MARTIN MARIETTA ENERGY SYSTEMS LIBRARIES

3 4456 0282432 6

NUREG/CR-4651
ORNL/TM-10100/V2
Vol. 2

Development of Riprap Design Criteria by Riprap Testing in Flumes: Phase II

Followup Investigations

Prepared by S.R. Abt, R.J. Wittler, J.F. Ruff, D.L. LaGrone,
M.S. Khattak, J.D. Nelson/CSU
N.E. Hinkle, D.W. Lee/ORNL

Colorado State University

Oak Ridge National Laboratory

Prepared for
U.S. Nuclear Regulatory
Commission

NOTICE

This report was prepared as an account of work sponsored by an agency of the United States Government. Neither the United States Government nor any agency thereof, or any of their employees, makes any warranty, expressed or implied, or assumes any legal liability of responsibility for any third party's use, or the results of such use, of any information, apparatus, product or process disclosed in this report, or represents that its use by such third party would not infringe privately owned rights.

NOTICE

Availability of Reference Materials Cited in NRC Publications

Most documents cited in NRC publications will be available from one of the following sources:

1. The NRC Public Document Room, 1717 H Street, N.W.
   Washington, DC 20555
2. The Superintendent of Documents, U.S. Government Printing Office, Post Office Box 37082, Washington, DC 20013-7082
3. The National Technical Information Service, Springfield, VA 22161

Although the listing that follows represents the majority of documents cited in NRC publications, it is not intended to be exhaustive.

Referenced documents available for inspection and copying for a fee from the NRC Public Document Room include NRC correspondence and internal NRC memoranda; NRC Office of Inspection and Enforcement bulletins, circulars, information notices, inspection and investigation notices; Licensee Event Reports; vendor reports and correspondence; Commission papers; and applicant and licensee documents and correspondence.

The following documents in the NUREG series are available for purchase from the GPO Sales Program: formal NRC staff and contractor reports, NRC-sponsored conference proceedings, and NRC booklets and brochures. Also available are Regulatory Guides, NRC regulations in the *Code of Federal Regulations,* and *Nuclear Regulatory Commission Issuances.*

Documents available from the National Technical Information Service include NUREG series reports and technical reports prepared by other federal agencies and reports prepared by the Atomic Energy Commission, forerunner agency to the Nuclear Regulatory Commission.

Documents available from public and special technical libraries include all open literature items, such as books, journal and periodical articles, and transactions. *Federal Register* notices, federal and state legislation, and congressional reports can usually be obtained from these libraries.

Documents such as theses, dissertations, foreign reports and translations, and non-NRC conference proceedings are available for purchase from the organization sponsoring the publication cited.

Single copies of NRC draft reports are available free, to the extent of supply, upon written request to the Division of Information Support Services, Distribution Section, U.S. Nuclear Regulatory Commission, Washington, DC 20555.

Copies of industry codes and standards used in a substantive manner in the NRC regulatory process are maintained at the NRC Library, 7920 Norfolk Avenue, Bethesda, Maryland, and are available there for reference use by the public. Codes and standards are usually copyrighted and may be purchased from the originating organization or, if they are American National Standards, from the American National Standards Institute, 1430 Broadway, New York, NY 10018.

NUREG/CR-4651
ORNL/TM-10100/V2
Vol. 2

Development of Riprap Design Criteria by Riprap Testing in Flumes: Phase II

Followup Investigations

Manuscript Completed: August 1988
Date Published: September 1988

Prepared by
S.R. Abt, R.J. Wittler, J.F. Ruff, D.L. LaGrone,
M.S. Khattak, J.D. Nelson, Colorado State University
N.E. Hinkle, D.W. Lee, Oak Ridge National Laboratory

Colorado State University
Fort Collins, CO 80523

Under Contract to:
Oak Ridge National Laboratory
Oak Ridge, TN 37831

Prepared for
Division of Low Level Waste Management and Decommissioning
Office of Nuclear Material Safety and Safeguards
U.S. Nuclear Regulatory Commission
Washington, DC 20555
NRC FIN B0279

MARTIN MARIETTA ENERGY SYSTEMS LIBRARIES
3 4456 0282432 6

ABSTRACT

Flume studies were conducted in which riprap embankments were subjected to overtopping flows. Embankment slopes of 1, 2, 8, 10, and 20% were protected with riprap containing median stone sizes of 1, 2, 4, 5, and/or 6 in. Riprap layer thickness ranged from 1.5 D_{50} to 4 D_{50}. Riprap design criteria for overtopping flows were developed in terms of unit discharge at failure, interstitial velocities and discharges through the riprap layer, resistance to flow over the riprap surface, effects of riprap layer thickness and gradation on riprap stability, and potential impacts of integrating soil into the riprap layer for riprap stabilization. A riprap design procedure is presented for overtopping flow conditions.

TABLE OF CONTENTS

Chapter	Page
ABSTRACT	iii
LIST OF FIGURES	vii
LIST OF TABLES	ix
NOTATION	xi
ACKNOWLEDGMENTS	xiii
1. INTRODUCTION	1
1.1 OBJECTIVES	1
1.2 PHASE I SUMMARY	1
1.2.1 Failure Relationships	2
1.2.2 Interstitial Velocities	2
1.2.3 Resistance to Flow	5
1.2.4 Incipient Stone Movement and Channelization	5
2. DESCRIPTION OF FACILITIES AND ARMORING MATERIALS	9
2.1 OUTDOOR FACILITY	9
2.2 INSTRUMENTATION	9
2.3 TEST MATERIAL PROPERTIES	11
3. EXPERIMENTAL PROGRAM	15
3.1 TEST PROCEDURE	15
3.2 PARAMETERS OF ANALYSIS	17
3.2.1 Manning's Roughness Coefficient	17
3.2.2 Shields' Coefficient	17
3.2.3 Darcy-Weisbach Friction Factors	17
3.3 ESTABLISHED DESIGN PROCEDURES	18
3.3.1 Safety Factors Method	18
3.3.2 Stephenson Method	22
3.3.3 U.S. Army Corps of Engineers Method	22
3.3.4 U.S. Bureau of Reclamation Method	26
3.3.5 Summary	26
3.4 ESTABLISHED PROCEDURES TO ESTIMATE RESISTANCE TO FLOW	28
3.4.1 Limerinos' Procedure	28
3.4.2 Stricker Procedure	28
3.4.3 Anderson, Paintal, and Davenport Procedure	29
3.4.4 Jarrett Procedure	29
3.4.5 Bathurst Procedure	29
3.4.6 U.S. Army Corps of Engineers Procedure	29
3.4.7 Summary	30
4. ROCK FAILURE AND ROCK MOVEMENT RELATIONSHIPS	31
4.1 FAILURE RELATIONSHIPS OF ANGULAR ROCK	31
4.1.1 Phase II Data	33
4.1.2 Composite Failure Relationship	33
4.2 RESISTANCE TO FLOW	33
4.2.1 Computation of Manning's n Value	33

4.2.2 Comparison of Phase I and Phase II Manning's n Value 37
4.3 RIPRAP GRADATION EFFECT ON RIPRAP STABILITY 39
4.3.1 Failure Relationship 40
4.4 RIPRAP LAYER THICKNESS. 40
4.4.1 Failure Trends 45
4.4.2 Layer Thickness Adjustment 45
4.5 SHAPE INFLUENCE ON RIPRAP STABILITY 48
4.5.1 Stability Comparison 48
4.6 STONE MOVEMENT AND CHANNELIZATION 50
4.6.1 Stone Movement to Failure Relationship 50
4.6.2 Rock Sizing to Resist Movement 54
4.6.3 Channelization to Failure Relationship 54
4.7 SUMMARY 54

5. INTERSTITIAL VELOCITIES THROUGH RIPRAP 57
5.1 COMPARISON OF PHASE I AND PHASE II INTERSTITIAL VELOCITIES. 57
5.2 CALCULATED VS MEASURED INTERSTITIAL VELOCITIES. 59
5.3 INTERSTITIAL VELOCITY RELATED TO D_{10} 59
5.4 INTERSTITIAL VELOCITY THROUGH FILTER MATERIAL 62
5.5 APPLICATION TO RIPRAP LAYER DESIGN. 62
5.6 SUMMARY 65

6. RIPRAP COVER 67
6.1 MATERIAL CLASSIFICATION AND PLACEMENT 67
6.2 RESULTS OF TEST NO. 23. 67
6.3 RESULTS OF TEST NO. 25. 69
6.4 RESULTS OF TEST NO. 53. 69
6.5 RIPRAP SOIL MATRIX. 71
6.6 RESULTS OF TEST NO. 52. 73
6.7 SUMMARY 73

7. RECOMMENDED DESIGN PROCEDURE 77
7.1 DESIGN PROCEDURE. 77
7.2 COMMENTS. 80

8. CONCLUSIONS. 81

9. REFERENCES 83

APPENDIX A - RIPRAP, FILTER, AND SOIL GRAIN SIZE DISTRIBUTION. . . . A-1

APPENDIX B - SUMMARY OF INTERSTITIAL VELOCITY PROFILES B-1

APPENDIX C - SUMMARY OF HYDRAULIC DATA C-1

LIST OF FIGURES

Figure		Page
1.1	Unit discharge and median stone size relationship at failure	3
1.2	Interstitial flow velocity relationships on steep embankments	4
1.3	Median stone size/slope parameter vs Manning's n for cascading flow conditions	6
1.4	Normalized unit discharge vs normalized time	7
2.1	Outdoor flume schematic	10
3.1	Riprap stability conditions as described in the Safety Factors Method	20
3.2	Angle of repose as a function of median stone diameter and shape	21
3.3	Graphical solution of Eq. 3.16	24
3.4	Sizing of riprap as a function of design shear stress	25
3.5	Parametric curve used to determine maximum stone size in riprap mixture as a function of channel bottom velocity	27
4.1	Comparison of unit discharge and median stone size relationship at failure for Phase II tests with Phase I tests at 10% slope	34
4.2	Consolidated relationship for riprap failure	35
4.3	Median stone size/slope parameter versus Manning's n	38
4.4	Gradation curve	41
4.5	Unit discharge at failure vs riprap layer coefficient of uniformity	42
4.6	Relating the coefficient of rock gradation to the coefficient of uniformity	43
4.7	Riprap layer stability as a function of median stone size	46
4.8	Coefficient of layer thickness vs riprap thickness for median stone sizes <6 in	47

Figure		Page

4.9 Comparison of angular- and rounded-rock stability..... 49

4.10 Riprap failure relationships from overtopping flow for angular and rounded rock..... 51

4.11 Normalized unit discharge vs normalized time for stone movement and channelization..... 53

5.1 Comparison of the Phase I and Phase II interstitial velocity data..... 60

5.2 Comparison of measured vs calculated interstitial velocities..... 61

5.3 Interstitial velocity expressed as a function of D and gradient..... 63

6.1 Soil cover with 14% clay prior to testing..... 72

6.2 Soil cover with 14% clay during channelized flow conditions..... 72

6.3 Riprap soil matrix prior to testing..... 74

6.4 Riprap soil matrix at failure..... 74

LIST OF TABLES

Table		Page
2.1	Riprap properties	13
2.2	Filter properties	14
3.1	Summary of experimental program	16
4.1	Summary of failure tests	32
4.2	Summary of average Manning's n for Phase II data	36
4.3	Summary of channel and movement discharges	52
5.1	Velocity profiles for interstitial flow through riprap in the outdoor flume at 10% slope	58
5.2	Interstitial velocities through filter GF5	64
6.1	Soil properties	68
6.2	Summary of soil cover tests	70

NOTATION

Symbol	Term
A	Cross-sectional area of flow
C_c	Bed critical Shield's coefficient
C_t	Coefficient of riprap layer thickness
C_f	Channel concentration factor
C_p	Coefficient representing method of stone placement
C_u	Coefficient of uniformity
C_R	Coefficient of gradation
D	Depth of flow
D_x	Soil diameter at which xpercent of the soil weight is finer
D_s	Stable stone size
D_{50}	Median stone size
F_d	Drag force
F_l	Lift force
f	Darcy-Weisbach friction factor
G_s	Specific gravity
g	Acceleration of gravity
i	Head loss gradient
k	Equivalent channel boundary surface roughness
K	Oliviers' constant
K_s	Shape factor of stone
n	Manning's roughness coefficient
n_p	Porosity
Q	Channel discharge
q	Unit discharge
q_f	Unit discharge at failure

Symbol	Term
R	Hydraulic radius of channel
r^2	Regression coefficient
S	Slope of embankment
S_m	Safety factor of riprap rolling down with no flow
SF	Safety Factors method
q_i	Interstitial unit discharge
t	Time elapsed after starting the test
t_f	Total time to failure
t_r	Thickness of riprap layer
V	Surface flow velocity
V_b	Localized bottom velocity of flow
W_c	Class weight of stone
W_s	Weight of stone
α	Slope angle
β	Wave front angle
γ	Unit weight
γ_s	Unit weight of surface-dry but saturated stone
γ_w	Unit weight of water
η	Stability number for riprap on a plane bed
η'	Stability number for riprap on a side slope
θ	Angle of slope measured from horizontal
ϕ	Friction angle
λ	Angle between horizontal and velocity vector
τ	Shear stress
τ_o	Bed shear stress
$\bar{\tau}_o$	Local boundary shear stress

ACKNOWLEDGMENTS

Research performed by Colorado State University under Subcontract No. ORNL-19X-55908C from Oak Ridge National Laboratory, operated by Martin Marietta Energy Systems, Inc. under contract with the U.S. Department of Energy. Research sponsored by Office of Nuclear Material Safety and Safeguards, U.S. Nuclear Regulatory Commission. The authors express their appreciation to the Colorado State University staff involved in the construction, testing and data reduction phases of this project.

1. INTRODUCTION

The protection of the public health and environment from the potential hazards of waste materials has stimulated the assessment of waste stabilization design procedures and methods. Current stabilization methods cap the waste materials with an earthen cover. In many cases, stabilizing materials are placed atop of the cover. Reclamation standards require that waste impoundments be designed and constructed to ensure the long-term stabilization for periods of 200 to 1000 years.

One means of providing long-term stabilization of a waste impoundment is to place a protective filter blanket and riprap layer over the cover. Nelson et al. (1986) indicated that when riprap protection is considered, alternative design procedures should be used for different zones of the impoundment. The riprap design should protect the impoundment from regional and localized flooding conditions that affect the embankment toe, side slopes, and cap.

Riprap design procedures should be conservative enough to ensure long-term cover stabilization, yet be economically advantageous to warrant the use of riprap. Established and field-tested design procedures exist that stabilize embankment toes and bank slopes for traditional channel flow conditions. However, many of the existing riprap procedures provide a conservative design that is not necessarily cost-effective. Also, many of the existing riprap design procedures were not developed specifically for overtopping flow conditions and, therefore, are not applicable to optimizing site protection and construction economics for reclamation.

1.1 OBJECTIVES

The objective of this investigation was to provide supplemental design criteria to the Phase I (Abt et al. 1987) study on long-term stabilization of uranium tailings impoundments subject to overtopping flows. A series of laboratory flume experiments were conducted to:

1. expand the applicability of the unit discharge, slope, and stone size relationships of a riprap system at failure;
2. verify interstitial velocity relationships;
3. verify resistance to surface flow relationships;
4. determine the effect that riprap layer thickness, stone shape, and stone layer gradation have on system stability; and
5. determine the stabilizing effects that soil cover and soil matrix have on the impoundment cover.

The results of the experimental program were combined with the results of Phase I when and where applicable.

1.2 PHASE I SUMMARY

Phase I (Abt et al. 1987) of the long-term stabilization analysis of riprap protection developed a series of overtopping flow relationships, without conservatism or "built-in" factors of safety, to evaluate existing design procedures for sizing riprap, for

determining the resistance to flow over riprap, and for estimating interstitial velocities within the riprap layer. From these relationships, a riprap design criteria was developed. A summary of the Phase I study and the specific findings follows.

A series of 52 flume experiments was conducted in which riprap was placed on an embankment(s) and subjected to overtopping flows. Embankment slopes of 1, 2, 8, 10, and 20% were protected with median stone sizes of 1, 2, 4, 5, and/or 6 in. in diameter. Data collected during these tests included unit discharge at failure; interstitial velocities in the stone layer; flow depth over the riprap surface; localized surface velocities over the riprap surface; and the stone, filter, and soil properties.

1.2.1 Failure Relationships

It was determined that the unit discharge at which the riprap layer failed was dependent upon the median stone size, D_{50}, of the riprap layer and upon the embankment or channel slope, S. A family of failure relationships resulted as shown in Fig. 1.1. Failure tests were conducted without tailwater. Therefore, by estimating the maximum unit discharge overtopping a riprap layer, the median stone size necessary to resist failure can be determined. The failure relationships portrayed in Fig. 1.1 do not reflect a safety factor in the sizing process.

1.2.2 Interstitial Velocities

The average interstitial velocity of flow through a rock layer was determined by a tracer-sensitive injection system. A salt solution was injected into each rock layer system, and the dilution curve was recorded. From the dilution curves, interstitial velocities in the rock layer were derived. A unique relationship resulted in which the interstitial velocity, V_i, and median stone size, D_{50}, were correlated to the embankment or channel slope, S; the stone properties coefficient of uniformity, C_u; and porosity, n_p; as presented in Fig. 1.2. After a power regression on the results was performed, the interstitial velocity was expressed as

$$V_i = 19.29 \; C_u^{-0.074} \; S^{0.46} \; n_p^{4.14^{1.064}} \; (g \, D_{50})^{0.5} \; , \qquad (1.1)$$

where velocity is in feet per second. Equation 1.1 allows the designer to estimate both the rock layer flow capacity and the average interstitial flow velocity as a function of the riprap properties and the embankment slope. Equation 1.1 was derived from riprap layer thicknesses of 3 in. to 12 in. placed on steep embankment faces.

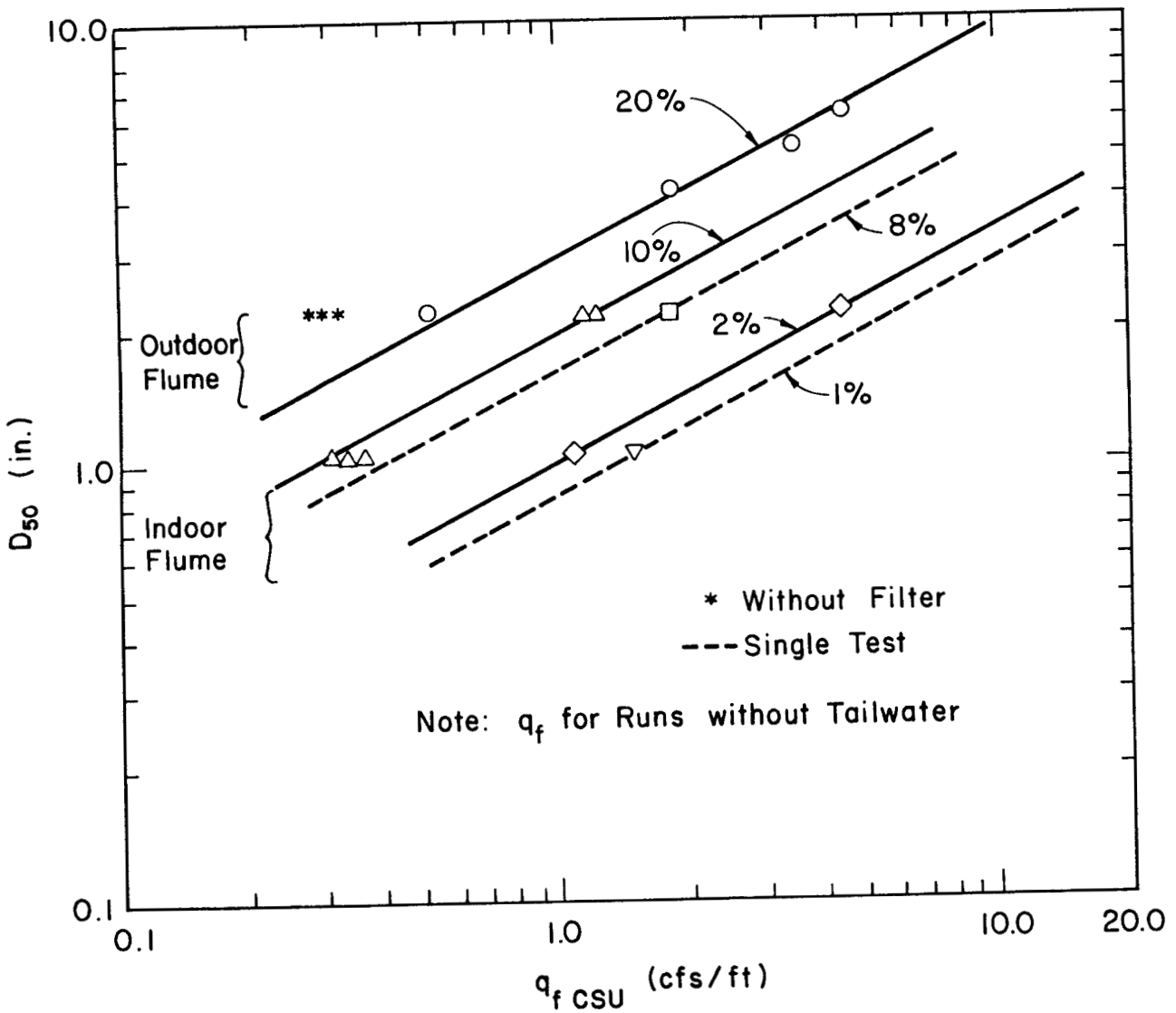

Figure 1.1. Unit discharge and median stone size relationship at failure.

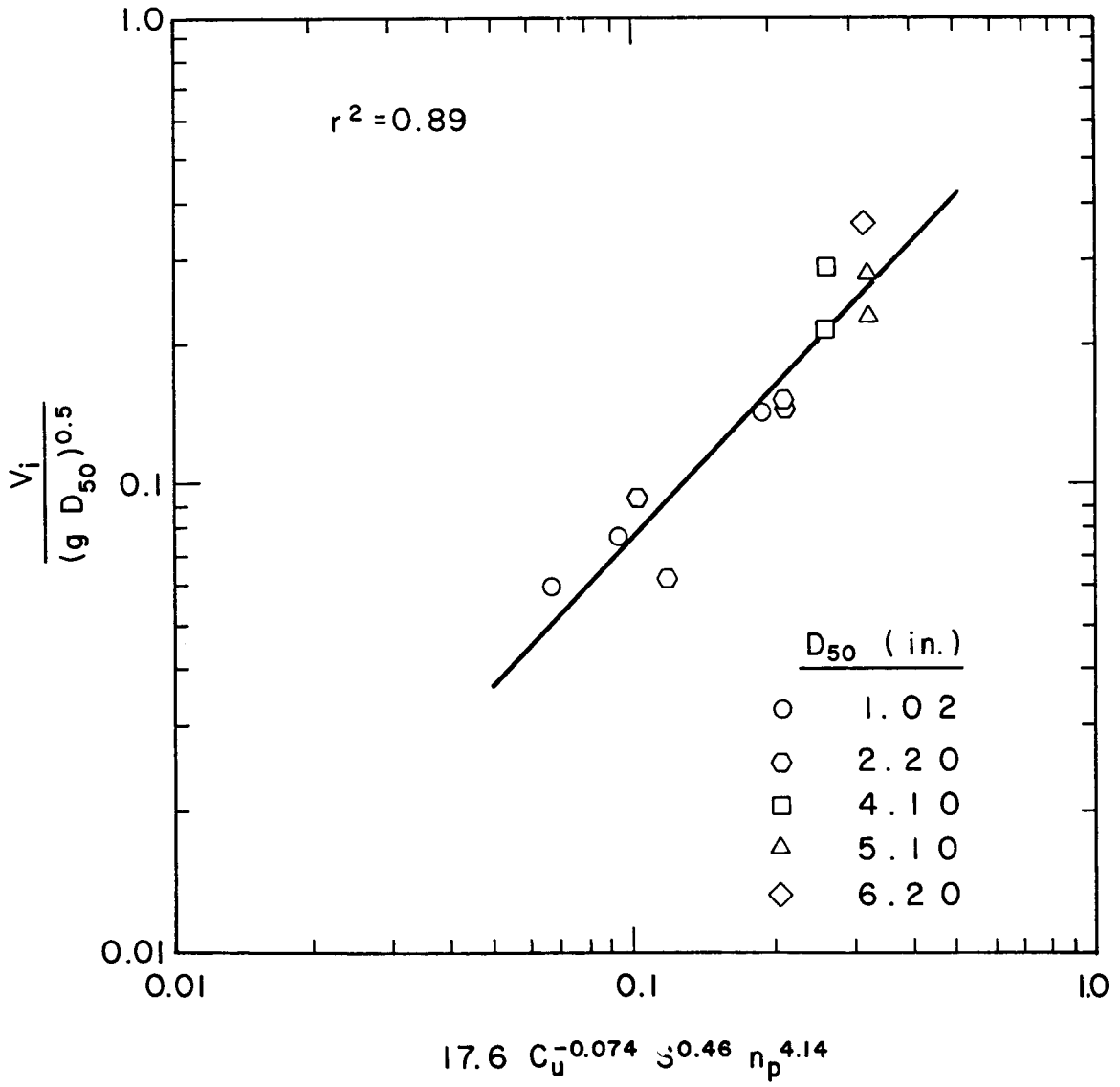

Figure 1.2. Interstitial flow velocity relationships on steep embankments.

1.2.3 Resistance to Flow

The resistance to surface flow was determined for each test in which surface flows resulted in riprap system failure. Extensive analysis of the data indicated that the estimated Manning's n values did not agree with existing relationships derived from flat, natural channels. The data analysis indicated that the product of the median stone size and the embankment or channel slope correlated to the Manning's n value as presented in Fig. 1.3. The n value can be expressed as

$$n = 0.0456\ (D_{50} \times S)^{0.159}, \tag{1.2}$$

where D_{50} is in inches. Equation 1.2 was derived for angular stone surfaces in cascading flow conditions.

1.2.4 Incipient Stone Movement and Channelization

The unit discharge in which stone movement was initially observed was recorded in four stone movement and failure tests. The unit discharge at stone movement was compared to the unit discharge at the riprap system failure. A graphical representation of the zone of rock movement is presented in Fig. 1.4, where the normalized unit discharge vs normalized time is portrayed. It was observed that stone movement occurred when the unit discharge approached 76% $\pm$ 3% of the unit discharge at failure. The stone movement appears to be independent of the shape of the rising limb of the normalized inflow hydrograph.

During many of the failure tests, small channels formed in the riprap layer. Channels formed as flow was diverted around the larger stones. Flow concentrated into localized zones, thereby increasing localized velocities and flow depths. Incipient channelization in the riprap layer was documented when possible. The zone of incipient channelization appeared to occur when the unit discharge approached 90% $\pm$ 5% of the unit discharge at failure, as indicated in Fig. 1.4. The channelization appeared to be independent of the shape of the normalized inflow hydrograph. Channelization of the total flow was expressed as the ratio of the unit discharge of the channelized flow to the unit discharge for the sheet flow. This flow channelization ratio was observed to exceed 3.0.

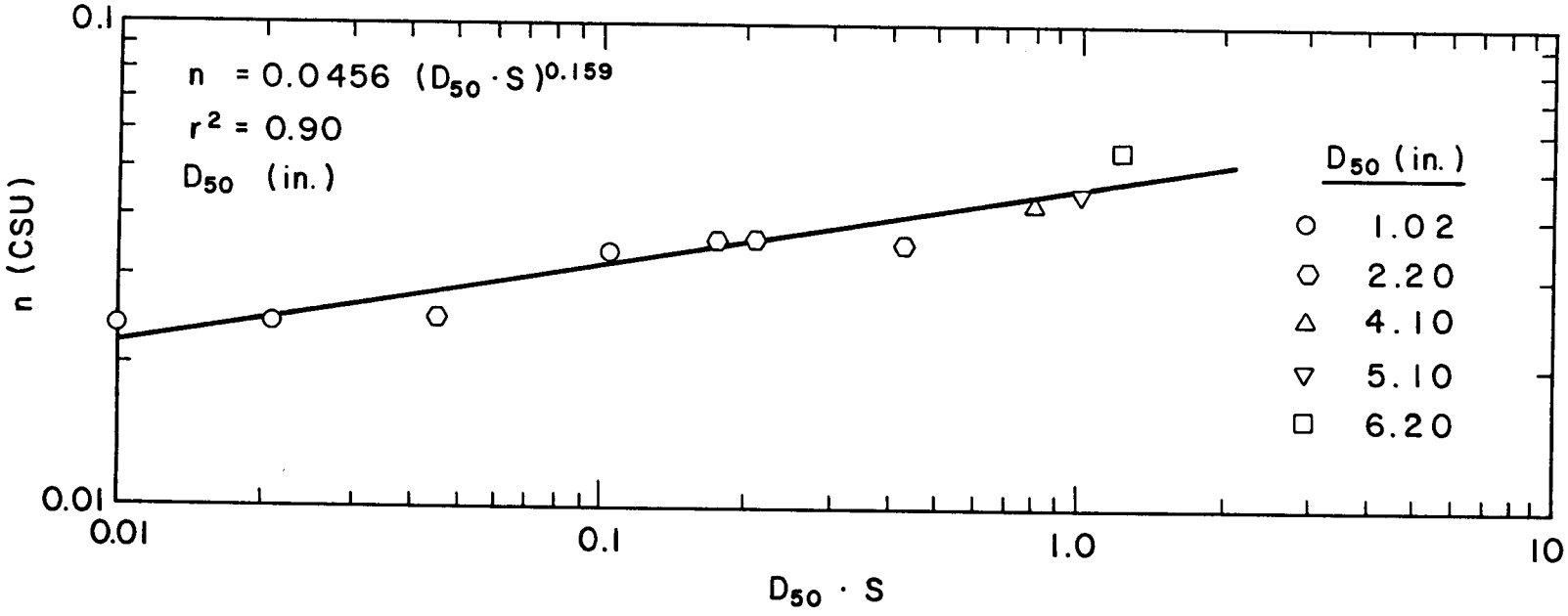

Figure 1.3. Median stone size/slope parameter vs Manning's n for cascading flow conditions.

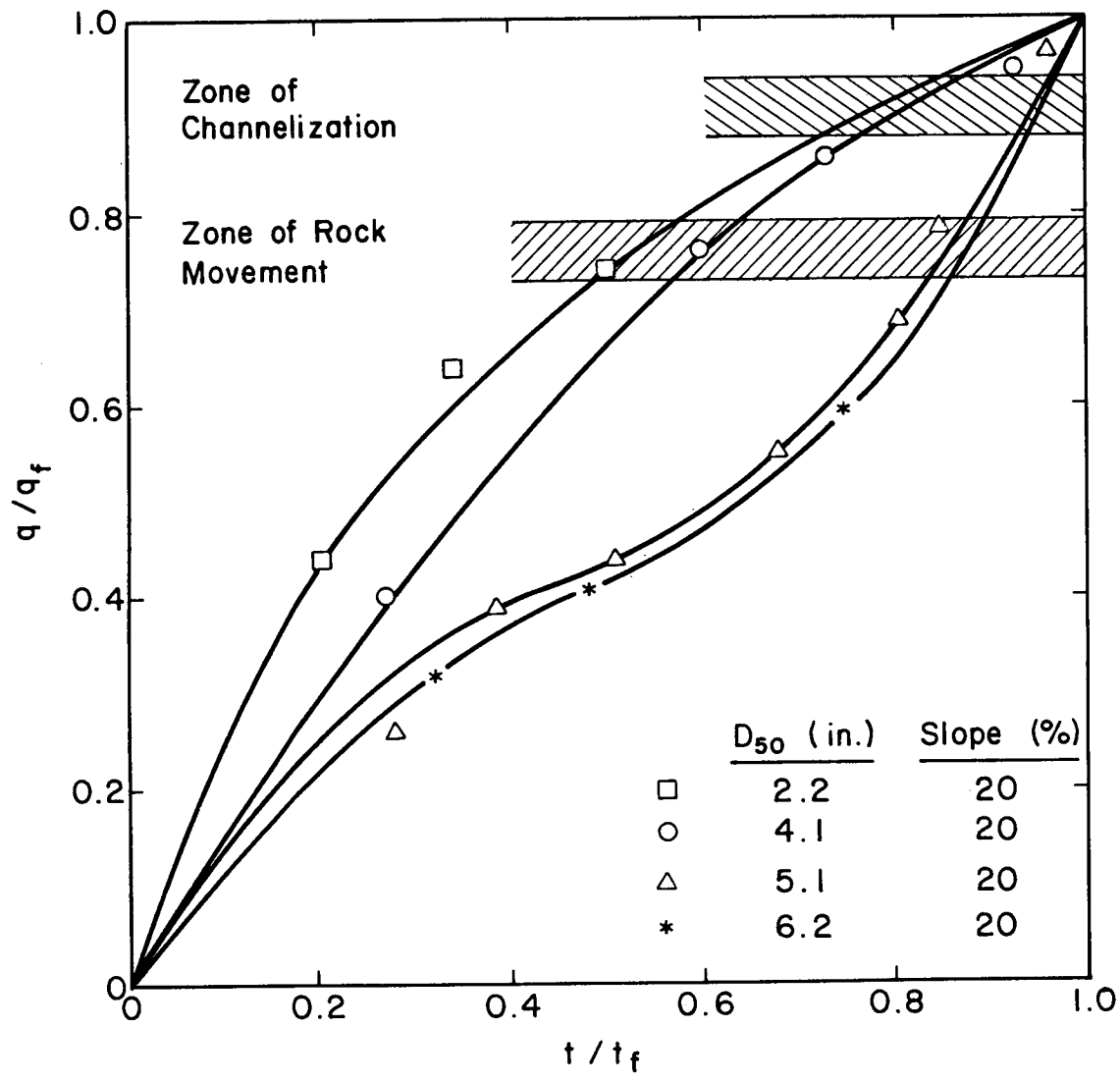

Figure 1.4. Normalized unit discharge vs normalized time.

2. DESCRIPTION OF FACILITIES AND ARMORING MATERIALS

The experimental program was conducted in an outdoor flume located at the Engineering Research Center of Colorado State University. The flume was used for simulating embankments with side slopes of 10 and 20%. The flume was modified to enable prototype testing of riprap-covered slopes for the evaluation of the layer stability when subjected to a variety of testing conditions. The flume configuration also served to test the stability of soil cover, soil matrix, and filter materials.

2.1 OUTDOOR FACILITY

The outdoor facility is a concrete flume that is 180 ft (54.9 m) long, 20 ft (6.1 m) wide and 8 ft (2.4 m) deep. The flume is shown in Fig. 2.1. The flume was modified so that the upper 20 ft served as an inlet basin for energy dissipation and wave suppression. A head wall was constructed and served as the inlet to the test section. The throat of the test section was 12 ft wide to allow a concentration of flow onto the embankment. The test embankment extended approximately 65 ft downstream of the headwall. The remainder of the flume was used for tailwater control and material recovery.

Water was supplied to the facility from Horsetooth Reservoir through an existing pipe network. A 36-in. butterfly valve located just upstream of the flume served to control inflow to the inlet basin. A sonic flow meter was used to determine inlet discharges. A V-notch weir was installed at the flume outlet to measure low flows ($\leq$5 cfs) and to check the sonic flow meter discharge measurements.

The test embankment was constructed of a moistened, compacted sand in the test section. The initial 15 ft of the embankment was horizontally placed to simulate the cover on top of a tailings pile. The embankment transitioned to a 10% slope to simulate the steep side slope of a reclaimed tailings pile. Geofabric was used to cover and stabilize the sand embankment. The geofabric allowed the embankment to be saturated and to move under a variety of loading conditions. However, the geofabric prevented the sand embankment from massive failure, thereby minimizing turn-around time between experiments.

A 6-in. thick sand/gravel filter layer was placed on top of the geofabric as specified by the appropriate filter design criteria for most of the tests. Riprap was placed on top of the filter material to the prescribed layer thickness.

A catwalk and an observation platform were constructed and placed on top of the flume. The catwalk served to allow access to any portion of the test section for data acquisition. The observation platform was used for videotaping and photographing each record test.

2.2 INSTRUMENTATION

The instrumentation consists of the equipment to monitor the water surface elevation and flow velocity through and over the riprap

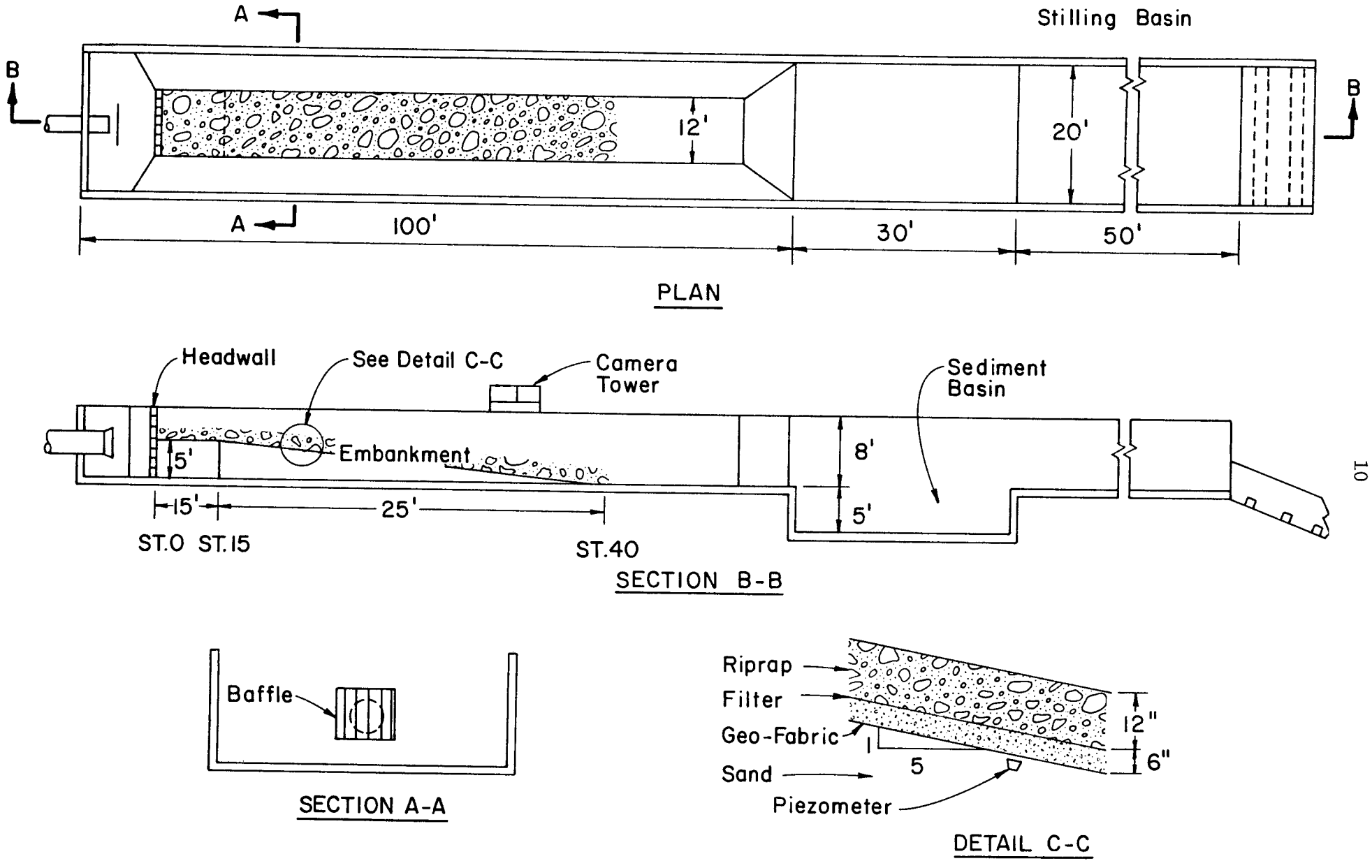

Figure 2.1. Outdoor flume schematic.

layer. Portable television equipment was used to videotape the riprapped embankments prior to, during, and after each test.

A tracer solution injection and recording system was developed to document the flow velocities through the riprap layer. The system was composed of a pressure-operated tracer injector, tracer-sensitive probes, multichannel selector, and multichannel strip chart recorder. Each tracer-sensitive probe was fabricated with three tracer-sensitive elements placed in the lower 8 in. of the probe. The tracer injector was fabricated with three injection ports. The injector port spacings were similar to the tracer-sensitive elements in the probe. Salt was used as the tracer.

The tracer-sensitive system was placed in the riprap layer such that the injector ports were approximately aligned with the elements in the tracer-sensitive probe. The injector and the tracer-sensitive probes were placed from 10 to 12 and from 20 to 24 in. apart in the rock layer. The flow was established in the flume such that the water surface was at an elevation just above the riprap surface. The tracer was then injected into the rock layer. An event marker on a strip chart recorder indicated when the injector was triggered. Output from the tracer-sensitive elements was also recorded on the strip chart, enabling the tracer-dilution curve to be observed and documented. Flow velocities were derived from the tracer-dilution curves recorded on the strip chart for each test condition.

Localized surface velocities in the outdoor flume were measured by a Marsh-McBirney® magnetic flow meter. The meter was periodically calibrated throughout the experimental program. Water surface elevations were monitored by piezometers installed in the embankments. Piezometers were placed at sections at the top of the embankment, near the crest of the embankment, at the upper one-third of the embankment slope, and at the lower one-third of the embankment slope. Piezometers were equally spaced at one-third intervals across each section to monitor potential differences in the flow distribution. Each piezometer was connected to a central manometer board to record the water surface elevation to the nearest 0.02 ft. During each test, flow depths were periodically estimated to the nearest 0.10 ft with a gaging rod to provide a check on the manometer system.

A Panasonic videotape camera and video cassette recorder system were used to visually document each failure test. Also, photographic equipment documented pre-test, test, and post-test embankment conditions.

2.3 TEST MATERIAL PROPERTIES

The riprap was obtained from a quarry located near Denver, Colorado. Nominal median stone sizes, D_{50}, tested were 2 and 4 in. Rock properties of coefficient of uniformity, unit weight, specific gravity, porosity, shape, and friction angle were determined in the Colorado State University Geotechnical Engineering Laboratory by

procedures outlined by the American Society for Testing Materials (ASTM). A summary of the riprap properties is presented in Table 2.1. The grain size distribution for each riprap size is presented in Appendix A.

A filter blanket underlaid the riprap layer in most of the tests. The filter criteria used to size the blanket was derived from Sherard et al. (1963) and is expressed as

$$\frac{D_{15}\ \text{(riprap)}}{D_{85}\ \text{(filter)}} < 5 \tag{2.1}$$

$$5 < \frac{D_{15}\ \text{(riprap)}}{D_{15}\ \text{(filter)}} < 40 \tag{2.2}$$

$$\frac{D_{50}\ \text{(riprap)}}{D_{50}\ \text{(filter)}} < 50 \tag{2.3}$$

A summary of the filter grain sizes and coefficients of uniformity is presented in Table 2.2. The grain size distribution for the filter materials is also provided in Appendix A.

Table 2.1. Riprap properties[a]

Test number	Riprap[b] D_{50} (in.)	Riprap gradation[c]	Filter gradation[c]	C_u[d]	γ[e] (lb/ft^3)	n_p[f]	ϕ[g]	G_s[h]
19-22	4.0 R	GR1	GF1	1.68	90	0.45	38	2.50
23-25	4.0 A	GR2	GF1	2.29	92	0.44	42	2.65
26-34	2.0 A	GR3	GF2	2.14	92	0.45	41	2.72
35-38	4.0 R	GR4	GF1	2.12	92	0.45	38	2.50
39-44	4.0 A	GR5	GF3	2.30	92	0.44	42	2.65
45-46	2.0 R	GR6	GF4	2.14	92	0.45	37	2.72
47-48	4.0 A	GR7	GF3	4.00	100	0.39	42	2.65
50-51	4.0 A	GR8	GF3	1.72	90	0.46	42	2.65
52-53	4.0 A	GR5	GF3	2.30	92	0.44	42	2.65

[a]All properties were determined in the Colorado State University Geotechnical Laboratory in accordance with American Society for Testing Materials guidelines.

[b]A = Angular Rock.
R = Round Rock.
D_{50} = Median stone size.

[c]Gradation curves designated by symbols are given in Appendix A.

[d]C_u = Coefficient of uniformity.

[e]γ = Unit weight.

[f]n_p = Porosity of rock layer.

[g]ϕ = Friction angle.

[h]G_s = Specific gravity,

Table 2.2. Filter properties[a]

Test number	Filter gradation[b]	Filter[c] D_{50} (in.)	Filter depth (in.)	Filter[d] C_u	Filter[c] D_{10} (in.)	Filter[c] D_{100} (in.)
19-25	GF1	0.50	6	11.21	0.061	1.70
26-34	GF2	0.19	6	5.87	0.046	1.00
35-38	GF1	0.50	6	11.21	0.061	1.70
39-44	GF3	0.44	6	13.40	0.047	1.50
45-46	GF4	0.19	6	6.11	0.045	1.00
47-48	GF3	0.44	6	13.40	0.047	1.50
49	GF5	0.44	6	13.40	0.047	1.50
50-53	GF3	0.40	6	13.40	0.047	1.50

[a]All properties were determined in the Colorado State University Geotechnical Laboratory in accordance with American Society for Testing Materials guidelines.

[b]Gradation curves designated by symbols are found in Appendix A.

[c]D_{50} = Median stone size.

D_{10} = 10% of stone is finer than indicated size on specified gradation curve.

D_{100} = All stone is finer than indicated size on specified gradation curve.

[d]C_u = Coefficient of uniformity.

3. EXPERIMENTAL PROGRAM

A series of 38 experiments was conducted including shakedown, rock movement, interstitial flow, and rock failure. The intent of these tests was to characterize riprap stability as a function of embankment or channel slope, median stone size, riprap layer thickness, riprap gradation, and riprap shape. A summary of the experimental program is presented in Table 3.1. The experimental variables encompassed the embankment slope, S; the discharge rate, Q; localized surface flow velocities, V; interstitial flow velocities, V_i; water surface depths above the bed, D; and time, t. Also, the riprap, filter, and soil properties, as reported in Sect. 2.3, were used throughout the analysis.

General observations were recorded, when appropriate, to document flow and riprap phenomena that could not be explicitly measured [e.g., incipient flow concentrations, filter blanket extraction and failure, riprap layer failure indicators, and stone movement (beyond bed adjustment)]. Therefore, qualitative observations during each test, and later verified during videotape playback, were recorded and incorporated into the analysis.

Riprap was dump-placed in all the tests conducted in this phase of the investigation. However, the stone surface was leveled to minimize the occurrence of man-made flow concentrations. The riprap layer thickness was determined with a self-leveling level. Predetermined locations on the filter served as a reference. Once the rock layer was graded, a square plate was placed on top of the rock and the elevation was determined. The difference between the top of the filter blanket and top of the rock layer was reported as the layer thickness.

3.1 TEST PROCEDURE

The rock movement and riprap failure test procedures were similar for all 38 experiments conducted. Once the test embankment and riprap were placed and the instrumentation set and checked, the flume inlet valve was opened. The riprap was inundated, and the bed was allowed to adjust and/or settle. The flow was increased until overtopping flow was observed. Once the flow stabilized, the discharge was determined, and localized velocities and water surface elevations were obtained along four cross sections when and where possible. After the data were recorded and observations were documented, the flow was increased. Generally, 12 to 20 minutes were required to increase and stabilize the flow, acquire data, and record results. The procedure was repeated until stone movement and failure occurred. A videotape recording was made of portions of each test.

The test procedure was modified for the soil cover and soil matrix tests. The compacted soils restricted the measurement of flow depth until the soil cover eroded. Therefore, only limited data could be collected and recorded in the riprap layer.

Table 3.1. Summary of experimental program

Number of Tests[a]	Slope (%)		Median stone size (in.)		Riprap layer thickness[b]				Shape of riprap	
	10	20	2	4	1.5	2	3	4	Angular	Rounded
3		x		x			x			x
1		x		x			x		x	
2	x		x		x				x	
2	x		x			x			x	
3	x		x				x		x	
2	x		x					x	x	
2	x			x	x					x
2	x			x			x			x
2	x			x	x				x	
2	x			x		x			x	
2	x			x			x		x	
2	x		x				x			x
2	x			x			x		x	
2	x			x			x		x	

[a]In addition, 1 test was conducted to measure interstitial velocities through the filter material, 2 shakedown tests were conducted, 2 witness tests were conducted, and 4 soil cover and soil matrix tests were conducted.

[b]The layer thickness is expressed as a multiple of the median stone size.

3.2 PARAMETERS OF ANALYSIS

The Manning's roughness coefficient, n, bed critical Shields' coefficient, C_c, and Darcy-Weisbach friction factor, f, were computed for each discharge tested. Coefficients are reported for each test in Appendix C.

3.2.1 Manning's Roughness Coefficient

The Manning's roughness coefficient (Chow 1959) can be estimated as

$$n = \frac{1.486}{Q} A R^{2/3} S^{1/2} , \tag{3.1}$$

where

n = Manning's roughness coefficient for the bed,
S = Channel slope (ft/ft),
A = Cross-sectional area of flow (ft),
Q = Channel discharge (cfs) of surface flow,
R = Hydraulic radius of channel (ft).

The ratio of depth of flow to transverse width of the embankment was on the order of 0.05 or less and was considered relatively small. Therefore, the channel was assumed to be a wide channel. Because the depth of flow, D, is approximately equal to the hydraulic radius for a wide channel, Eq. 3.1 can be modified to

$$n = \frac{1.486}{Q} A D^{2/3} S^{1/2} . \tag{3.2}$$

3.2.2 Shields' Coefficient

The bed critical Shields' coefficient (Simons and Senturk 1977) is an indicator of incipient stone movement on the rock bed. The Shields' coefficient, C_c, is defined as

$$C_c = \frac{DS}{(G_s-1)\ D_{50}} , \tag{3.3}$$

where

D = Depth of flow (ft),
S = Channel slope (ft/ft),
G_s = Specific gravity of the rock,
D_{50} = Median stone size of the riprap (ft).

3.2.3 Darcy-Weisbach Friction Factors

The Darcy-Weisbach friction factor (Ruff et al. 1985) was computed for each test discharge. The Darcy-Weisbach friction factor, f, is defined as

$$f = \frac{8gDS}{V^2}, \tag{3.4}$$

where

g = Acceleration of gravity (ft/s^2),
V = Average velocity of flow (ft/s),
D = Depth of flow (ft),
S = Channel slope (ft/ft).

3.3 ESTABLISHED DESIGN PROCEDURES

Currently, several riprap design procedures are routinely used to determine the appropriate stone size for protection of impoundment covers, embankments, channel, and unprotected slopes from the impact of flowing waters. Four riprap design procedures that are referenced are:

1. Safety Factor Method (SF),
2. The Stephenson Method (STEPH),
3. The U.S. Army Corps of Engineers Method (COE), and
4. The U.S. Bureau of Reclamation Method (USBR).

A summary of each method is presented.

3.3.1 Safety Factors Method

The Safety Factors Method (Richardson et al. 1975) for sizing riprap allows the designer to evaluate rock stability from flow parallel to the cover and adjacent to the cover. The Safety Factors Method can be used by assuming a stone size and then calculating the safety factor, SF, or allowing the designer to determine a SF and then computing the corresponding stone size. If the SF is greater than unity, the riprap is considered safe from failure; if the SF is unity, the rock is at the condition of incipient motion; and if SF is less than unity, the riprap will fail.

The following equations are provided for riprap placed on a side slope or embankment where the flow has a nonhorizontal (downslope) velocity vector. The safety factor, SF, is:

$$SF = \frac{\cos\theta \tan\phi}{\eta' \tan\phi + \sin\theta \cos\beta}, \tag{3.5}$$

where

$$\eta' = \eta\left[\frac{[1 + \sin(\lambda + \beta)]}{2}\right], \tag{3.6}$$

$$\eta = \frac{21\,\tau_o}{(G_s - 1)\,\gamma\, D_{50}}, \tag{3.7}$$

$$\tau_o = \gamma\, DS, \tag{3.8}$$

and

$$\beta = \tan^{-1}\left[\frac{\cos\lambda}{(2\sin\theta)/(\eta\tan\phi) + \sin\lambda}\right] \tag{3.9}$$

The angle, λ, as shown in Fig. 3.1, is the angle between a horizontal line and the velocity vector component, V_r, measured in the plane of the side slope. The angle, θ, is the side slope angle shown in Fig. 3.1, and β is the angle between the vector component of the weight, W_s, directed down the side slope and the direction of particle movement. The angle, ϕ, is the angle of repose of the riprap, τ_o is the bed shear stress (Simons and Senturk 1977), D_{50} is the representative median stone size, G_s is the specific weight of the rock, D is the depth of flow, γ is the specific weight of the liquid, S is the slope of the channel, and η' and η are stability numbers. In Fig. 3.1, the forces F_l and F_d are the lift and drag forces, and the moment arms of the various forces are indicated by the value e_i as i = 1 through 4. Figure 3.2 illustrates the angle of repose for riprap material sizes.

Riprap is often placed along side slopes where the flow direction is close to horizontal or the angularity of the velocity component with the horizontal is small (i.e., = 0). For this case, the above equations reduce to:

$$\tan \beta = \frac{n \tan \phi}{2 \sin \theta} \tag{3.10}$$

and

$$\eta = \left[\frac{S_m^2 - (SF)^2}{(SF)\ (S_m^2)}\right] \cos \theta \ , \tag{3.11}$$

where

$$S_m = \frac{\tan \phi}{\tan \theta} \ . \tag{3.12}$$

The term S_m is the safety factor of the rock particles against rolling down the slope with no flow. The safety factor, SF, for horizontal flow may be expressed as:

$$SF = \frac{S_m}{2} \left[\left(S_m^2\ \eta^2\ \sec^2 \theta + 4\right)^{0.5} - S_m\ \eta \sec \theta\right] \ . \tag{3.13}$$

Riprap may also be placed on the cover or side slope. For a cover sloping in the downstream direction at an angle, α, with the horizontal, the equations reduce to:

$$SF = \frac{\cos \alpha \tan \phi}{\eta \tan \phi \sin \alpha} \tag{3.14}$$

Historic use of the Safety Factors Method has indicated that a minimum SF of 1.5 for non-probable maximum flood applications (i.e., 100-year events) provides a side slope with reliable stability and protection (Simons and Senturk 1977). However, an SF of slightly greater than 1.0 is recommended for probable maximum flood or maximum credible flood circumstances. It is recommended that the riprap thickness be a minimum of 1.5 times the D_{50}. Also, a bedding or filter layer should underlay the rock riprap. The filter layer

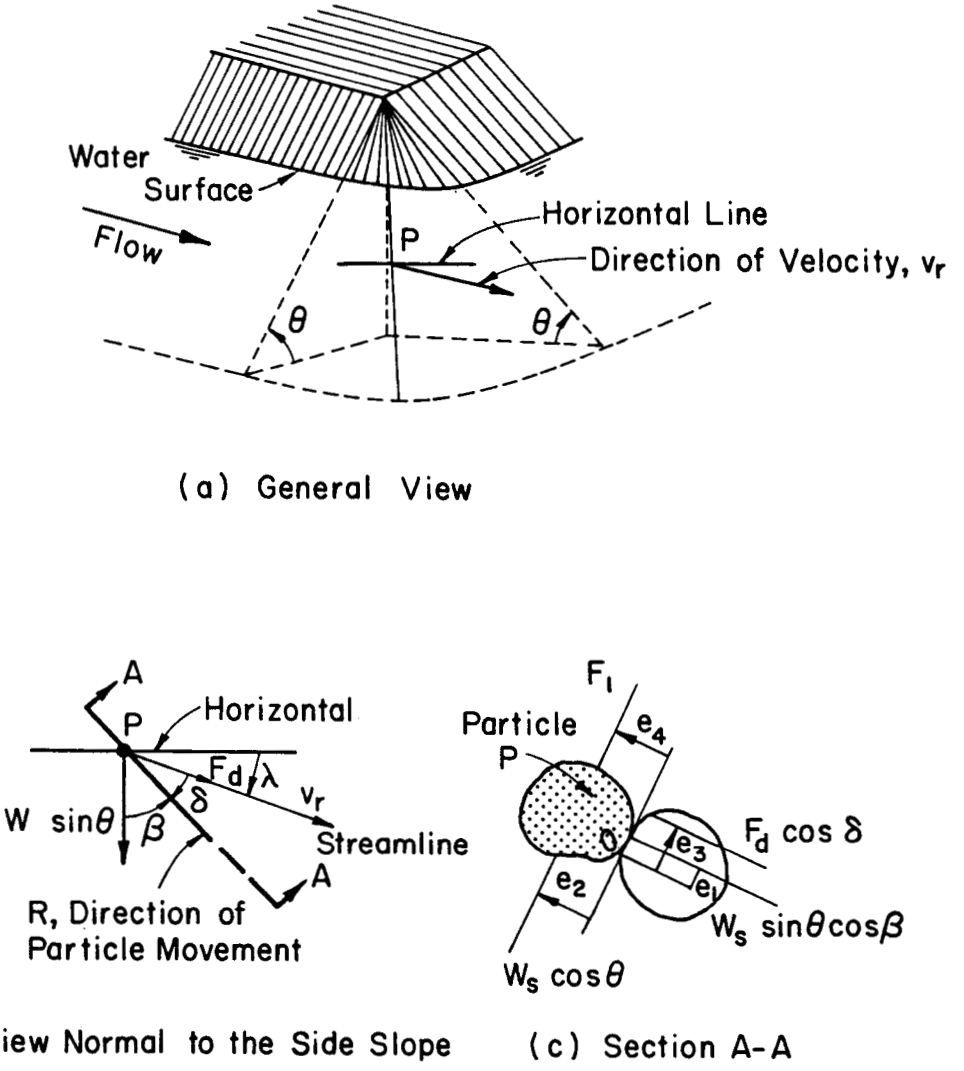

Figure 3.1. Riprap stability conditions as described in the Safety Factors Method.

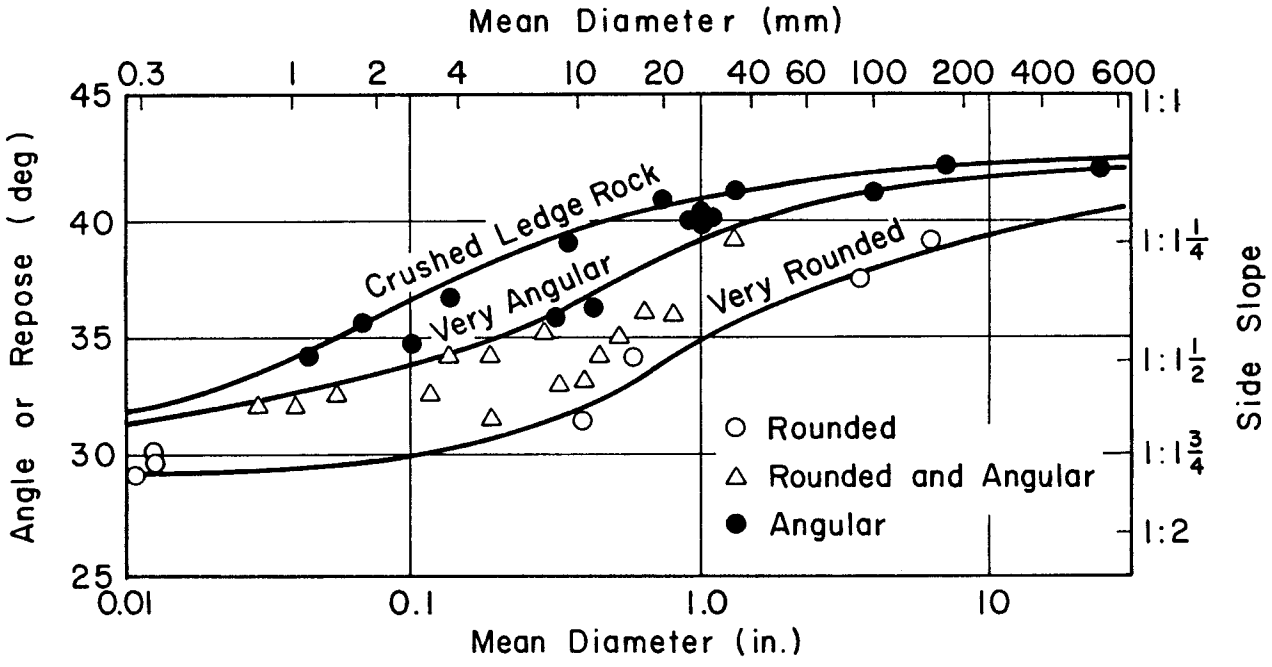

Figure 3.2. Angle of repose as a function of median stone diameter and shape.

thickness should minimally range from 6 to 12 in. In cases where the Safety Factors Method is used to design riprap along embankments or slopes steeper than 4H:1V, it is recommended that the toe be firmly stabilized.

3.3.2 Stephenson Method

The Stephenson Method for sizing rockfill to stabilize slopes and embankments is an empirically derived procedure developed for emerging flows (Stephenson 1979). The procedure is applicable to a relatively even layer of rockfill acting as a resistance to through and surface flow. It is ideally suited for the design and/or evaluation of embankment gradients and rockfill protection for flows parallel to the embankments, cover, or slope.

The sizing of the stable stone or rock requires the designer to determine the maximum flow rate per unit width, q; the rockfill porosity, n_p; the acceleration of gravity, g; the relative density of the rock, G_s; the angle of the slope measured from the horizontal, θ; the angle of friction, ϕ; and the empirical factor, C.

The stone or rock size, D_{50}, is expressed by Stephenson as

$$D_{50} = \left[\frac{q(\tan\theta)^{7/6}\, n_p^{1/6}}{C\, g^{1/2}\, [(1-n_p)(G_s-1)\cos\theta\,(\tan\phi - \tan\theta)]^{5/3}} \right]^{2/3} . \quad (3.15)$$

where the factor C varies from 0.22 for gravel and pebbles to 0.27 for crushed granite. The stone size calculated in Eq. 3.15 is the representative median diameter, D_{50}, at which rock movement is expected for unit discharge, q. The maximum flow rate, q, is then multiplied by Oliviers' constant, K, to ensure stability. Oliviers' constants are 1.2 for gravel and 1.8 for crushed rock. The rockfill layer should be well graded and at least two times the D_{50} in thickness. A bedding layer or filter should be placed under the rockfill.

The Stephenson Method does not account for uplift of the stones due to emerging flow. This procedure was developed for flow over and through rockfill on steep slopes. Therefore, it is recommended that the Stephenson Method be applied as an embankment stabilization for overflow or sheetflow conditions. Alternative riprap rockfill design procedures should be considered for toe and stream bank stabilization.

3.3.3 U.S. Army Corps of Engineers Method

The U.S. Army Corps of Engineers has developed perhaps the most comprehensive methods and procedures for sizing riprap revetment. Their criteria are based on extensive field experience and practice (COE 1970; COE 1971). The U.S. Army Corps of Engineers Method is primarily applicable to embankment toe and bank protection and has been developed to protect the embankment from local shear forces and localized velocities.

The toe of a slope or embankment is generally subjected to the greatest concentration of erosive forces and therefore must be protected. The effective stone size, D_{50}, can be estimated after the depth of flow, D, is determined. The local boundary shear, $\bar{\tau}_o$ can be computed as

$$\bar{\tau}_o = \frac{\gamma_w V^2}{\left(32.6 \log_{10} \frac{12.2\ D}{k}\right)^2}, \tag{3.16}$$

where γ_w is the unit weight of water in pounds per cubic foot, V is the average cross-sectional velocity in feet per second, k is the equivalent channel boundary surface roughness in feet, and D is the depth of flow in feet. By substituting D_{50} for k, the local boundary shear at any point on the wetted perimeter can be determined. The design shear stress, τ_o, should be based on critical local velocities and shall serve as the design shear for the toe and channel bottom. A graphic solution to Eq. 3.16 is presented in Fig. 3.3.

The design shear for riprap placed on the channel slope or bank can be determined as

$$\tau_o = \tau \left[1 - \frac{\sin^2 \theta}{\sin^2 \phi}\right]^{0.5} \tag{3.17}$$

where

$$\tau = a(\gamma_s - \gamma_w)\ D_{50}, \tag{3.18}$$

as θ is the angle of the side slope with the horizontal, ϕ is the angle of repose of the riprap (normally about 40°), γ_s is the specific weight of surface-dry but saturated stone, and the value of a is 0.04. The side slope shear, τ_o, is the design shear for sizing the riprap revetment.

The average stone size can then be determined as

$$D_{50} = \frac{\tau}{0.04\ (\gamma_s - \gamma_w)} \tag{3.19}$$

for the toe and channel bottom and

$$D_{50} = \frac{\tau_o}{0.04\ (\gamma_s - \gamma_w)} \tag{3.20}$$

for the channel side slopes where γ_s and γ_w are the specific weights of the stone and water, respectively. The same procedure can be used for bank protection. A graphic representation of Eq. 3.19 is provided in Fig. 3.4.

The Corps of Engineers Method was developed for channelized flows. Therefore, this procedure should be used to evaluate and/or design rock protection for the portions of the cover or embankment

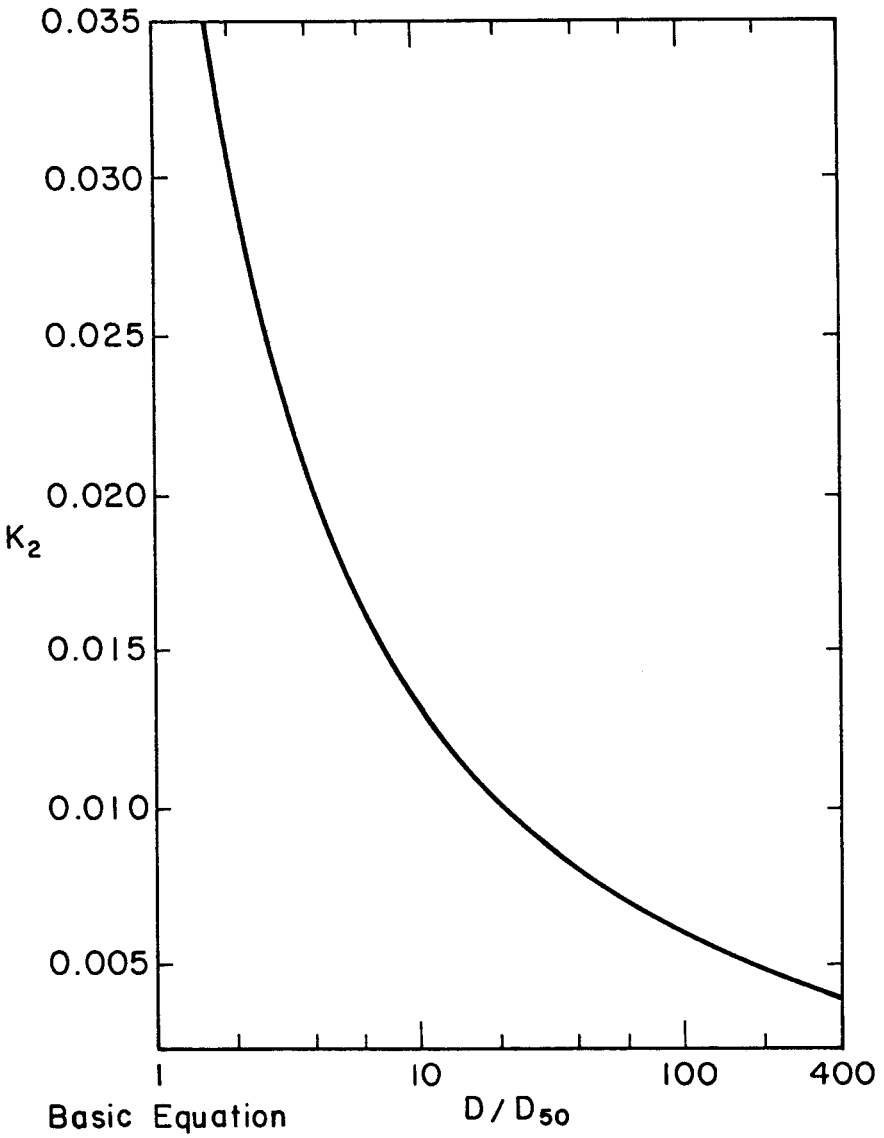

Basic Equation

$$\tau_0 = K_2 V^2$$

where

$$K_2 = \frac{\gamma_w}{\left[32.6 \log_{10}(12.2D/D_{50})\right]^2}$$

γ_w = Specific Weight of Water

D = Flow Depth

D_{50} = Theoretical Spherical Diameter of Average Stone Size

Figure 3.3. Graphical solution to Eq. 3.16. Source: Hydraulic Design of Flood Control Channels, EM 1110-2-1601, U.S. Army Corps of Engineers, July 1970.

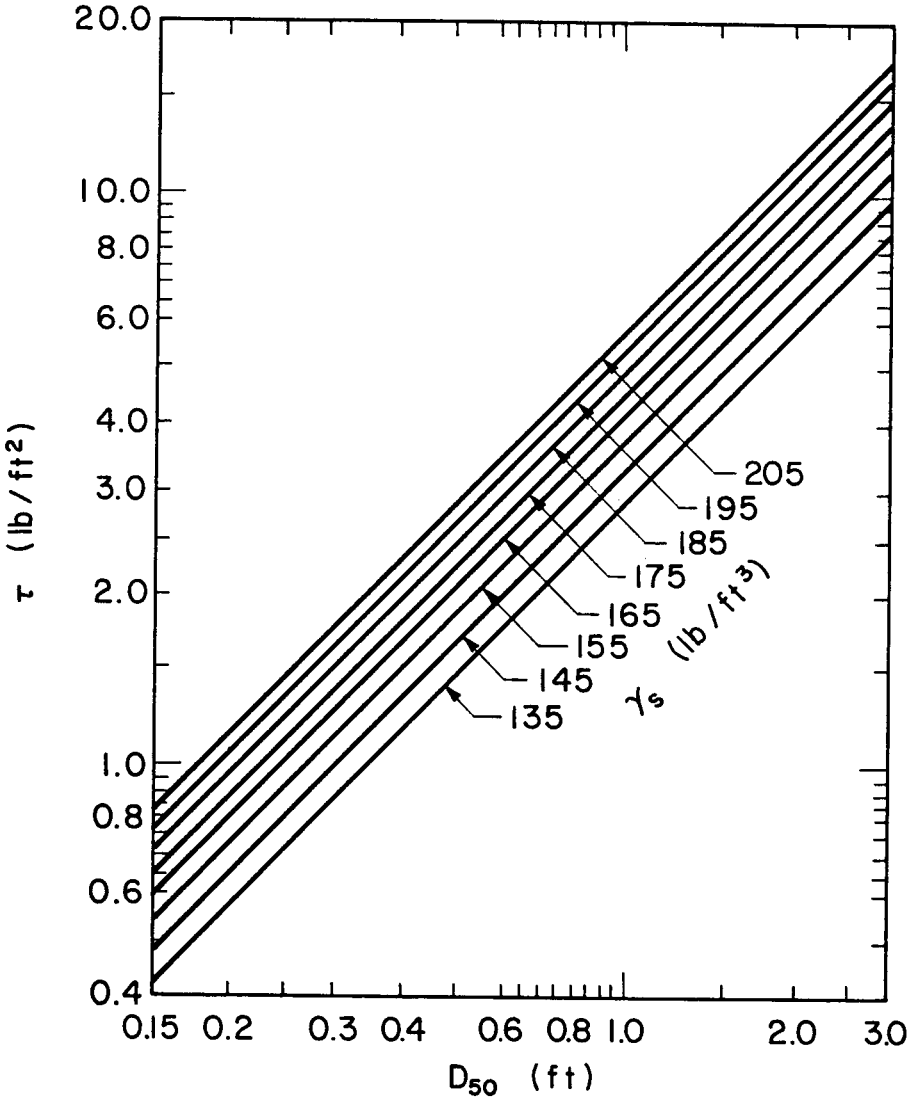

Basic Equation

$\tau = 0.040 (\gamma_s - \gamma_w) D_{50}$

where

τ = Design Shear Stress on Bottom of Channel

γ_s = Specific Weight of Stone

γ_w = Specific Weight of Water (62.4 lb/ft³)

D_{50} = Theoretical Spherical Diameter of Average Size Stone

Figure 3.4. Sizing of riprap as a function of design shear stress. Source: Engineering and Design, Additional Guidance for Riprap Channel Protection, ETL-1110-2-120, Office of the Chief of Engineers, U.S. Army Corps of Engineers, May 1971.

that are in the floodplain. This method is ideal for stabilizing cover and embankment toes.

3.3.4 U.S. Bureau of Reclamation Method

The U.S. Bureau of Reclamation (USBR) Method (DOI 1978) for riprap design was developed for the prevention of damage in and near stilling basins. The USBR procedure is empirically based upon extensive laboratory testing and field observations. Riprap failure was determined to occur because alternative design procedures underestimate the required stone size in highly turbulent zones, and there is a tendency for inplace riprap to be smaller and more stratified than specified. The USBR method is a velocity-based design procedure.

The USBR method estimates the maximum stone size, D_{100}, as a function of the localized bottom velocity of flow, V_b, in feet per second. One means of predicting the maximum stone size is by the Mavis and Laushey (1948) procedure:

$$D_{100} = \left[\frac{V_b}{0.5\ (G_s - 1)^{0.5}} \right]^2 , \qquad (3.21)$$

where D_{100} is the maximum stone size in millimeters and G_s is the particle specific gravity. If the bottom velocity cannot be determined, local velocity may be substituted to size the rock. The local velocity can be determined by U.S. Army Corps of Engineers methods (COE 1970).

The stone size and stone weight can be determined from Fig. 3.5 for a given bottom velocity, V_b. The resulting stone size is conservative. The riprap should be composed of a well-graded mixture of stone. Riprap should be placed on a filter blanket or bedding layer. The riprap layer should be 1.5 times the thickness of the largest stone diameter. The filter blanket should be at least 6 in. thick.

It is recommended that the USBR Method be considered for only the design of rock along the toe of the slope or where flow concentrations require substantial energy dissipation. This method would be well suited in areas where a hydraulic jump may occur. The USBR Method is not necessarily recommended for bank and cover protection, because of its conservatism.

3.3.5 Summary

It is apparent that design procedures exist that adequately size riprap layers for protecting low-gradient channel beds and banks, energy dissipation and impact basins, and steep embankments. However, these procedures fail to address other components of the riprap design process (e.g., layer thickness, effects of rounded rock, and effects of rock gradation).

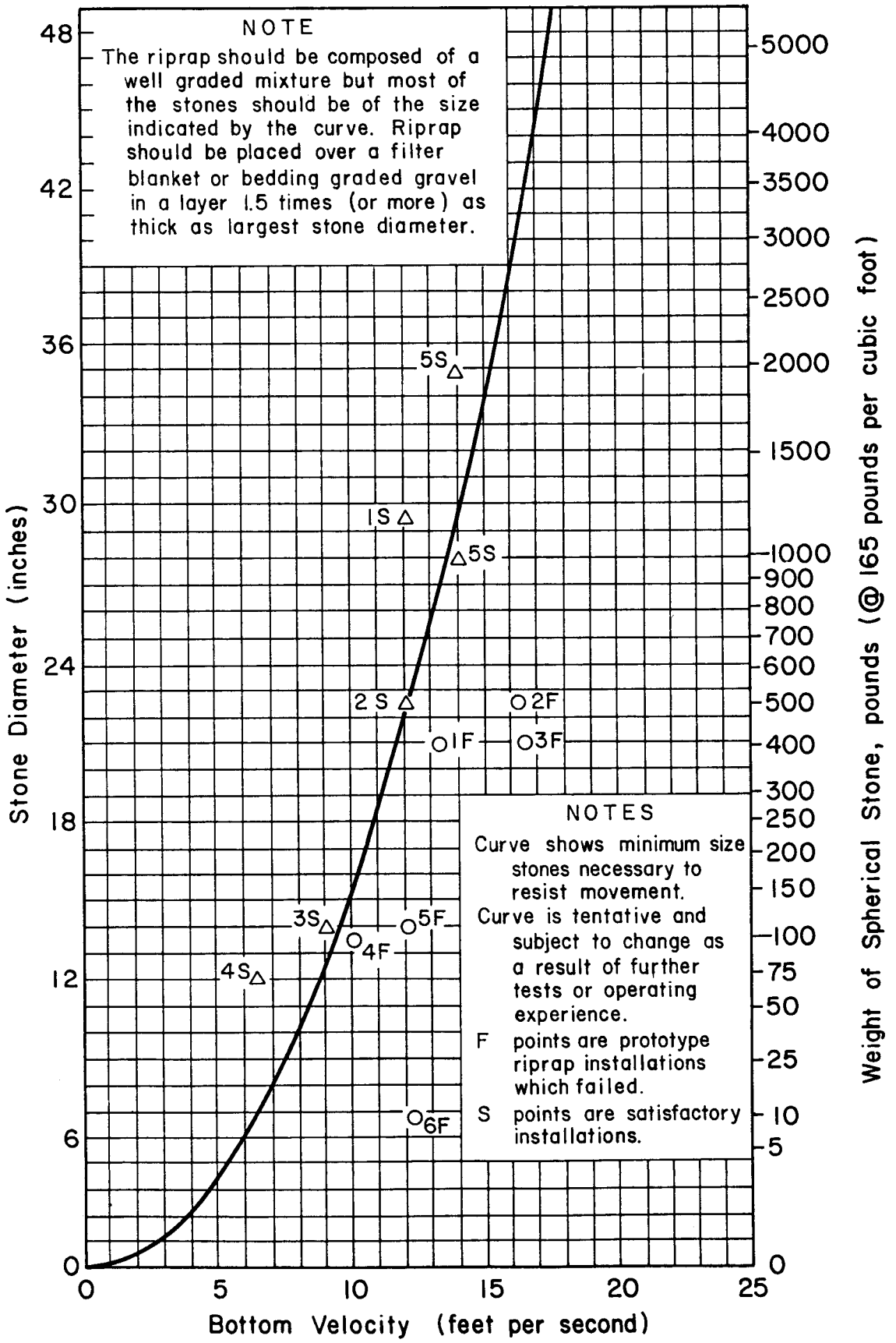

Figure 3.5. Parametric curve used to determine maximum stone size in riprap mixture as a function of channel bottom velocity.

3.4 ESTABLISHED PROCEDURES TO ESTIMATE RESISTANCE TO FLOW

The estimation of flow resistance in steep, armored channels has long been an art of the practicing hydraulic engineer. The Manning's roughness coefficient, n, is perhaps the most commonly used means of expressing flow resistance. The Manning's roughness coefficient has been shown to be a function of surface roughness, vegetation, channel irregularity, channel alignment, channel shape, and flow depth (Chow 1959). Also, the resistance to flow is affected by the stone shape and size in gravel and cobble bed channels (Barnes 1967).

Several procedures are used to determine the resistance to flow by the Manning's roughness coefficient. These procedures were derived from data obtained in gravel, rock and cobble bed, and natural streams. Six frequently cited procedures for determining resistance to flow are:

1. Limerinos (1970),
2. Strickler (1923),
3. Anderson, Paintal and Davenport (1970),
4. Jarrett (1984),
5. Bathurst (1985), and
6. U.S. Army Corps of Engineers (COE 1970).

Each procedure is summarized below.

3.4.1 Limerinos' Procedure

Limerinos (1970) collected data in California gravel-bed rivers to develop an equation to estimate Manning's roughness coefficient. His analysis yielded the expression:

$$n = \frac{0.113\ D^{1/6}}{1.16 + 2.00 \log \left(\frac{D}{D_{84}}\right)}, \tag{3.22}$$

where D is the mean flow depth in meters and D_{84} is the characteristic bed material size for the reach in meters. Limerinos related flow resistance to the relative submergence, D/D_{84}.

3.4.2 Strickler Procedure

Strickler (1923) proposed a formula for determining the Manning coefficient as only a function of a characteristic bed material. His expression is

$$n = a\ (D_{90})^{1/6}, \tag{3.23}$$

where D_{90} is in feet. The coefficient, a, ranges from 0.0385 to 0.041. Although the Strickler equation was derived for low-gradient, natural channels, it is commonly used indiscriminately. The Strickler expression should be used only where channel slopes are less than 2% and a high, in-bank flow condition exists.

3.4.3 Anderson, Paintal, and Davenport Procedure

Anderson et al. (1970), using data from natural rivers, also proposed a formula for determining the Manning coefficient on the basis of particle size as

$$n = 0.0395\ (D_{50})^{1/6}, \tag{3.24}$$

where D_{50} is in feet. The channel slope in the Anderson et al. experiments was less than 2%, and the relative roughness was small; and the expression is independent of slope and depth of flow.

3.4.4 Jarrett Procedure

Jarrett (1984) performed several on-site surveys by making 75 discharge measurements on 21 streams having slopes greater than 0.2%, with the purpose of estimating the Manning roughness coefficient, n, as well as to provide the hydraulic data on the streams. From the data, Jarrett developed an equation for predicting Manning's n in natural channels expressed as

$$n = 0.39\ S^{0.38}\ R^{-0.16}, \tag{3.25}$$

where S is the stream gradient (channel slope) and R is the hydraulic radius. He concluded that n varies directly with slope, n varies inversely with depth, and streams thought to be in the supercritical flow range were often in the subcritical flow range because of the high resistance to flow.

3.4.5 Bathurst Procedure

Bathurst (1985) studied the flow resistance of gravel and boulder-bed rivers with slopes ranging from 0.4 to 4.0%. On many sites, boulders protruded through the surface and inhibited flow. Bathurst performed an empirical analysis relating the flow resistance to the relative submergence, D/D_{84}, resulting in the expression:

$$\left(\frac{8}{f}\right)^{1/2} = 5.62\ \log\left(\frac{D}{D_{84}}\right) + 4\ , \tag{3.26}$$

where f is the Darcy-Weisbach friction factor. The relative submergence values ranged from 0.43 to 7.10.

3.4.6 U.S. Army Corps of Engineers Procedure

The U.S. Army Corps of Engineers (COE 1970) presented a procedure for estimating the Manning's n developed for low-gradient, deep-channeled flows. The generalized equation is expressed as

$$n = \frac{R^{1/6}}{23.85 + 21.95\ \log_{10}\left(\frac{R}{k}\right)} \tag{3.27}$$

where n is the Manning's roughness coefficient, R is the hydraulic radius in feet, and k is the equivalent roughness height in feet.

Equivalent roughness, k, for a stone-lined channel may be referenced to the theoretical spherical diameter of the median stone size, D_{50}. The effective height of the irregularities forming the roughness elements is called the roughness height. Values of k for natural rivers range between 0.1 and 3.0 (COE 1970).

3.4.7 Summary

Recent studies indicate that the depth of flow, characteristic boundary roughness, and channel slope influence the resistance to flow, as often expressed by the Manning's roughness coefficient. Further, it is apparent that the resistance to flow may greatly vary, depending upon the field conditions from which the procedure was derived. The procedures cited were derived from natural streams with bed materials containing predominately rounded stones and cobbles.

4. ROCK FAILURE AND ROCK MOVEMENT RELATIONSHIPS

The results of the Phase II riprap testing program were used to verify the findings of the Phase I riprap testing report (Abt et al. 1987) and to extend the current design guidelines for the long-term protection of uranium tailings impoundments. The tests performed in Phase II extended the existing data base relative to riprap failure criteria and rock movement criteria. Data were also obtained to provide stone shape, riprap gradation and riprap layer thickness criteria. Data acquisition and analysis were similar to and consistent with procedures used in the Phase I report.

Rock movement and failure criteria determined in Phase I testing were also used throughout the Phase II test program. Rock movement was observed during each test at two distinct times. First, rock movement occurred for only a few seconds when flow commenced or when the flow was incrementally increased. This movement consisted of settling of the riprap layer or slight movement of individual stones to a more stable position. Second, incipient movement of the stones occurred when the forces exerted by the channel flow just overcame the resistance force of a stone to motion. Individual stones would initiate movement by rolling over the rock layer.

The criterion for incipient failure of the riprap layer was visual observation of exposed filter blanket, or more often, geofabric. In many cases, concentrated flows would remove riprap from a localized zone along the embankment. However, rock movement from upslope would subsequently fill and stabilize the scoured area. When rock movement could no longer adequately replace the material in the scoured area, failure was observed. Catastrophic failure occasionally occurred prior to filter cloth exposure because of the dynamic rock movement along the bed and because of poor conditions for observing the filter blanket resulting from the significant turbulence, bubbles, and air entrainment in the cascading flows.

A series of 17 tests was conducted in which rock movement or rock failure were recorded. Riprap failure occurred during 15 of the 17 tests. A summary of the Phase II test parameters and remarks that will be used for the data analysis is presented in Table 4.1. Complete test results are presented in Appendix B and Appendix C. Because the results of both Phase I and Phase II will be incorporated in the analysis of failure relationships, the failure data of both test series will be combined wherever possible.

4.1 FAILURE RELATIONSHIPS OF ANGULAR ROCK

Failure relationships were determined for angular and rounded stone shapes placed on 10 and 20% slopes. Tests were also conducted to analyze the stability of an angular-shaped, riprap layer with respect to riprap gradation, riprap layer thickness, and riprap flow resistance.

Table 4.1. Summary of failure tests[a]

Test number	Median stone size D_{50} (in.)	Stone shape	Riprap Thickness[b] (in.)	Slope	Q (cfs)	q_f (cfs/ft)	Remarks
20	4.00	ROUNDED	12.00	0.20	8.65	0.72	Rock movement observed
21	4.00	ROUNDED	12.00	0.20	11.38	0.95	Complete slope failure
22	4.00	ROUNDED	12.00	0.20	11.12	0.95	Complete slope failure
24	4.00	ANGULAR	12.00	0.20	1.28	0.11	Test stopped on request of NRC[c]
27	2.00	ANGULAR	3.00	0.10	9.21	0.77	Complete slope failure
29	2.00	ANGULAR	4.00	0.10	10.21	0.85	Complete slope failure
31	2.00	ANGULAR	6.00	0.10	11.99	1.00	Complete slope failure
32	2.00	ANGULAR	6.00	0.10	13.32	1.11	Complete slope failure
34	2.00	ANGULAR	8.00	0.10	14.80	1.23	Complete slope failure
36	4.00	ROUNDED	6.00	0.10	23.84	1.99	Complete slope failure
38	4.00	ROUNDED	12.00	0.10	25.11	2.09	Complete slope failure
40	4.00	ANGULAR	6.00	0.10	40.80	3.40	Complete slope failure
42	4.00	ANGULAR	8.00	0.10	42.13	3.51	Complete slope failure
44	4.00	ANGULAR	12.00	0.10	45.45	3.79	Complete slope failure
46	2.00	ROUNDED	6.00	0.10	8.27	0.69	Complete slope failure
48	4.00	ANGULAR	12.00	0.10	28.93	2.41	Complete slope failure
51	4.00	ANGULAR	12.00	0.10	49.41	4.12	Complete slope failure

[a]All tests were conducted without tailwater and with a filter blanket thickness of 6 in.

[b]All riprap was dump-placed.

[c]NRC = Nuclear Regulatory Commission.

4.1.1 Phase II Data

Four of the Phase II failure tests were conducted to verify model-prototype similarities between Phase I and Phase II test results. Because many of the Phase I tests were conducted in an indoor flume with a shortened model embankment, it was important to correlate the indoor model embankment results to the outdoor prototype embankment results. Therefore, some Phase II tests were used to check experiment repeatability.

All four failure tests (Nos. 31, 32, 44, and 51) were conducted in the outdoor flume on an embankment with a 10% slope and riprap layer thickness of three times D_{50} (2- and 4-in. median rock sizes).

In Fig. 4.1, the Phase I and Phase II results are presented. It is seen that the results of the Phase II experiments closely agree with the results and predicted relation at failure presented in the Phase I report for the 10% embankment. Therefore, it was concluded that test repeatability and model-prototype similarity was achieved.

4.1.2 Composite Failure Relationship

In the Phase I tests involving median rock sizes of 1 to 6 in., layer thicknesses of two to three times D_{50}, and embankment slopes ranging from 1 to 20%, a family of curves exists that relates unit discharge at failure to the median rock size (Fig. 4.1). Because the failure relationships are parallel and slope dependent, a regression analysis of the Phase I and Phase II data resulted in a composite relationship as presented in Fig. 4.2. A power regression was performed on the parametric expression relating the median stone size, D_{50}, to the embankment slope, S, and unit discharge at failure, q_f. The results are expressed as:

$$D_{50} = 5.23\ S^{0.43}\ q_f^{0.56} \tag{4.1}$$

Based upon the test parameters previously described, Eq. 4.1 should not be used for D_{50} greater than 6 in., for rounded rock, or for slopes greater than 20%. Application of Eq. 4.1 beyond the limits prescribed would be strictly at the users' risk.

4.2 RESISTANCE TO FLOW

The resistance to flow, expressed as the Manning's roughness coefficient, significantly impacts channel design procedures used by the practicing engineer. The Phase I report presented an alternative procedure for estimating the Manning's n value for riprap-lined channels or embankment faces where roughness is a function of the median stone size and the slope, as presented in Eq. 1.2.

4.2.1 Computation of Manning's n Value

The riprap resistance to flow over the riprap surface was estimated for each of the ten failure test conditions summarized in Table 4.2. Each value presented in Table 4.2 is the average of the

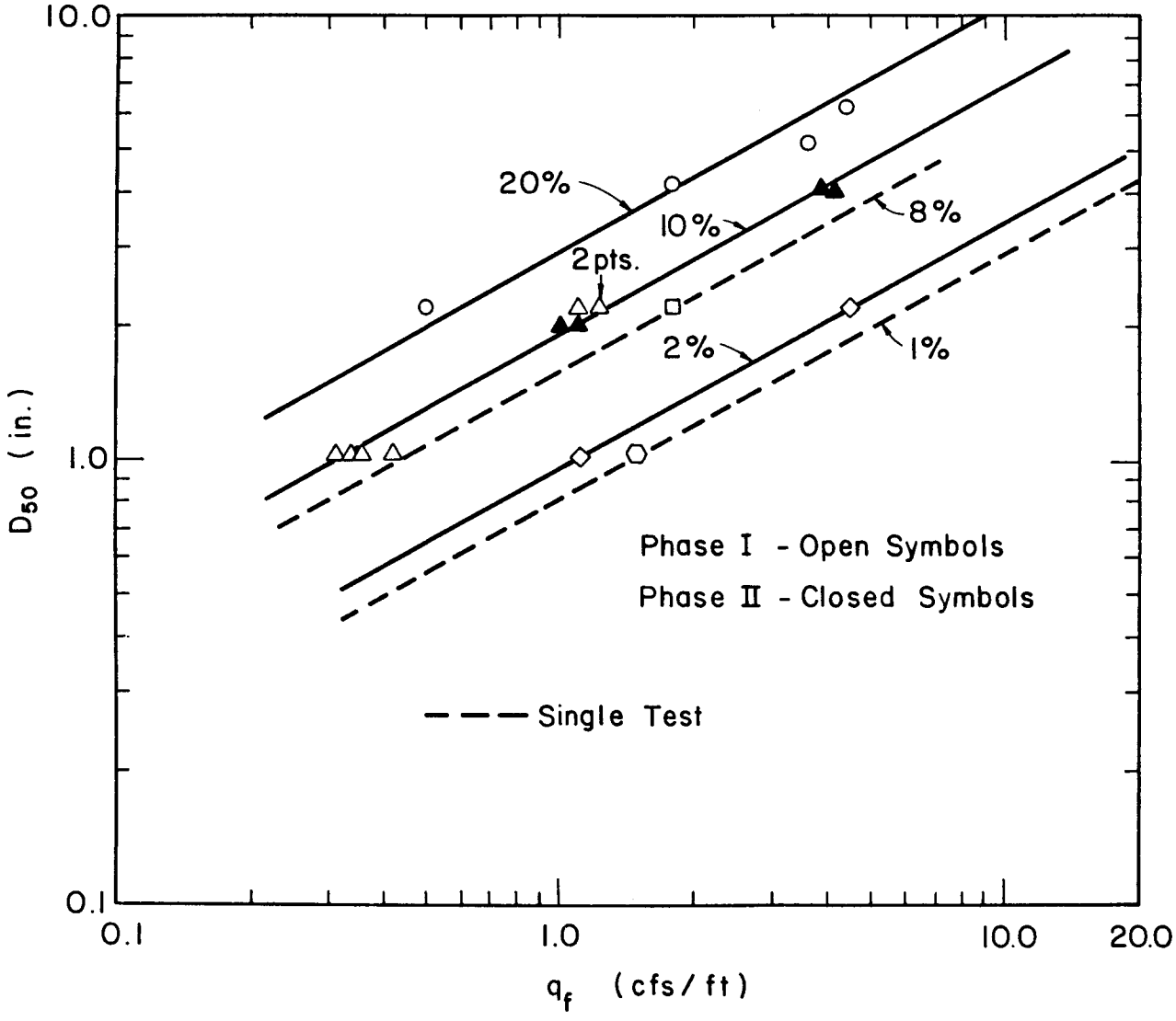

Figure 4.1. Comparison of unit discharge and median stone size relationship at failure for Phase II tests with Phase I tests at 10% slope.

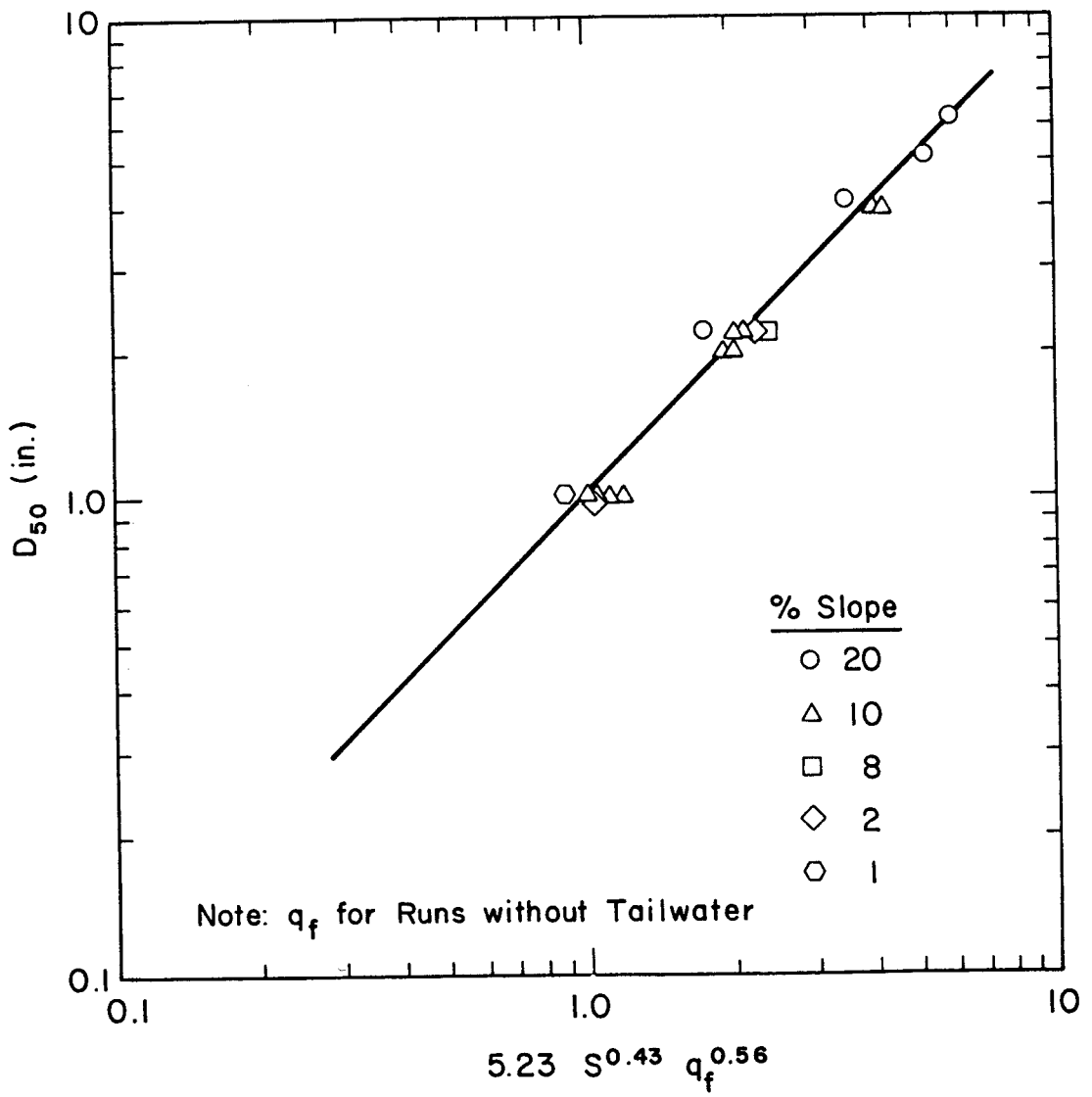

Figure 4.2. Consolidated relationship for riprap failure.

Table 4.2. Summary of average Manning's n for Phase II data[a]

Test run	Median stone size D_{50} (in.)	Riprap thickness (in.)	$\frac{D}{D_{50}}$	Number of data points[b]	n[c]
27	2.0	3.0	1.02	10	0.038
29	2.0	4.0	1.50	11	0.059
31	2.0	6.0	1.18	18	0.029
32	2.0	6.0	1.47	13	0.044
34	2.0	8.0	1.56	35	0.049
40	4.0	6.0	1.66	20	0.061
42	4.0	8.0	1.70	33	0.046
44	4.0	12.0	1.54	30	0.050
48	4.0	12.0	1.32	26	0.058
51	4.0	12.0	1.59	24	0.045

[a]All tests were conducted on a 10% channel slope.

[b]Number of data observations from which the n is derived.

[c]Colorado State University value.

individual data sets collected for each test prior to riprap layer failure. For example, ten n values, ranging from 0.032 to 0.044, were determined from the data collected in test 27. The average n value for test 27 is 0.038, as presented in Table 4.2. These average values better indicate data trends than do the individual data points from which these averages were derived. The individual data sets are presented in Appendix C.

In the analysis, the Manning's roughness coefficient, n, the bed Shields' coefficient, C_c , and the Darcy-Weisbach friction factor, f, were computed by the equations presented in Chapter 3. Because the Manning's, Shields', and Darcy-Weisbach coefficients are interrelated, the analysis concentrates on the Manning's roughness coefficient.

The Manning's roughness value is difficult to determine for riprap in cascading flow situations. The Manning's roughness coefficient, n, was expressed in Eq. 3.2 as a function of the surface discharge, the depth of flow in a wide channel, the embankment or channel slope, and the cross-sectional area of flow. Other factors that affect Manning's roughness coefficient include surface roughness, channel irregularity, channel alignment, flow depth, silting and scouring, obstructions, and channel shape. Chow (1959) and Barnes (1967) present a comprehensive list of n values for open-channel flow applications. Manning's n values commonly range from 0.017 for smooth channels to 0.07 for cobble bed streams.

The Manning's n value for the 2-in. rock ranged from 0.029 to 0.059 for the test runs presented in Table 4.2. The average n value of the five 2-in. tests is 0.044. The Manning's n values for the 4-in. rock ranged from 0.045 to 0.058, yielding an average n value of 0.052. The average n value for the 2- and 4-in. median stone sizes varies about the mean by approximately 34 and 12%, respectively. The n values presented are derived for supercritical flow conditions.

The flow depth/median stone size ratio (D/D_{50}) is presented in Table 4.2 for each of the ten tests in which the Manning's n value was estimated. The D/D_{50} values ranged from 1.02 to 1.70. The high resistance to flow in conjunction with the low-flow-depth/median-stone-size ratio indicates extensive separation and air entrainment over the riprap surface.

4.2.2 Comparison of Phase I and Phase II Manning's n Values

Four failure tests were conducted in Phase II, (Nos. 31, 32, 44, and 48) in which the riprap layer thickness, rock gradation, and angular shape were similar to the Phase I tests. The computed Manning's n values for these four tests are plotted with the Phase I results in Fig. 4.3. It is evident that the Phase II results are generally higher than the Phase I results by as much as 40%. The Phase II data indicate that the Phase I relationship may not necessarily be conservative.

The increase in Manning's n in Phase II may be attributed to differences between the Phase I and Phase II test conditions. During

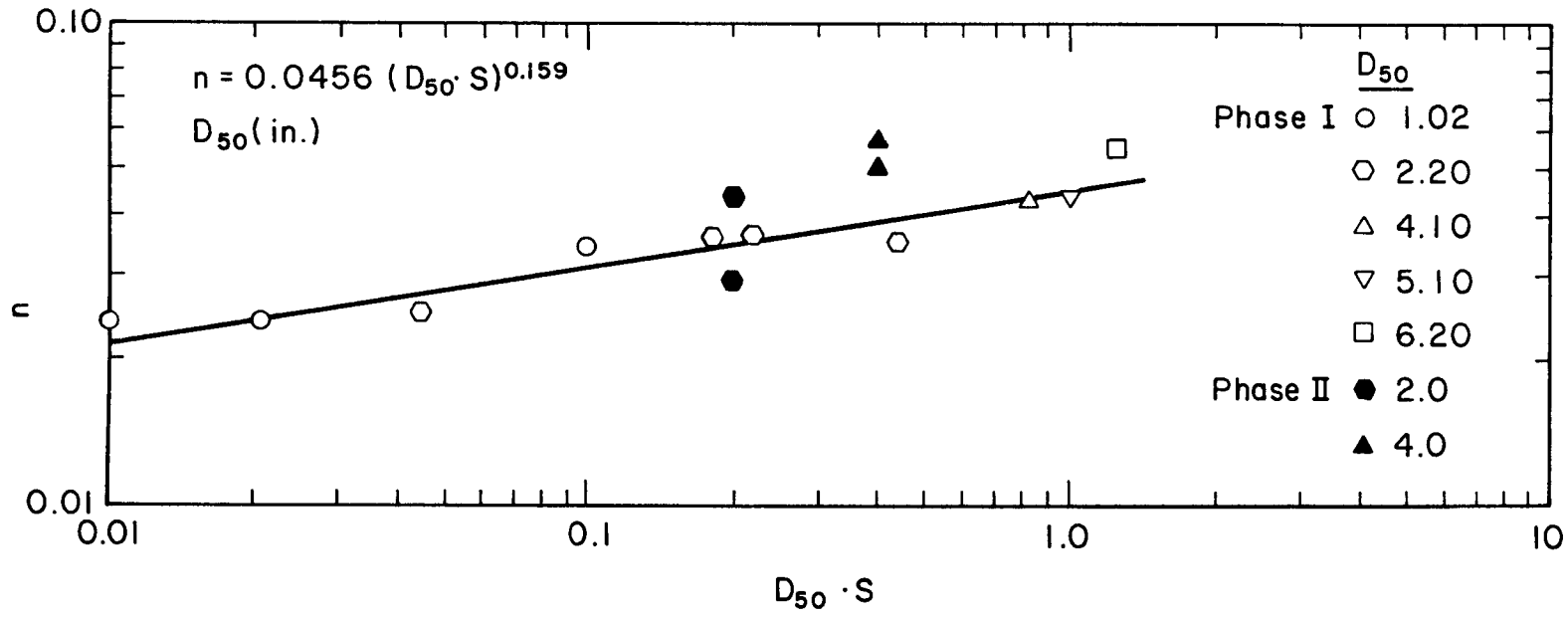

Figure 4.3. Median stone size/slope parameter vs Manning's n.

Phase I, the 10% slope failure tests were conducted in the indoor flume. Water surface measurements were obtained with a point gage in turbulent flow. Slight differences in recording the depth of flow were found to significantly affect the resulting n values. A series of piezometers was used in Phase II to collect water surface elevations. The variability of the piezometers was greater than the point gage in the indoor tests. The scatter of data is due, in part, to the inability of the instrumentation to record highly accurate readings in turbulent flow.

The resistance to flow relationship presented in Fig. 4.3 may underestimate the actual resistance to flow in a riprap-lined channel or embankment face. However, Eq. 1.2 provides an improved means of estimating the resistance to flow over procedures presented in Chapter 3. The n values resulting from the Phase II experiments are currently insufficient to modify the relationship presented in Fig. 4.3. However, the Phase II results indicate that the n value estimation expression presented in the Phase I report may not be as conservative as originally anticipated.

4.3 RIPRAP GRADATION EFFECT ON RIPRAP STABILITY

One criterion for riprap design that has not been investigated yet, which may impact rock stability, is the riprap layer gradation for overtopping flow conditions. Segregation during stock piling, movement, and placement operations make it difficult to monitor and maintain a uniform gradation throughout the riprap layer. However, failure to maintain a uniform gradation during placement operations may reduce layer stability.

Existing gradation criteria have been developed for stable channel and coastal protection conditions. Simons and Senturk (1977) recommended that the gradation of stone riprap follow a smooth size distribution, have a maximum size to median size ratio of about 2.0, and have a median size to 20% size ratio of about 2.0. They suggest that a gradation with a coefficient of uniformity, C_u, of approximately 2.5 should be sufficient to provide erosion protection.

The U.S. Army Corps of Engineers (COE 1970) recommended that stones should be well graded throughout the in-place layer. The Corps of Engineers' criteria for gradation stipulate that the largest stone should not be less than two times the median stone and should not exceed five times the median stone. The Corps of Engineers' upper limit coefficient of uniformity is approximately 1.75. The Corps of Engineers identifies riprap by weight and not by rock size.

The Federal Highway Administration (Richardson et al. 1975) and the California Division of Highways (CDH 1970) also have general gradation guidelines. The recommended upper limit gradation curves for the Federal Highway Administration and the California Department of Transportation have coefficients of uniformity of approximately 2.7 and 1.1, respectively.

Although standards for riprap gradation exist, the differences in these standards are substantial. For example, the coefficients of uniformity for the procedures cited range from approximately 1.1 to 2.7. The effects of gradation upon riprap stability remains unknown.

4.3.1 Failure Relationship

In an attempt to evaluate gradation effects on riprap layer stability, three Phase II failure tests were conducted, (Nos. 44, 48, and 51) in which the median stone size, D_{50} = 4.0 in.; embankment slope, S = 10%; riprap layer thickness, t_r = 12 in.; and stone shape, angular; were held constant. Rock gradation, expressed as the coefficient of uniformity, was the only variable modified in all three tests. The gradation curves of the riprap layers tested are presented in Fig. 4.4. The coefficients of uniformity tested ranged from 1.72 to 4.0.

The unit discharges at failure for the coefficients of uniformity of 1.72, 2.30, and 4.0 are 4.12, 3.79, and 2.41 cfs, respectively. The unit discharges at failure were correlated to the coefficients of uniformity as presented in Fig. 4.5. The resulting relationship indicates that gradation significantly impacts the riprap stability for the rock size, layer thickness, and slope tested. The increase in coefficient of uniformity from 1.72 to 4.0 reduced the unit discharge at failure by about 40%.

The sizing of riprap for overtopping conditions should account for the variability in rock gradation to maintain a stable riprap layer. Therefore, a gradation coefficient, C_{GR}, was derived from the data in Fig. 4.5 by relating the coefficient of uniformity to the variation of stability as indicated by the unit discharge at failure. A coefficient of uniformity of 2.3 was related to the gradation coefficient of 1.0, as shown in Fig. 4.6, to maintain consistency with the gradation standards presented by the U.S. Army corps of Engineers (COE 1970). Multiplying the riprap median stone size by the gradation coefficient yields an adjusted D_{50} that will maintain the desired level of riprap layer stability.

In general, the more uniform the gradation, the more resistant the rock layer to overtopping flow. Although the results portrayed in Fig. 4.5 are limited, the relationship in Fig. 4.6 provides a means for adjusting the median stone size to maintain a stable riprap layer.

4.4 RIPRAP LAYER THICKNESS

The riprap layer thickness has traditionally been expressed in terms of the median stone size, D_{50}. For example, the U.S. Army Corps of Engineers (COE 1970) channel protection guidelines indicate that the riprap layer should not be less than the spherical diameter of the upper limit size stone or less than 1.5 times the spherical diameter of the median stone size, whichever is greater. Because the procedure was developed for protecting channel beds and banks, the riprap layer should not be less than 12 in. thick. When riprap is placed underwater, the layer thickness should be increased by 50% to account

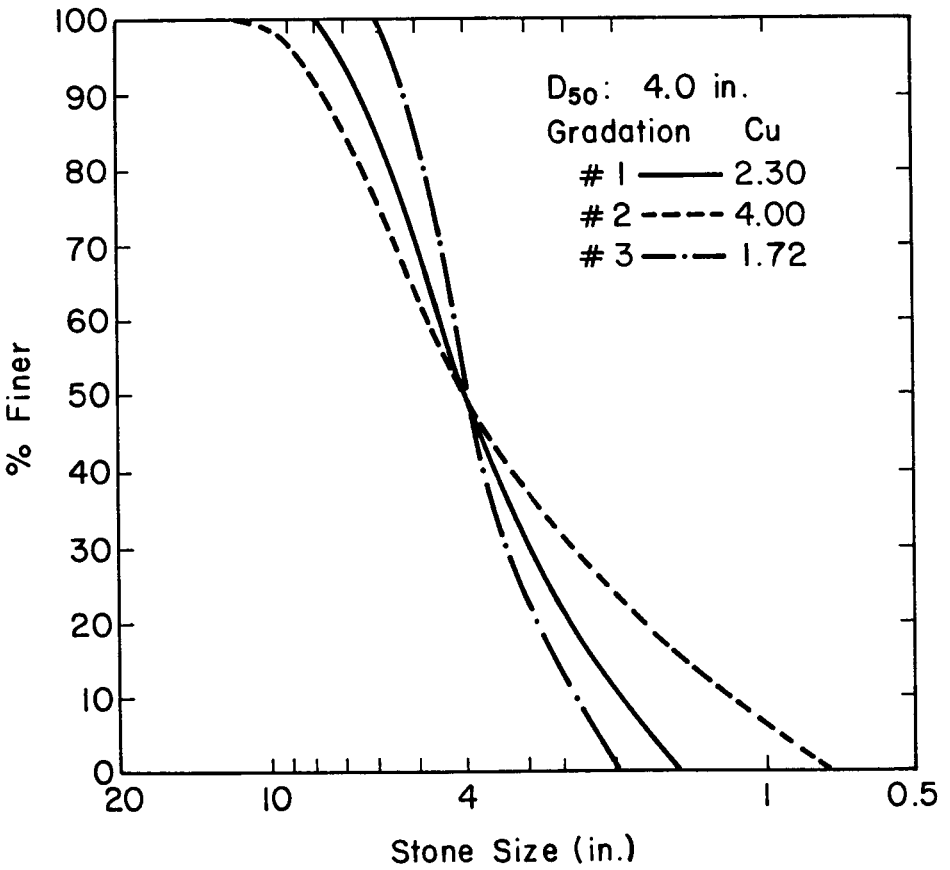

Figure 4.4. Gradation curve.

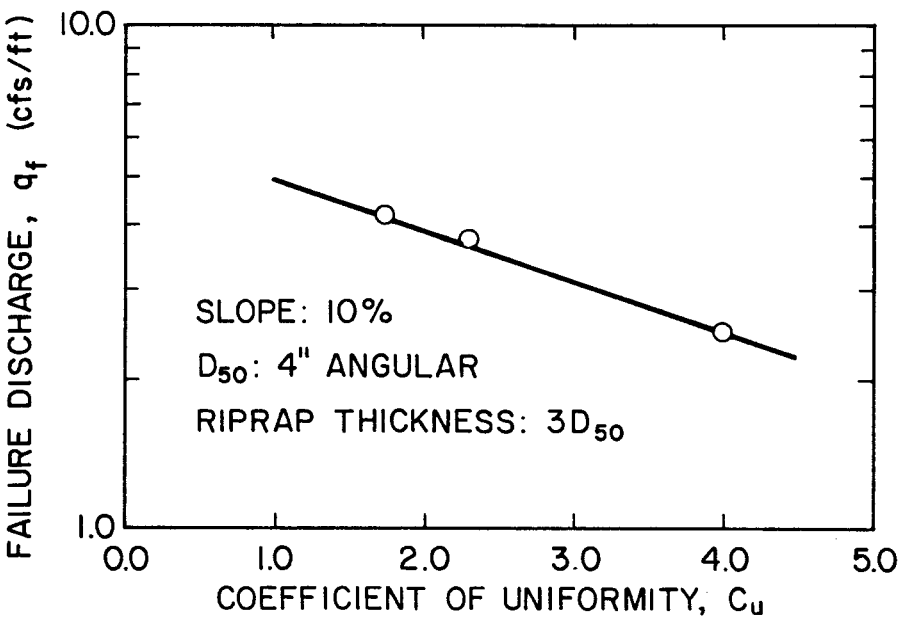

Figure 4.5. Unit discharge at failure vs riprap layer coefficient of uniformity.

Figure 4.6. Relating the coefficient of rock gradation to the coefficient of uniformity.

for uncertainties associated with placement. Further, should riprap be subjected to large floating debris or to wave action, it is advised that the stone size be increased and that the riprap thickness be increased by 6 to 12 in.

The California Department of Transportation (CDH 1970) has developed a procedure for determining riprap layer thickness for the protection of embankments along streams and rivers. The riprap thickness criterion is based on the orientation, side slope, stone shape, and class of stone. The general expression for estimating the riprap layer thickness is

$$T_r = C_p \, K_s \sin \theta \, \sqrt[3]{W_c} \tag{4.2}$$

where t_r is the riprap thickness normal to the face slope, K is the shape factor of stone (commonly 0.40), θ is the side slope angle, W_c is the class weight of stone, and C_p is a coefficient representing machine placement or dump placement, and ranges from 1.5 to 1.875, respectively. It is recommended that the thickness, t_r, be 1.5 times the long axis of the critical stones.

Simons and Senturk (1977) indicated that the thickness of riprap should be sufficient to accommodate the largest stones in the riprap. Further, for a well-graded riprap without voids, a layer thickness equal to the largest stone should be adequate. When strong wave action is of concern, the thickness should be increased by 50%.

The American Society of Civil Engineers Task Committee (Vanoni 1975) recommended that a blanket revetment on river banks should be characterized by a graded material placed such that all voids are filled and all rocks are keyed into the mass. The maximum rock size is limited to about 1-1/2 times the median rock size. Minimum riprap thickness should be 1-1/2 times the median rock size.

Stephenson (1979) developed a procedure for estimating the thickness of the riprap layer sufficient to resist potential high velocities from overtopping flows on rock protected embankments. It was reasoned that the stone thickness must be great enough to resist the sliding between adjacent stone layers. Stephenson equated the friction drag per unit area to the shear resistance and solved for the minimum lining or layer thickness. The minimum layer thickness, t_r, was expressed as

$$t_r = \frac{R \, i}{(G_S - 1)(n_p + 1) \cos \theta \, (\tan^2 \phi - \tan^2 \theta)^{1/2}} \tag{4.3}$$

where ϕ is the angle of friction, θ is the angle of bank slope from horizontal, R is the hydraulic radius, i is the head loss gradient, G_s is the specific gravity of the material, and n_p is the porosity of the rock fill.

On the basis of Stephenson's experimental data, the layer thickness criterion was expressed as

$$t_r \simeq 1.5\ D_s, \tag{4.4}$$

where D_s is the stable stone size. It was noted that the relationship expressed in Eq. 4.4 rarely controls the layer thickness.

4.4.1 Failure Trends

Eight failure tests were designed and conducted in Phase II to evaluate the rock layer stability as a function of the riprap layer thickness. The 2- and 4-in. median stone sizes were tested on a 10% slope. The riprap layers had coefficients of uniformity ranging from 2.14 to 2.30. Each riprap layer was subjected to an overtopping flow until the riprap failed. The riprap layer thicknesses were correlated to the unit discharge at failure for each median stone size, as presented in Fig. 4.7.

It was observed that the unit discharge required to fail the rock layer increased as the rock layer thickness increased. For 2-in. rock, an increase in riprap thickness from 1.5 to 4.0 D_{50} increased the layer stability by approximately 60%. For 4-in. rock, an 11% increase in stability is observed by increasing the riprap layer thickness from 1.5 to 3 D_{50}. The riprap layer was enhanced as the weight of the additional stone layer compressed and wedged the lower stone layer(s). The stone weight, in conjunction with the vibration of the flow, transformed the lower riprap layer into an armored condition.

The increase in riprap-layer stability with increase in rock-layer thickness appears to be dependent upon the median stone size. As the median stone size increases, the need for a thickened riprap layer decreases. With median stone sizes of < 6 in., a riprap layer thickness beyond the traditional 1.5 times the median stone size is warranted. However, when the median stone size is > 6 in., the traditional guideline of 1.5 times the median stone size is prudent.

4.4.2 Layer Thickness Adjustment

The thickening of the riprap layer for median stone sizes < 6 in. was shown (in Section 4.4.1) to increase the layer stability. In instances where small riprap sizes are warranted (< 6 in.), the design riprap layer thickness should be adjusted to maintain the riprap stabilty. A coefficient of layer thickness, C_t, is needed to adjust the median stone size and compensate for the riprap layer thickness. Figure 4.8 presents the coefficient of layer thickness as a function of the design riprap layer thickness. The relation in Fig. 4.8 was derived from the Phase II failure tests for 2-in. riprap on a 10% slope. A riprap layer thickness of 3.0 D_{50} corresponds to a coefficient of layer thickness equal to 1.0.

The coefficient of layer thickness is used as follows. The design riprap layer thickness is determined by one of the procedures

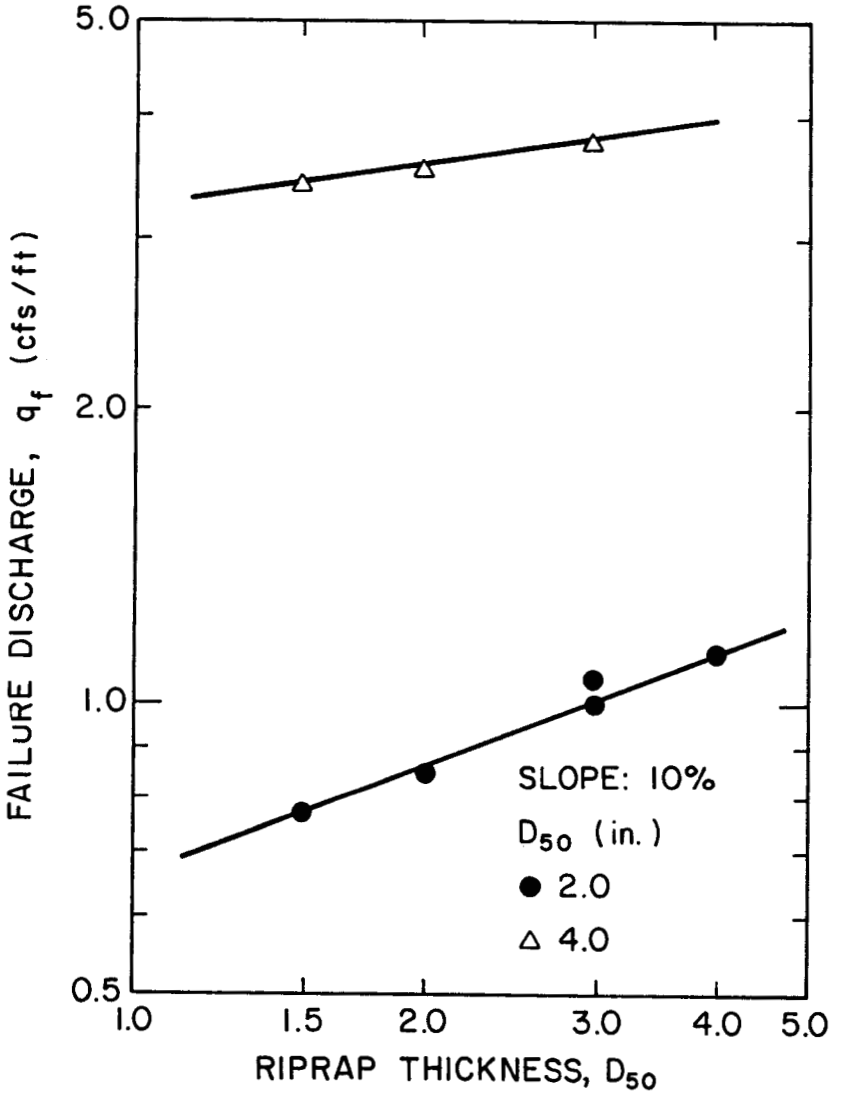

Figure 4.7. Riprap layer stability as a function of median stone size.

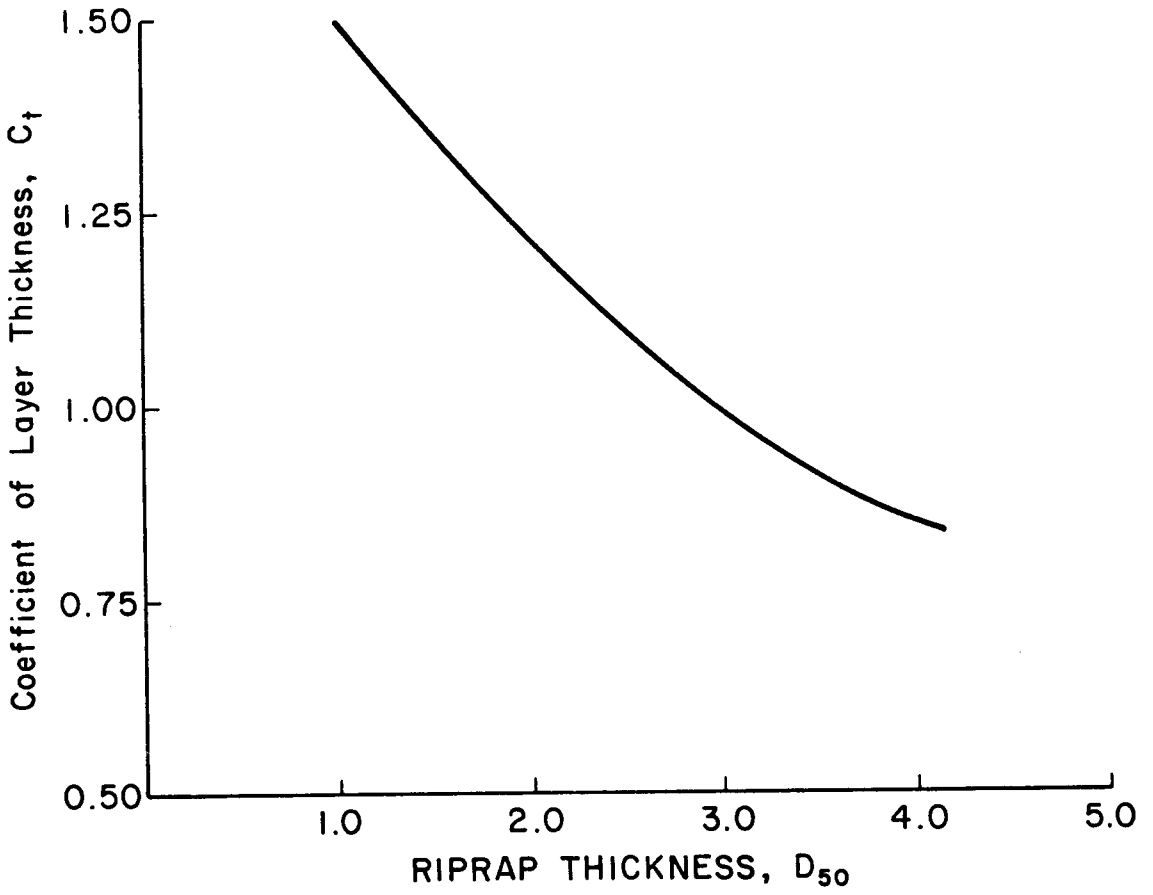

Figure 4.8. Coefficient of layer thickness vs riprap thickness for median stone sizes < 6 in.

presented in Section 4.4. Then, enter Fig. 4.8, using the design riprap layer thickness (expressed in median stone size) and determine the coefficient of layer thickness. The coefficient of layer thickness is multiplied by the design median stone size, resulting in an adjusted median stone size.

4.5 SHAPE INFLUENCE ON RIPRAP STABILITY

Riprap specifications have traditionally stipulated that a high-quality, angular-shaped stone (preferably crushed) be used for placement in the field. Angular stone tends to interlock or wedge and subsequently resist sliding and rolling. In addition, fewer fines are required to fill the voids of crushed material compared with a similarly graded rounded stone.

Unfortunately, high-quality rock sources (i.e., granite, limestone, etc.) for quarrying operations either do not exist near many uranium disposal sites, or the cost to haul high-quality rock to the disposal site is prohibitive. Some disposal sites have rounded, alluvial rock available that may be considered for surface and erosion protection of reclaimed uranium mill tailings. Therefore, it is important to determine the influence the rounded shape has on stability.

A series of five failure tests was conducted in Phase II, (Nos. 21, 22, 36, 38, and 46) with rounded-shaped stones of 2 and 4-in. in diameter on 10 and 20% slopes. The riprap properties are presented in Table 2.1.

Round rock was defined as rock with no intersecting surfaces but rather a single, continuous, smooth-curved surface. During mining, transport, and handling, a portion of the rock fractured and became faced. The faced rock comprised approximately 5% of the rounded rock tested in Phase II.

4.5.1 Stability Comparison

To compare the stability of rounded with angular rock, the unit discharges at failure for 2- and 4-in. rounded and 2- and 4-in. angular-shaped rocks were plotted, as shown in Fig. 4.9, for a 10% slope with 3 D_{50} layer thickness. It was observed in Fig. 4.9 that the rounded stones failed at a unit discharge 32 and 45% lower than the angular rock for the 2- and 4-in. rock sizes, respectively. Although these results represent only one set of test conditions, they are indicative of the stability relationship between angular and rounded stones.

The numerical results support the test observations. Usually, when the angular stones moved, they traveled a short distance and wedged into other stones. When the rounded stones moved, they often rolled down the entire embankment without intermediate lodging.

To generalize the results from the rounded-rock tests, the five rounded-rock failure points were plotted on Fig. 4.2, as presented in

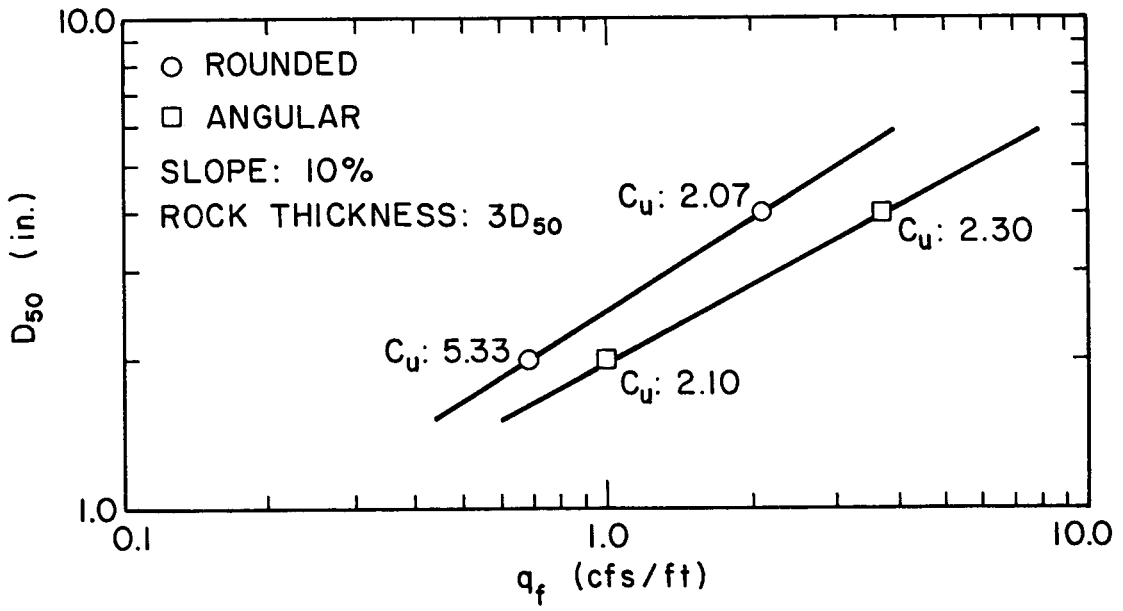

Figure 4.9. Comparison of angular- and rounded-rock stability.

Fig. 4.10. It is observed in Fig. 4.10 that a linear relationship, parallel to the best-fit curve for the angular-shaped rock, can be fit to the rounded-rock results. The difference in the stability between the rounded- and angular-shaped stones is about 40%.

The relationships presented in Fig. 4.10 provide the user the ability to size riprap for rounded- and angular-shaped stones on the basis of the design embankment slope and design unit discharge. Although the rounded-stone data base is quite limited, it provides an indication of relative riprap stability.

4.6 STONE MOVEMENT AND CHANNELIZATION

It was reported in Phase I that stone movement, resulting from the impinging flow, must be considered to prevent failure of the riprap layer. Stone movement was recorded in Phase I for 2-, 4-, 5-, and 6-in. stones on a 20% slope. The stone movement was determined to initiate when the unit discharge approached about 76% $\pm$ 3% of the unit discharge at failure. Stone movement was independent of bed settlement and shifting due to changes in discharge.

The Phase I report also indicated that small channels formed in the riprap layer, conveying unit discharges greater than were expected under sheet-flow conditions. The channels appeared to form as flows were diverted around the larger stones and directed into areas or zones of the smaller stones. The smaller stones moved, creating a gap between the larger stones. The flow concentrated into these gaps, thereby increasing the localized velocity and discharge.

An attempt was made to quantify the degree of channelization through the riprap layer. A channel concentration factor, C_f, was formulated as the ratio of the flow through the channelized riprap to the flow expected under sheet-flow conditions. The channel concentration factor ranged from 1.0 to 3.0.

The unit discharge at channelization was recorded and compared to the unit discharge at failure for 2-, 4-, 5-, and 6-in. stones. It was reported that channelization occurred at about 90% $\pm$ 5% of the unit discharge at failure.

4.6.1 Stone Movement to Failure Relationship

During each of the Phase II failure tests, the unit discharge at which stone movement occurred was recorded. In a manner similar to that in Phase I, stone movement observations were verified with videotape recordings. A summary of the unit discharge at stone movement, at channelization, and at failure are presented in Table 4.3. The stone movement can be normalized by dividing the unit discharge at movement by the unit discharge at failure. The average ratio of the unit discharge at movement to unit discharge at failure is 0.73. A graphical presentation of the normalized discharge to the normalized time is presented in Fig. 4.11. The Phase I and Phase II unit discharge at movement to unit discharge at failure ratios of 0.76 and 0.73, respectively, indicate a small change in the incipient stone

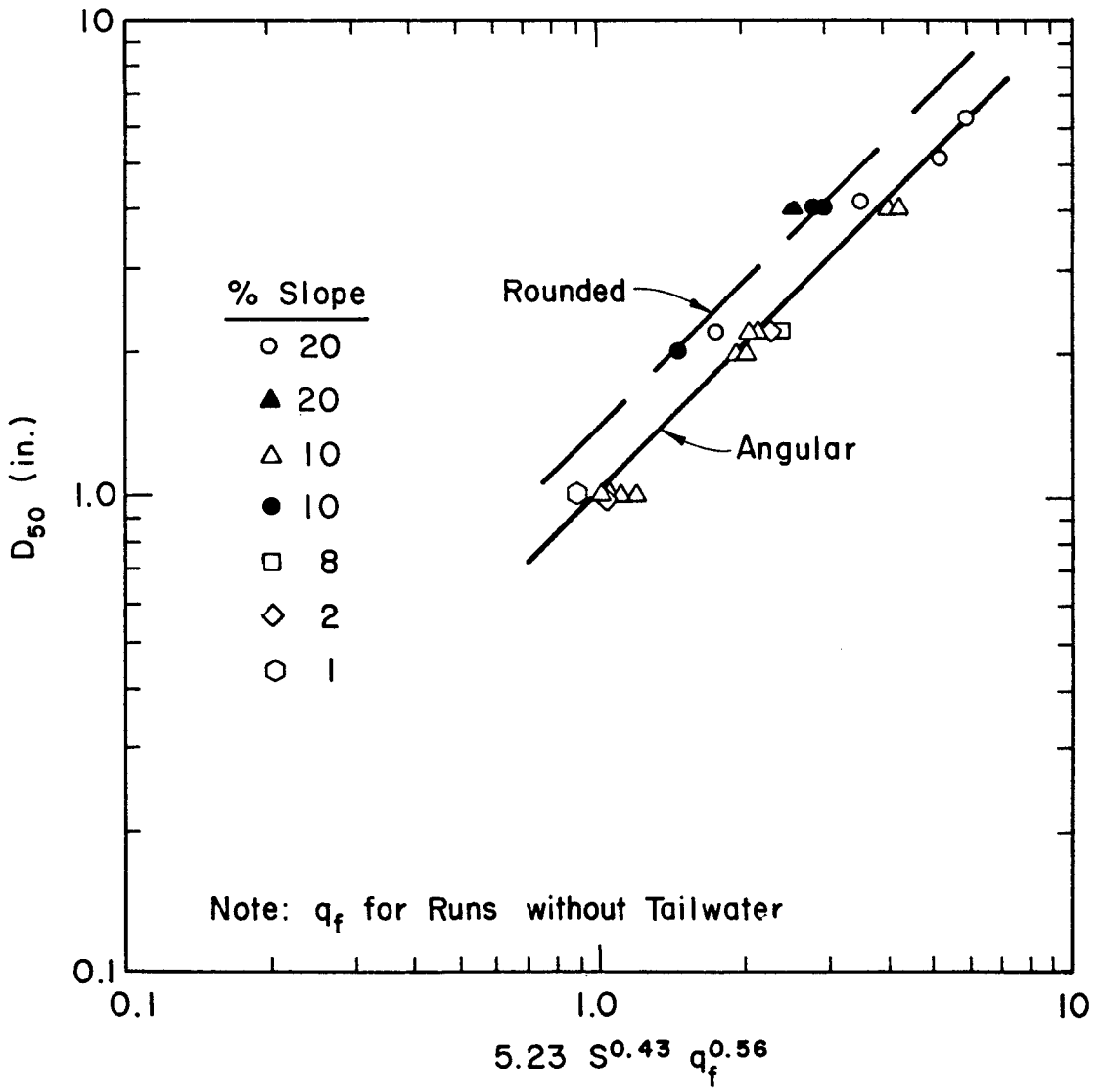

Figure 4.10. Riprap failure relationships from overtopping flow for angular and rounded rock.

Table 4.3. Summary of channel and movement discharges[a]
(All values are in cfs/ft.)

Run number	Rock Shape[b]	$q_{(move)}$	$q_{(chan)}$	$q_{(fail)}$	$\frac{q_{(move)}}{q_{fail}}$	$\frac{q_{(chan)}}{q_{fail}}$
21	R	0.75	0.84	0.95	0.79	0.88
22	R	0.75	0.83	0.94	0.80	0.89
27	A	0.45	0.63	0.77	0.59	0.82
29	A	0.56	0.73	0.85	0.66	0.85
31	A	0.62	0.82	1.00	0.62	0.82
32	A	0.84	0.95	1.11	0.76	0.86
34	A	1.10	1.18	1.23	0.89	0.96
36	R	1.51	1.67	1.99	0.76	0.84
38	R	1.39	1.80	2.09	0.66	0.86
40	A	2.71	3.17	3.40	0.80	0.93
42	A	2.72	3.23	3.51	0.77	0.92
44	R	2.95	3.24	3.79	0.78	0.86
46	A	4.58	0.57	0.69	0.67	0.83
48	A	1.88	2.17	2.41	0.78	0.90
51	A	3.10	3.68	4.12	0.75	0.89
				Average	0.73	0.87

[a] $q_{(move)}$ = unit discharge at incipient motion of the rock

[b] $q_{(chan)}$ = unit discharge at channelization of the rock

$q_{(fail)}$ = unit discharge at rock failure

[b] R - rounded rock.
A - angular rock.

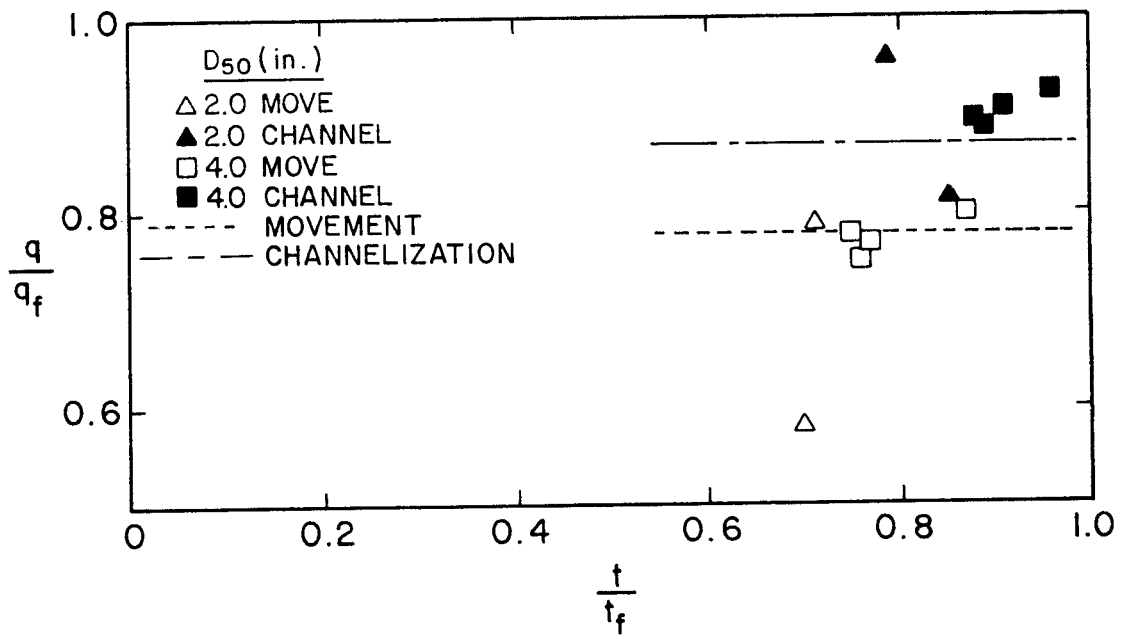

Figure 4.11. Normalized unit discharge vs normalized time for stone movement and channelization.

movement between phases. Inclusion of the Phase I data with the Phase II data without rounded stone and soil cover yields an average unit discharge at a movement to unit discharge at failure ratio of 0.74.

4.6.2 Rock Sizing to Resist Movement

A relationship was presented in Eq. 4.1 for predicting the median stone size of the riprap layer on the bases of the embankment slope and the unit discharge at failure. Stone movement can be prevented by adjusting the unit discharge at failure. The adjusted unit discharge at failure, q_f^* is defined as the design unit discharge divided by the stone movement to stone failure ratio of 0.74 expressed as

$$q_f^* = \frac{q_{design}}{0.74} = 1.35\ q_{design} \tag{4.5}$$

Eq. 4.1 is modified to yield a median stone size that will resist stone movement at the design unit discharge where

$$D_{50} = 5.23\ S^{0.43}\ (q_f^*)^{0.56} \tag{4.6}$$

Eq. 4.6 is applicable to only angular-shaped riprap.

4.6.3 Channelization to Failure Relationship

Flow channelization was observed and documented in 15 failure tests during Phase II. The unit discharge at which flow channelization was observed in the riprap layer is presented in Table 4.3. Although an attempt to identify initial channelization was made during each test, documentation of initial channelization was verified from the videotape recordings. The unit discharges at channelization were normalized to the appropriate unit discharges at failure. A representation of the normalized unit discharge to time, normalized at failure, is shown in Fig. 4.11.

The average ratio of the unit discharge at channelization to the unit discharge at failure was 0.88 for angular-shaped riprap. The Phase I report indicated that the average ratio of unit discharge at channelization to unit discharge at failure was 0.90. The average Phase I and Phase II ratio of 0.89 shall be considered the critical channelization ratio. On the basis of these results, it is possible to predict the unit discharge at which channelization will occur on a riprap embankment.

4.7 SUMMARY

The Phase I and Phase II failure test data resulted in a composite relationship for angular shaped rock as presented in Fig. 4.2 and expressed in Eq. 4.1. The composite failure relationship related the median stone size to the embankment slope and unit discharge at failure for overtopping flow conditions.

The effect of riprap gradation on riprap stability was also studied. The results indicate that the more uniform the gradation, the more resistant the rock layer to overtopping flow. It is recommended that riprap gradations, expressed as a coefficient of uniformity, should be 2.5 or less.

The thickness of the riprap layer was investigated to determine its effect on riprap stability. It was concluded that a layer thickness of 1.5 times the median stone size, or 1.0 times the D_{100}, is adequate for median stone sizes of 6 in. or larger. However, the layer thickness or the median stone size should be increased for median stone sizes less than 6 in.

Failure tests were conducted to determine the stability of rounded-rock subjected to overtopping flow conditions. The failure test results indicated that rounded-rocks are about 40% less stable than angular-rocks of the same median stone size. The rounded-rock failure relationship is presented in Fig. 4.10.

Since riprap should be sized to resist movement rather than failure, a means was presented to adjust the unit discharge at failure. Therefore, Eq. 4.1 used to calculate the median stone size, was modified to incorporate the adjusted unit discharge at failure as presented in Eq. 4.6.

5. INTERSTITIAL VELOCITIES THROUGH RIPRAP

The measurement of interstitial velocities through the riprap layers was performed in Phase II to verify the velocity relationships presented in Phase I. Because riprap gradation and riprap shape were constants in Phase I, both parameters varied in Phase II to provide a basis for indicating how riprap gradation and riprap shape affect interstitial velocities.

Interstitial velocity profiles were measured and recorded for each riprap test configuration (D_{50} and layer thickness) to estimate the average interstitial velocity of flow. Profiles were measured as described in Chapter 2 in the upper third of the embankment (station 20-22) and in the lower third of the embankment (station 50-52). In each case, the water surface was at or near the rock surface. A summary of the interstitial velocity profiles in the riprap are presented in Table 5.1.

It is observed in Table 5.1 that at 10% slope, average interstitial velocities range from 0.45 to 0.63 fps for angular 2-in. rock and from 0.36 to 0.91 fps for angular 4-in. rock. Although there is considerable variation in the velocity profiles through the riprap layer, the larger velocities appear in the zone near the rock surface, usually in the top 2 in., with velocities decreasing with depth into the layer. In a few instances, velocities through the riprap exceeded 1.0 fps. The variation in velocity is attributed primarily to the partial blockage in the flow path between the injector and the sensor. In some cases, a large stone inhibited the direct flow path between the instruments. Injectate had to flow around the stone, and the extended flow path resulted in reduced velocity.

The average interstitial velocities presented in Table 5.1 indicate that the interstitial velocity of flow through 2-in. rounded riprap (~0.39 fps) is lower than interstitial velocities through 2-in. angular riprap (~0.52 fps) by nearly 25%. The 4-in. rounded riprap yielded interstitial velocities of ~0.55 fps, while the 4-in. angular riprap interstital velocities were ~0.64 fps. The stone shape appears to influence the interstitial flow of the riprap layer.

The affect of stone gradation on interstitial velocity through the riprap layer was also investigated. Phase II tests (Nos. 43, 47, and 50) were conducted in which the riprap coefficients of uniformity of 2.3, 4.0, and 1.72 yielded interstitial velocities of ~0.84, ~0.42 and ~0.79 fps, respectively. The median stone size, layer thickness, and slope were constant. The results indicate that the large coefficient of uniformity (4) reduces the interstitial velocity through the riprap layer by 50% compared with the uniformly graded riprap layers. The riprap layers with coefficients of uniformity of 1.72 and 2.30 produced similar interstitial velocities.

5.1 COMPARISON OF PHASE I AND PHASE II INTERSTITIAL VELOCITIES

Nine of the fourteen interstitial velocity tests conducted in Phase II used angular-shaped riprap, as reported in Phase I. With

Table 5.1. Velocity profiles for interstitial flow through riprap in the outdoor flume (12 ft) at 10% slope.

Test number	Median stone size[a] D50 (in.) (1)	Riprap Thick-ness (in.)	Distance from headwall[b] (ft)	Q (cfs)	Depth of flow (in.)	Velocity of flow through riprap at Y in. below riprap surface (fps)												Average interstitial velocity (fps)
						Y=10	Y=8	Y=6.5	Y=6	Y=5	Y=4.5	Y=3.5	Y=3	Y=2	Y=1.5	Y=0.5	Y=0.0	
26	2.0	3.0	20-22	1.10	0.00										0.45			0.45
26	2.0	3.0	50-52	1.12	0.00										0.46			0.46
28	2.0	4.0	20-22	1.16	0.00								0.31				0.62	0.47
28	2.0	4.0	50-52	0.91	-0.27								0.36				0.64	0.50
30	2.0	6.0	20-22	1.84	0.00				0.52		0.41		0.63		0.52		1.06	0.63
30	2.0	6.0	50-52	1.79	0.17				0.59		0.44				0.65		0.49	0.54
33	2.0	8.0	20-22	2.05	0.73		0.45		0.39	0.51		0.48		0.56		0.61		0.50
33	2.0	8.0	50-52	2.11	0.75		0.46		0.63	0.77		0.51		0.53		0.64		0.59
35	4.0	6.0	20-22	0.97	-0.61		0.45						0.34					0.40
35	4.0	6.0	50-52	0.94	-0.31		0.36						0.47		0.83			0.55
37	4.0	12.0	20-22	3.05	-0.32	0.40			0.71									0.58
37	4.0	12.0	50-52	4.20	0.82	0.40			1.31				0.67					0.73
39	4.0	6.0	20-22	2.40	0.36				0.49		0.48		0.75		0.44		0.30	0.49
39	4.0	6.0	50-52	2.52	1.16				0.38		1.00		0.65		0.46			0.62
41	4.0	8.0	20-22	2.52	0.67		0.47	0.39		0.60		0.56		1.20		1.10		0.72
41	4.0	8.0	50-52	2.37	0.44		0.77	0.60		0.42		0.83		0.50		0.83		0.66
43	4.0	12.0	20-22	3.33	-0.47	0.60							0.76				1.15	0.84
45	2.0	6.0	20-22	1.64	0.45				0.28		0.37		0.41		0.48			0.39
45	2.0	6.0	50-52	1.94	0.41				0.21		0.35				0.49		0.48	0.38
47	4.0	12.0	20-22	2.46		0.30			0.42								0.33	0.35
47	4.0	12.0	50-52	2.40		0.40			0.64				0.40					0.48
50	4.0	12.0	20-22	4.64	-0.23	0.90			0.60				0.63				1.45	0.91
50	4.0	12.0	50-52	5.58	0.20	0.50			0.53								0.94	0.66

[a]R - Round Rock

[b]Nominal distances of the tracer injector and tracer sensor, respectively.

specific test parameters from Appendix B, the average upstream and downstream interstitial velocities (Nos. 26, 28, 30, 33, 39, 41, 43, 47, and 50) are plotted in Fig. 5.1 along with Phase I data from equivalent tests using the dimensionless relationship in Eq. 1.1.

Figure 5.1 indicates that the interstitial velocity data obtained at 10% slope in Phase II compare favorably to the data recorded in Phase I for slopes ranging from 1 to 20%. Therefore, it appears appropriate to use Eq. 1.1 to estimate interstitial velocities through riprap layers on slopes $\leq$ 20%. It is, however, recommended that the data base be expanded to median riprap sizes > 6 in. and riprap layer thicknesses > 12 in. before Eq. 1.1 is applied to engineering problems.

5.2 CALCULATED VS MEASURED INTERSTITIAL VELOCITIES

In an attempt to verify the interstitial velocity measurements obtained with the injection system, the average interstitial velocity was also calculated. Because the total discharge (Q) supplied to the flume, the average cross-sectional area of flow, and the porosity of the rock layer were measured parameters, the average calculated interstitial velocity, V_c, is

$$V_c = \frac{Q}{An_p} , \tag{5.1}$$

where discharge is in cubic feet per second and area is in square feet. The average measured interstitial velocity data from both Phase I and Phase II tests, as presented in Fig. 5.1, were compared with the average calculated interstitial velocity. A comparison of the measured vs calculated interstitial velocities is presented in Fig. 5.2. The diagonal line plotted in Fig. 5.2 indicates perfect agreement between measured and calculated average interstitial velocities. The data indicate that there is generally a good fit between the measured and calculated velocities considering the wide range of slopes, rock sizes, and rock-layer thicknesses tested. However, the velocity may not be strictly proportional to the inverse of porosity, and other factors may be important.

The velocity of flow through the voids of the riprap layer is a function of the rock size and the gradation. In part, the more well graded the riprap, the more small particles available to fill the voids between the rocks, resulting in a lower porosity. Because the interstitial velocity was related to median stone size, as evident in Eq. 1.1, it is possible that the gradation, expressed as the coefficient of uniformity, C_u , is related to the interstitial velocity.

5.3 INTERSTITIAL VELOCITY RELATED TO D_{10}

It was determined in the Phase I study that the interstitial velocity, V_i, through the riprap and/or filter layer(s) is a function of the material properties and the gradient expressed as

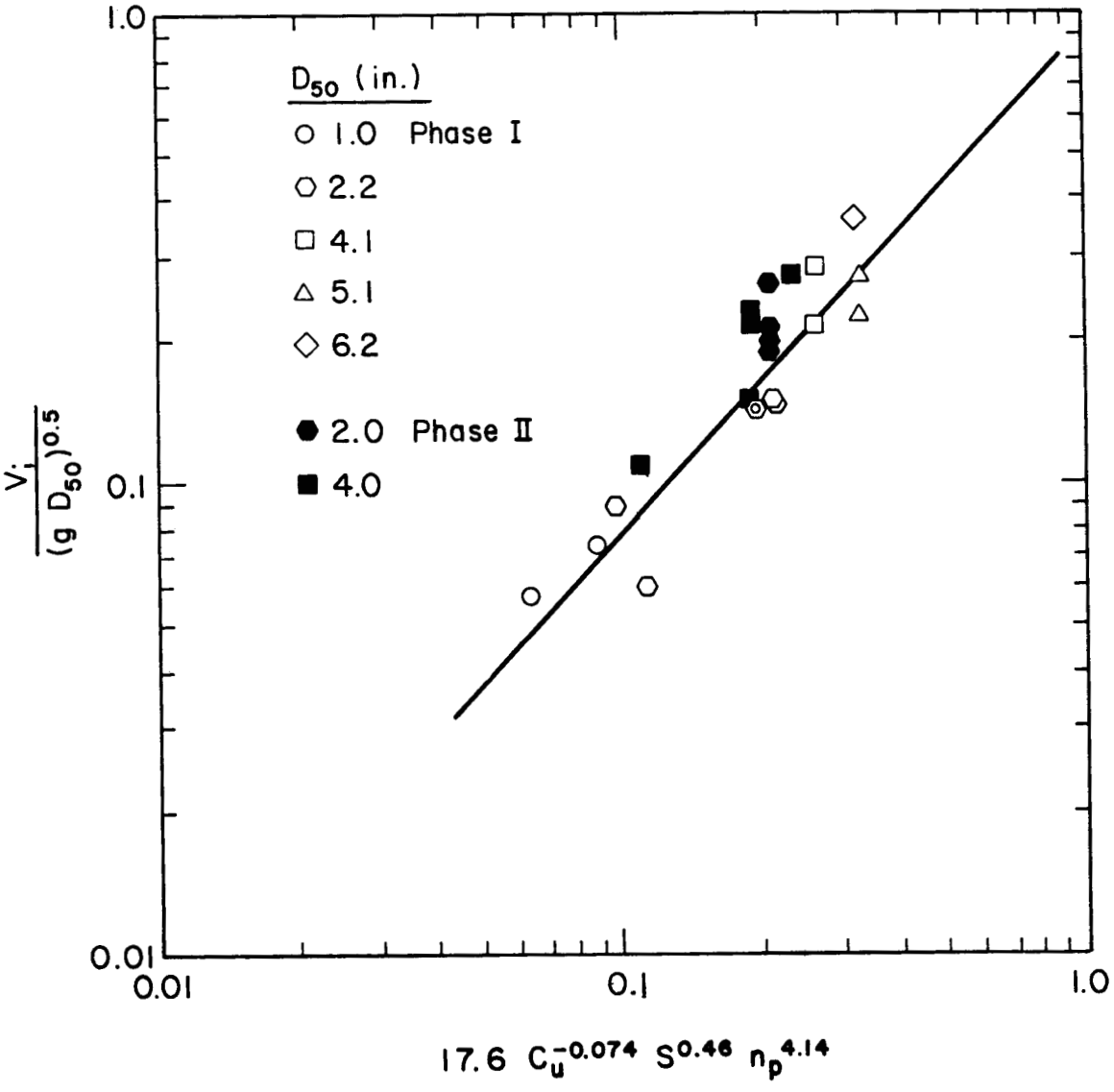

Figure 5.1 Comparison of the Phase I and Phase II interstitial velocity data.

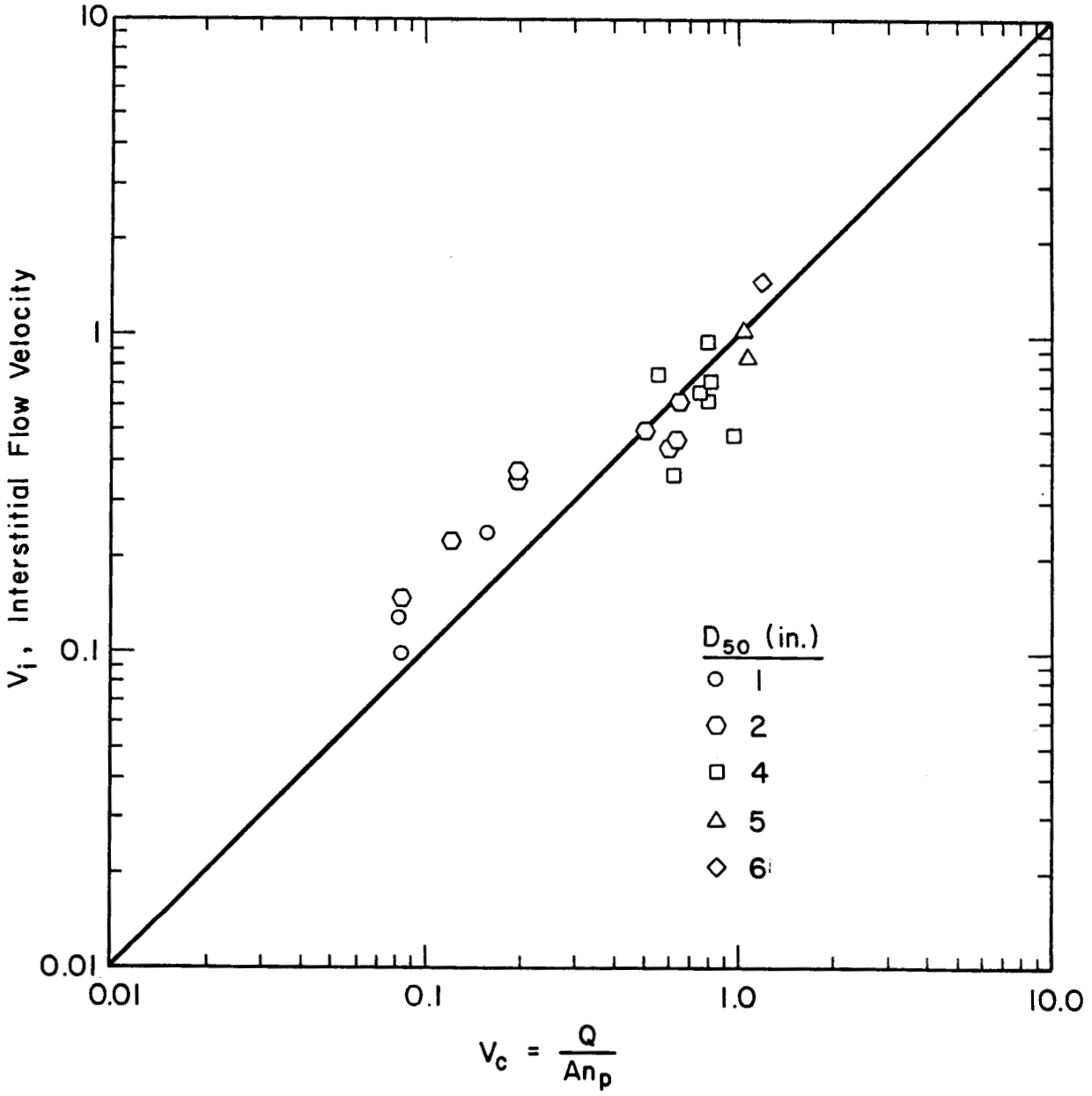

Figure 5.2. Comparison of measured vs calculated interstitial velocities.

$$V_i = 19.29\ (C_u^{-0.074}\ S^{0.46}\ n_p^{4.14})^{1.064}\ (g\ D_{50})^{0.5} \tag{5.2}$$

During the preliminary design process, the median stone size, D_{50}, is often estimated. However, the material properties of coefficient of uniformity, C_u, and the rock layer porosity, n_p, are unknown. Therefore, an analysis was conducted to correlate the interstitial velocity through the rock layer to the rock size and slope. The variables C_u and n_p were eliminated from the analysis.

A sensitivity analysis was performed relating the rock size and gradient to the interstitial velocity. Representative stone sizes of D_{50}, D_{40}, D_{30}, D_{20}, D_{15} and D_{10}, in conjunction with the slope, were correlated to the measured interstitial velocity. The analysis indicated that the D_{10} stone diameter (at which 10% of the weight is finer) provided the highest coefficient of correlation of the stone sizes tested. The interstitial velocities depicted in Fig. 5.1 and the interstitial velocities measured for the rounded-rock riprap layers (Phase II tests 35, 37, and 45) were plotted as shown in Fig. 5.3. A linear regression analysis yielded the expression

$$V_i = 0.232\ (g\ D_{10}\ S)^{1/2}, \tag{5.3}$$

where V_i is the interstitial velocity in feet per second, g is the acceleration of gravity in feet per second squared, D_{10} is in inches, and S is the gradient expressed in decimal form. The correlation coefficient of the relationship presented in Eq. 5.2 is $r^2 = 0.92$.

5.4 INTERSTITIAL VELOCITY THROUGH FILTER MATERIAL

Interstitial velocity profiles were measured for filter material GF5, median grain size of 0.44 in. (Table 2.2), which was considered representative of the filter materials used throughout the Phase II program (Appendix A). The average interstitial velocities of flow through filter GF5 are presented in Table 5.2. The average interstitial velocity through the GF5 filter material is 0.08 fps.

The filter material interstitial velocities were nearly two orders of magnitude smaller than the surface velocities and one order of magnitude smaller than the riprap interstitial velocities. Thus, the volume of flow through the filter is signficantly less than the volume of flow through the riprap layer.

5.5 APPLICATION TO RIPRAP LAYER DESIGN

The design of the median stone diameter, riprap gradation, and riprap layer thickness is dependent upon the unit discharge over the riprap layer surface. Because a portion of the design discharge tributary to the riprap layer will flow through the layer, the surface discharge can be reduced by an amount equal to the through-flow discharge.

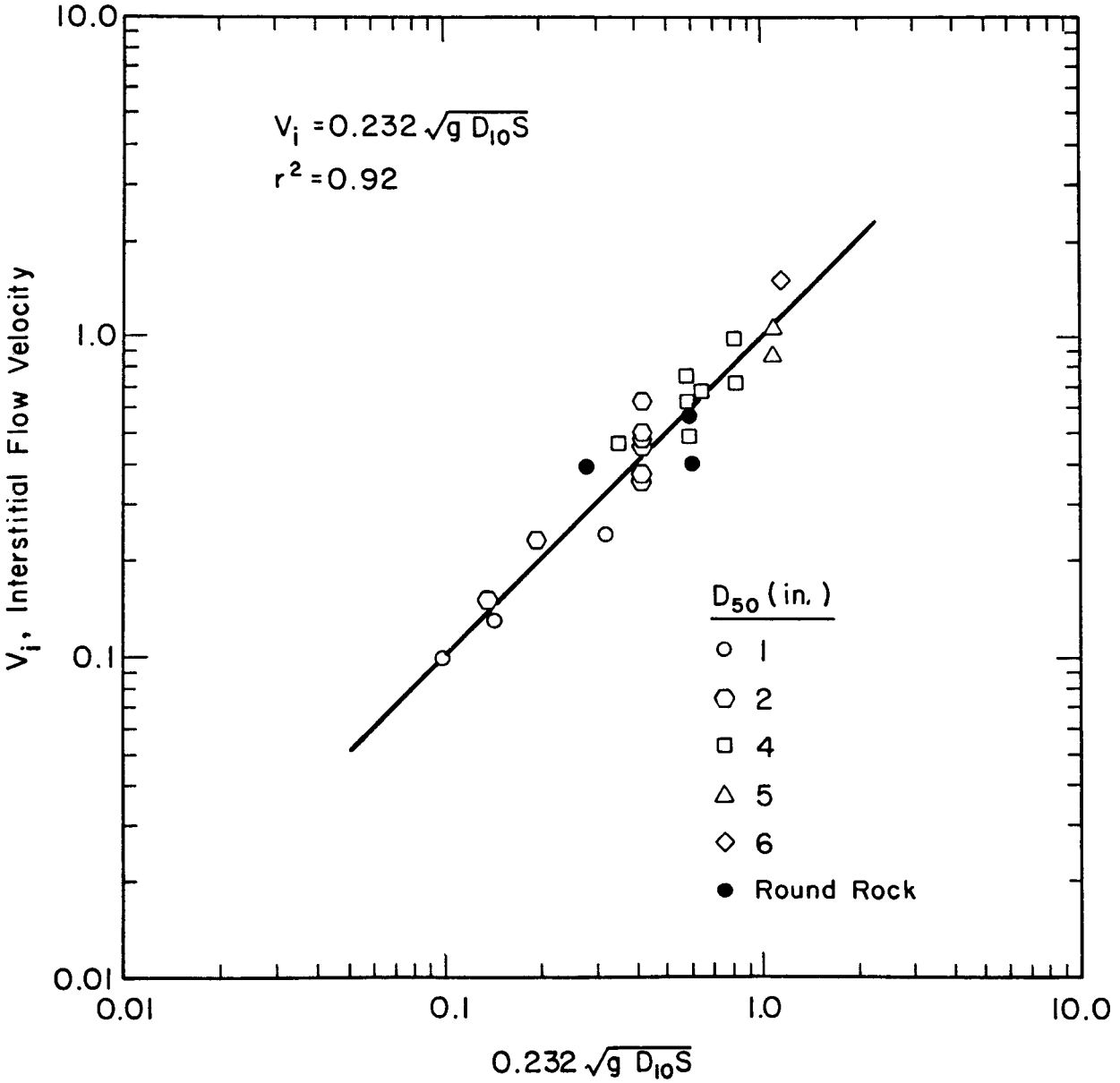

Figure 5.3. Interstitial velocity expressed as a function of D_{10} and gradient.

Table 5.2. Interstitial velocities through filter GF5

Q (cfs)	Depth of filter (in.)	Velocity of flow through riprap at 4 in. below filter surface (ft/s) Y = 1.5	Y = 4.5	Average velocity (ft/s)
0.09	6.0	0.11	0.05	0.08
0.10	6.0	0.10	0.04	0.07
0.23	6.0	0.12	0.06	0.09
			Average	0.08

To calculate the adjustment of the design surface discharge, q_{design}:

1. Multiply the estimated interstitial velocity resulting from Eq. 5.2 or Eq. 5.3 by the estimated riprap-layer thickness yielding the unit discharge of through flow in cubic feet per second.
2. Subtract the through-flow unit discharge from the design unit discharge, leaving the adjusted surface unit discharge in cubic feet per second.

5.6 SUMMARY

Interstitial velocities through the riprap layers were recorded and compared to the interstitial velocity data in Phase I. A comparison of the Phase I and Phase II results substantiated the use of Eq. 1.1 derived in Phase I.

The interstitial velocities measured in Phase I and Phase II were compared with the calculated interstitial velocities. The data indicate a favorable comparison although other factors not identified in this study appear to influence the velocity estimate.

An analysis conducted to simplify Eq. 5.2 indicated that the interstitial velocity can be expressed as a function of the rock size D_{10}, the acceleration of gravity and the embankment slope. The simplified interstitial velocity relationship is presented in Eq. 5.3.

The interstitial velocity was measured for a generic filter material with median grain size of 0.44 in. The velocity of flow through the filter was one order of magnitude smaller than the riprap interstitial velocities and two orders of magnitude smaller than the surface velocities.

6. RIPRAP COVER

Although riprap is one of the most effective means of erosion protection and slope stabilization, it is often considered visually obtrusive. Therefore, a series of three tests in Phase II (Nos. 23, 25, and 53) was conducted in which riprap was placed on the embankment and then covered with compacted soil. The integration of soil material as part of the erosion protection plan provides a base to support vegetation while reducing the visual obtrusiveness of the reclaimed site. The following sections discuss soil cover placement and testing.

6.1 MATERIAL CLASSIFICATION AND PLACEMENT

The three soil materials used were laboratory tested and classified. The soil properties of each material are summarized in Table 6.1. The soils were classified in accordance with the Universal Soil Classification System as a sandy-silt mixture, a clayey loam, and a clayey sand for tests 23, 25, and 53, respectively.

Soil cover placement was as follows. After the embankment and riprap layer were prepared in a manner similar to other tests without a soil cover, a thin layer of soil (2 to 3 in.) was placed on top of the riprap. The soil was vibrated into the rock. Another thin layer of soil was placed and vibrated. This process was repeated until the soil depth was 12 in. over the riprap surface. Soil densities were maintained at 92% $\pm$ 2% of the modified proctor.

The embankments with soil cover were tested in a manner slightly different from that of the riprap-covered embankments. Instead of water flowing directly into the soil at the headwall-embankment interface, the flume was modified to enable water to flow over the soil cover surface and down the embankment. The soil cover was allowed to erode away, exposing the riprap protective layer. Flow was gradually increased until the riprap layer failed.

Test No. 23 was an exception to the prescribed procedure in that flow was allowed to enter the soil at the headwall-embankment interface. All other testing procedures were as outlined in Section 3.2. The soil cover in test No. 23 was a sandy-silt composition without clay content. The cover was placed such that flow ponded at the headwall-soil cover interface, and soil was placed over the entire toe of the slope. The depression near the headwall-soil interface filled, allowing water to simultaneously enter the riprap and overflow onto the soil surface.

6.2 RESULTS OF TEST NO. 23

When flow overtopped the soil surface along the embankment crest, the flow cut into the sandy soil cover, leaving numerous rills down the embankment face. As the initial flow reached the middle of the embankment, a portion of the soil cover near the toe was "blown" out by the hydrostatic pressure of water stored in the riprap layer under the soil cover. The cavity in the soil cover served as a base for a

Table 6.1. Soil properties[a,b]

Test number	Riprap D_{50} (in.)	Slope	Soil thickness (in.)	Soil type	γ_{max} (%)	Soil D_{50} (in.)	C_u	Sand (%)
23	4.0	0.20	12.0	SM[c]	93.8	0.0180	4.6	82%
25	4.0	0.20	12.0	CL[d]	90.0	0.0031	13.8	54%
52	4.0	0.10	0.0	SC[e]	90.0	0.0157	7.9	86%
53	4.0	0.10	12.0	SC[e]	91.0	0.0157	7.9	86%

[a] All properties were determined in the Colorado State University Geotechnical Laboratory in accordance with American Society for Testing and Materials guidelines.

[b] Gradation curves found in Appendix C.

[c] SM: Poorly graded sand-silt mixture.

[d] CL: Inorganic clays of low to medium plasticity.

[e] SC: Clayey sands, poorly graded clay mixtures.

D_{50} = Median stone or soil size.

γ_{max} = Theoretical soil density.

C_u = Coefficient of uniformity.

headcut as the surface flow reached the slope toe. Within a 10-minute period, the flow reached a unit discharge of 0.11 cfs and had cut several gullies completely through the soil cover to the riprap surface. Throughout the test, the pond atop the cover served as a water source and driving force for flow through the riprap layer. Flow through the riprap transported soil in the riprap void spaces to the embankment toe.

The test was stopped after about 25 minutes. The riprap had not failed, although the majority of the soil cover had eroded. The findings based upon this test are as follows:

1. The soil cover should have some type of material to ensure a minimum level of bonding between soil particles. The sandy-silt material is not acceptable for a soil cover because of its high potential for erosion.
2. Ponding upstream of the slope crest or anywhere on the reclaimed pile should be avoided. Seepage from the pond tends to remove the soil in the riprap, serves as a moisture source to the radon barrier, and generally weakens the erosion protection layer on the embankment.
3. The toe of the embankment slope should not be covered, but rather allowed to drain. Water tends to accumulate in the riprap and filter layers if covered, resulting in the potential for hydrostatic pressure under the cover, which could result in the catastrophic loss of soil and the initiating of a headcut through the cover.

6.3 RESULTS OF TEST NO. 25

The second soil cover tested (No. 25) comprised a clayey-loam material with over 40% clay compacted to 90% modified proctor. The soil covered an angular riprap layer with median stone size of 4 in. placed at a layer thickness of 3 times D_{50} on a 20% slope.

The soil cover was overtopped and determined to be highly resistant to erosion. In the early stages of testing ($q \leq 1.0$ cfs), soil loss was due to individual soil particles being lifted from the surface and transported in the sheet flow. When the unit discharge exceeded 1.0 cfs, soil was removed in clumps, thereby pitting the soil cover surface. As the unit discharge approached 1.40 cfs, flow began to channelize, causing headcutting along the flume wall. The headcut incised very quickly to the riprap layer. More than 80% of the flow was diverted into the gully, causing the gully to widen because it could no longer incise. The channelization of flow soon failed the entire riprap layer in the bottom of the gully at a unit discharge of 1.53 cfs, as shown in Table 6.2. The predicted unit discharge at failure of the riprap layer (from Eq. 4.1) was 2.45 cfs.

6.4 RESULTS OF TEST NO. 53

Test No. 53 was conducted in the same manner as test No. 25. However, the soil cover was graded toward the center of the embankment

Table 6.2. Summary of soil cover tests[a]

Test number	Slope	Q (cfs)	q_f (cfs)	q_f^{*b} (cfs)	Remarks
23	0.20	0.12	0.01	0.13	Riprap covered with 12-in. sandy silt
25	0.20	18.33	1.53	0.13	Riprap covered with 12-in. clayey loam
52	0.10	48.05	4.00	4.6	Riprap filled with clayey sand, flush with surface
53	0.10	27.36	2.28	4.6	Riprap covered with 12-in. of clayey sand

[a]All tests were conducted with dump-placed angular-shaped riprap of 4-in. median stone size, 12-in. riprap layer thickness, 6-in. filter thickness.

[b]Adjusted unit discharge to resist movement.

to ensure flow concentrated away from the flume walls, as shown in Fig. 6.1. Once the embankment was prepared, flow overtopped the embankment. As the unit discharge approached 1.0 cfs, a gully developed along the flume centerline. The gully penetrated through the soil cover to the riprap barrier. Flow began to channelize, thereby widening the gully, as shown in Fig. 6.2. The riprap layer failed at a unit discharge of 2.28 cfs (Table 6.2). The predicted unit discharge of the riprap layer at failure (Eq. 4.1) due to overtopping was 4.10 cfs.

The findings from these soil cover tests are summarized as follows:

1. The clay content of the soil used for the cover is an important indicator of the cover stability. The higher the clay content, the more stable the slope when subjected to sheet-flow conditions.
2. The greater the clay content of the soil cover, the more energy of the flow is required to erode the gully sidewalls as flow is channelized. The slower the sidewall degradation, the greater the potential for premature riprap layer failure.
3. The soil cover thickness directly influences the extent of gullying. The thicker the cover, the greater the chance that concentrated flow through the gully may cause premature failure of the riprap barrier.

On the basis of the findings, it is recommended that a soil cover thickness above a riprap barrier not exceed 3 to 4 in. Thin soil layers can be easily eroded without excessive gullying. As the soil thickness increases, stability of the erosion barrier decreases.

6.5 RIPRAP SOIL MATRIX

One test (No. 52) was conducted to determine the feasibility of protecting an embankment with a soil-rock matrix. The matrix should be comprised of rock to resist the design unit discharge and soil to fill the rock voids and reduce infiltration as well as provide a soil base for vegetation.

Two methods were considered for mixing and placement of the matrix barrier. The first method entailed the mixing of the rock and soil in a stock pile. The rock-soil material would be dumped on the embankment, vibrated, and tested. Problems resulting from implementation of this method included: how much soil to mix with the rock; how to avoid segregation and localized areas without rock protection; how much compaction is needed; and how to ensure adequate rock protection and maintain quality control.

The second method of soil-rock matrix placement was to place the riprap to the prescribed thickness over the entire embankment. Then, place a thin soil layer, 3 to 4 in. thick, over the riprap layer and vibrate the soil into the rock. Repeat the soil placement and vibration until the soil is adjacent to the rock surface, as shown in Fig. 6.3. The rock layer remains intact, ensuring the quality of the erosion barrier. The soil fills the voids and reduces the visual obtrusion of the reclaimed pile.

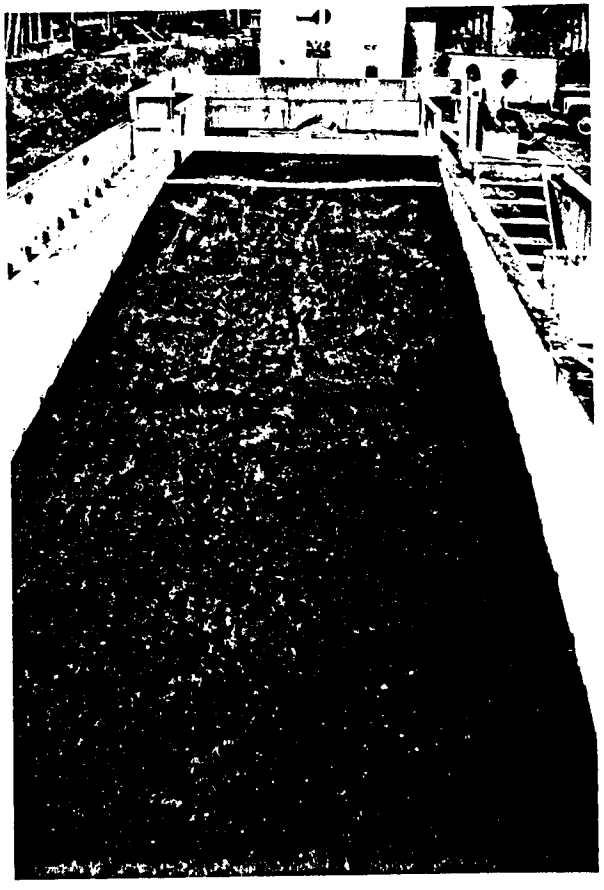

Figure 6.1. Soil cover with 14% clay prior to testings.

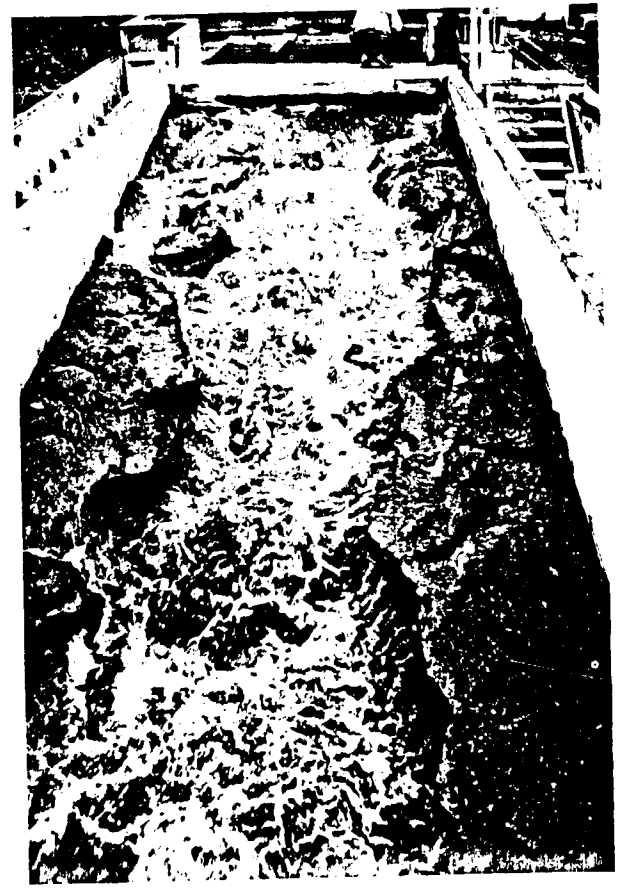

Figure 6.2. Soil cover with 14% clay during channelized flow conditions.

The second method of soil matrix mixing and placement was selected for this test to ensure the quality and integrity of the barrier. It was also anticipated that the vibration used during soil placement would densify the rock, thereby increasing matrix stability.

6.6 RESULTS OF TEST NO. 52

The overtopping flow eroded the soil away from the riprap as the flow over the embankment crest increased. Little rock movement was observed when the unit discharge was below 1.5 cfs. The soil particles tended to stabilize the rock, reducing rock layer adjustment. When the unit discharge exceeded 3.0 cfs, the soil had eroded from the void spaces in the top rock layer, resulting in rock movement in many isolated locations. The second layer of rock in the riprap began to move when the unit discharge approached 3.5 cfs. The soil matrix layer had a localized failure when the unit discharge reached 4.0 cfs (Table 6.2). Figure 6.4 shows the matrix at failure. The design unit discharge at failure for the riprap layer (from Eq. 4.1) is 3.65 cfs. Therefore, the rock-soil matrix was nearly 10% more stable than the riprap layer without soil. Because of the manner in which the test was conducted, the strengthened erosion barrier at failure is attributed to the compactive process.

It is recognized that these results do not reflect the erosive effects of lesser rainfall and runoff events on the soil matrix that occur prior to the major runoff event simulated in test No. 52. Also, the antecedent moisture conditions in the matrix prior to the major runoff event were ignored. Therefore, the amount of erosion on the matrix cover prior to a major runoff event and the antecendent moisture conditions of the matrix could potentially reduce the effectiveness of the matrix stability.

The riprap soil matrix appears to lend a unique solution to erosion protection. The riprap provides the long-term aspect of erosion control. The vibration of the riprap densifies the rock layer by tightly wedging stones together. The soil fills the void spaces, stabilizing the rock from movement, reducing moisture infiltration, and providing a vegetative base. Because soil is not placed above the riprap surface, the opportunity for gullying and channelized flow through the soil is significantly reduced. Although the riprap surface is not completely hidden, visual degradation is reduced.

6.7 SUMMARY

Three tests were conducted in which soil covers and rock-soil matrices were evaluated. The test results indicated that cover materials should be cohesive in nature. Covers should be contoured to eliminate potential ponding. When riprap underlies a soil cover, the toe of the riprap should be exposed to allow drainage. On the basis of the findings, the soil cover thickness over a riprap barrier should not exceed 3 to 4 in. or the cover has an increased chance of gullying.

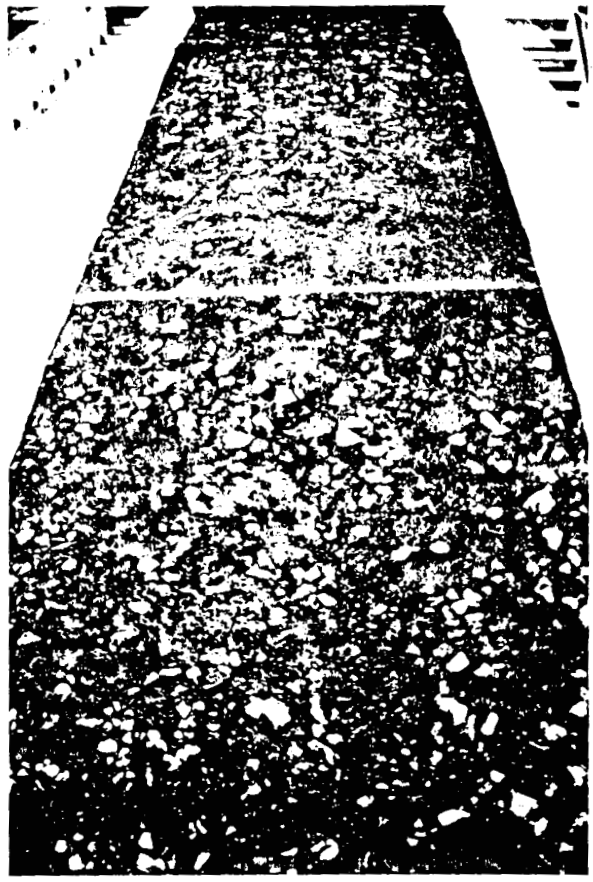

Figure 6.3. Riprap soil matrix prior to testing.

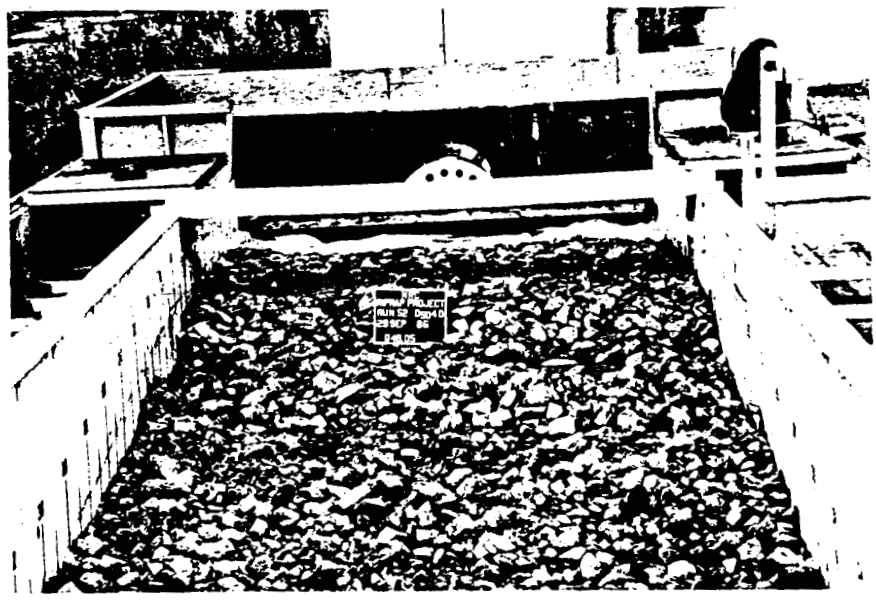

Figure 6.4. Riprap soil matrix at failure.

The rock-soil matrix appeared to provide the most stable condition of the soil cover experiments. The vibrated rock increased the rock layer density while the soil reduced rock movement. The rock-soil matrix increased the cover stability by 10% over the riprap only condition.

7. RECOMMENDED DESIGN PROCEDURE

The Phase I and Phase II studies report the findings of 90 laboratory tests that address the application of riprap for protecting embankment slopes from overtopping flows. Although the data base is limited, it is possible to provide the user with a design procedure for sizing riprap. This chapter will outline the assumptions, equations, and/or graphics necessary to apply the findings of the Phase I and Phase II studies.

7.1 DESIGN PROCEDURE

Step 1. Determine the design unit discharge

Determine the design embankment slope(s) and the peak unit discharge, q, resulting from the tributary runoff at a point near the toe-of-the-slope (Nelson et al. 1987), and determine the shape of available rock sources (angular or round). Define the initial design unit discharge by adjusting the tributary unit discharge with the flow concentration factor, C_f, as

$$q'_{design} = q \times C_f \ , \tag{7.1}$$

where C_f = 1.0 for overland sheet flow,
2.0 for a high probability of concentrated flow, and
3.0 for a high probability of channelized flow.

The values of the flow concentration factor is based on data from Abt et al. (1987).

Step 2. Estimate the median stone size (D_{50}) of the riprap layer

To size the median stone and prevent stone movement, adjust the design unit discharge by

$$q^*_{design} = 1.35 \ q'_{design} \ . \tag{7.2}$$

Then, estimate the median stone size as

Angular stone

Apply Eq. 4.1, using the embankment slope from Step 1:

$$D_{50} = 5.23 \ S^{0.43} \ (q^*_{design})^{0.56} \ , \tag{7.3}$$

where D_{50} is expressed in inches.

Rounded rock

Compute a conditional value of the rock size, D_c, where

$$D_c = 5.23 \ S^{0.43} \ (q^*_{design})^{0.56} \ . \tag{7.4}$$

Then, from Fig. 4.10, obtain the median stone size for rounded-shape

riprap, as D_{50}, expressed in inches.

Step 3. Estimate the riprap layer thickness

Estimate the minimum riprap layer thickness, t_r, using the median stone size, D_{50}, computed in Step 2 by

$$t_r = 1.5\ D_{50} \tag{7.5}$$

or

$$t_r = D_{100}\ , \tag{7.6}$$

whichever thickness is greater. A riprap layer thickness greater than that prescribed in Eq. 7.5 or Eq. 7.6 can be specified.

Step 4. Estimate interstitial discharge

The average velocity of flow through the riprap layer can be determined by one of two means developed in the Phase I and Phase II reports. Method I requires that extensive testing of the rock source be conducted. Method II allows the user the opportunity to estimate interstitial velocities without significant testing of the rock source.

Method I

The average velocity of flow through the stone layer, V_i, can be estimated by determining the embankment slope, S; the coefficient of uniformity, $C_u = D_{60}/D_{10}$; the porosity, n_p; and the median stone size, D_{50}, of the source riprap. The average velocity through the riprap layer is computed by Eq. 1.1 as

$$V_i = 19.29\ [C_u^{-0.74}\ S^{0.46}\ n_p^{4.14}]^{1.064}\ (g\ D_{50})^{0.5}\ , \tag{7.7}$$

where velocity is in feet per second.

Method II

The average velocity of flow through the stone layer, V_i, can be estimated by determining the embankment slope, S, and the soil particle size at which 10% of the soil weight is finer, D_{10}. The average velocity is computed by Eq. 5.2 as

$$V_i = 0.232\ (g\ D_{10}\ S)^{1/2}\ , \tag{7.8}$$

where velocity is in feet per second and g is the acceleration of gravity, 32.2 ft/s^2.

Interstitial Discharge

The interstitial unit discharge, q_i, is estimated by multiplying the interstitial velocity, V_i, (using either Eq. 7.7 or Eq. 7.8) by the thickness of the rock layer, t_r expressed in feet, and multiplying by 1.0 foot, yielding

$$q_i = V_i t_r \times 1.0 \ , \tag{7.9}$$

where discharge is in cubic feet per second. The interstitial unit discharge, q_i, is assumed to be zero for covers comprised of a rock-soil matrix.

Step 5. Adjustment of the design surface discharge

The design surface unit discharge, q'_{design}, should be adjusted to reflect that a portion of the discharge, q_i, is through the riprap layer. Therefore,

$$q_{design} = q'_{design} - q_i \ , \tag{7.10}$$

where q_{design} is in cubic feet per second.

Step 6. Adjustment of the median stone size

The median stone size should be adjusted to reflect a reduced surface discharge. Repeat Step 2, substituting the adjusted unit discharge, q_{design}, for q'_{design} in Eq. 7.2. Then, compute the median stone size based upon a redefined value of q^*_{design}.

Step 7. Adjustment of the riprap layer thickness

Using the adjusted median stone size from Step 6, compute the adjusted riprap layer thickness as outlined in Step 3.

Step 8. Median stone size adjustment for gradation

The median stone size, D_{50} , of the riprap layer should be modified on the basis of the riprap gradation. Determine the coefficient of uniformity, C_u, of the riprap source material. Then, enter Fig. 4.6 with the coefficient of uniformity, and obtain the coefficient of rock gradation, C_{GR}. Multiply the median stone size resulting from Step 6 by the coefficient of gradation as

$$D'_{50} = D_{50} \times C_{GR} \ , \tag{7.11}$$

where D'_{50} is in inches.

Step 9. Median stone size adjustment for layer thickness

For $D_{50} \geq 6$ in.:

Adjustment is not required.

$D_{50} < 6$ in.:

In the case(s) where the adjusted design unit discharge for stone movement results in a median stone size, D'_{50} of < 6 in., it was recommended that a riprap layer thicker than 1.5 D_{50} may be warranted. However, the median stone size can be adjusted to compensate for the reduced layer thickness. To modify the median stone size, D'_{50}, from

Step 8, obtain the design riprap layer thickness resulting from Step 3. From Fig. 4.8, determine the coefficient of layer thickness, C_t. Multiply the median stone size, D' , from Step 8 by the coefficient of layer thickness as

$$D^*_{50} = D'_{50} \times C_t \ , \tag{7.12}$$

where D^*_{50} is in inches.

7.2 COMMENTS

The research presented strongly supported the use of a filter layer beneath the riprap layer. The filter tends to bed and stabilize the stones, prevents migration of particles beneath the filter, and reduces any pressure gradient that may exist from seepage. However, information indicating the optimal filter thickness is not available. Therefore, the use of a filter layer > 6 in. thick is highly recommended.

8. CONCLUSIONS

A series of 90 laboratory experiments was conducted in the Phase I and Phase II studies in which riprapped embankments were subjected to overtopping flows. Embankment slopes of 1, 2, 8, 10, and 20% were protected with riprap layers, 1.5 to 4 D_{50} in thickness, comprising median stone sizes of 1, 2, 4, 5, and/or 6 in. Design criteria were developed for overtopping flows addressing stone size, stone shape, layer thickness, stone gradation, interstitial velocity, resistance to surface flow, and the effects of flow concentration on riprap stability. Specific findings are as follows:

- A unique riprap design relationship was developed to determine median stone size on the basis of the unit discharge and embankment slope for overtopping flows.

- A design criterion was developed to size rounded riprap for potential erosion-control applications. The rounded riprap required oversizing of about 40% to provide the same level of protection as the angular riprap.

- The median stone size should be increased by increasing the design unit discharge by 35% to prevent rock movement.

- Two procedures were derived to estimate interstitial velocities though the riprap layer. Both procedures are based on a representative stone size and embankment slope.

- A unique procedure was derived to estimate the resistance to surface water flow using the Manning's n coefficient. The resistance to flow was found to be a function of the stone size and embankment slope for angular-riprap-covered slopes.

- Flow channelization occurred along the riprap-protected embankment when the unit discharge approached 88% of the unit discharge at failure.

- A procedure was developed to adjust the median stone size on the basis of the proposed riprap layer thickness for stone sizes < 6 in. The stone layer should not be < 1.5 D_{50}.

- Riprap gradation was determined to significantly influence riprap stability. It was recommended that the coefficient of uniformity be ≤ 2.3. A procedure was developed to adjust the median stone size on the basis of the riprap gradation.

- The application of soil covers over riprap layers caused premature barrier failure. Soil covers should not exceed 3 to 4 in. thick above the riprap surface.

- The application of a riprap-soil matrix without soil cover was determined to stabilize the riprap barrier. In many cases, the matrix may increase stability beyond riprap alone.

- Flow concentrations will occur on riprapped embankments. Flow concentration factors of 1.0 to 3.0 are recommended to adjust the design unit discharge.

- A riprap design procedure was developed for sizing the median stone size for rock protection subjected to overtopping flow.

9. REFERENCES

Abt, S. R., et al., May 1987, Development of Riprap Design Criteria by Riprap Testing in Flumes: Phase I, USNRC Report NUREG/CR-4651, prepared for NRC by Colorado State University and Oak Ridge National Laboratory.

Anderson, A. G., A. S. Paintal, and J. T. Davenport, 1970, Tentative Design Procedure for Riprap Lined Channels, Report 108, National Cooperative Highway Research Program.

Barnes, H. H., 1967, Roughness Characteristics of Natural Channels, Water-Supply Paper 1849, U.S. Geological Survey.

Bathurst, J. C., 1985, "Flow Resistance Estimation in Mountain Rivers," J. Hydrol. Eng., III (4), Paper 19661.

CDH (California Division of Highways, Department of Public Works), 1970, Bank and Shore Protection in California Highway Practice, p. 423.

Chow, V. T., 1959, Open-Channel Hydraulics, McGraw-Hill Book Co.

Codell, R. B., 1986, "Runoff from Armoured Slopes," Proceedings from Geo-technical and Geo-hydrological Aspects of Waste Management, Colorado State University, Fort Collins, Colorado.

COE (U.S. Army Corps of Engineers), July 1970, Hydraulic Design of Flood Control Channels, EM 1110-2-1601, U.S. Army Corps of Engineers.

COE (U.S. Army Corps of Engineers), May 1971, Engineering and Design, Additional Guidance for Riprap Channel Protection, ETL-1110-2-120, Office of the Chief of Engineers, U.S. Army Corps of Engineers.

DOI (U.S. Department of the Interior), 1978, Hydraulic Design of Stilling Basins and Energy Dissipators, Engineering Monograph 25, Bureau of Reclamation, U.S. Department of the Interior.

Jarrett, R. D., 1984, "Hydraulics of High-Gradient Streams," J. Hydrol. Eng., ASCE 101 (11), 1519-39.

Lacey, G., 1946-1947, "A General Theory of Flow in Alluvium," J. Inst. Civ. Eng., London, Vol. 27, Paper 55118, pp. 16-47.

Limerinos, J. T., 1970, Determination of the Manning's Coefficient from Measured Bed Roughness in Natural Channels, Water Supply Paper 1898-B, U.S. Geological Survey, Washington, D.C.

Mavis, F. T., and L. M. Laushey, 1948, "A Reappraisal of the Beginnings of Bed Movement-Competent Velocity," Proceedings of the International Association for Hydraulic Structurs Research, Stockholm, Sweden.

Nelson, J. D., et al., May 1986, Methodologies for Evaluating Long-Term Stabilization Designs of Uranium Mill Tailings Impoundments, Phase I Report, NUREG/CR-4620, U.S. Nuclear Regulatory Commission, Silver Spring, Maryland.

Richardson, E. V., et al., 1975, Highways in the River Environment - Hydraulics and Environmental Design Considerations, U.S. Department of Transportation. Available from Publications Office, Engineering Research Center, Colorado State University, Fort Collins, Colorado 80523.

Ruff, J. F., et al., August 1985, Riprap Tests in Flood Control Channels, prepared by Colorado State University for the U.S. Army Corps of Engineers, Waterways Experiment Station, Vicksburg, Miss., CER85-86JFR-AS-SRA-EVR17.

Sherard, J. C., L. P. Dunnigan, and J. R. Talbot, June 1984, "Basic Properties of Sand and Gravel Filters," J. Geotech. Eng. Div., ASCE 110 (6).

Sherard, J. L., et al., 1963, Earth and Earth Rock Dams, John Wiley.

Simons, D. B. and F. Senturk, 1977, Sediment Transport Technology, Water Resources Publications, Fort Collins, Colorado.

Stephenson, D., 1979, "Rockfill in Hydraulic Engineering," pp. 50-60 in Developments in Geotechnical Engineering, Vol. 27, Elsevier Scientific Publishing Co.

Strickler, A., 1923, "Beitrage zur Frage der Geschwindigkeits-formel und der Rauhigkeitszahlen fur Strome, Kanale und Geschlossene Leitungen" (Some contributions to the problems of the velocity formula and roughness factor for rivers, canals and closed conduits), Mitt. Eidg. Amtes Wasserwirtsch., Bern, Switzerland, No. 16 g.

Vanoni, V. A., ed., 1975, Sedimentation Engineering, prepared by the American Society of Civil Engineers, Task Committees for Preparation of Manual on Sedimentation, Sedimentation Committee of Hydraulics Division, Manuals and Reports on Engineering Practice, 54, New York, N.Y.

APPENDIX A

RIPRAP, FILTER, AND SOIL GRAIN SIZE DISTRIBUTION

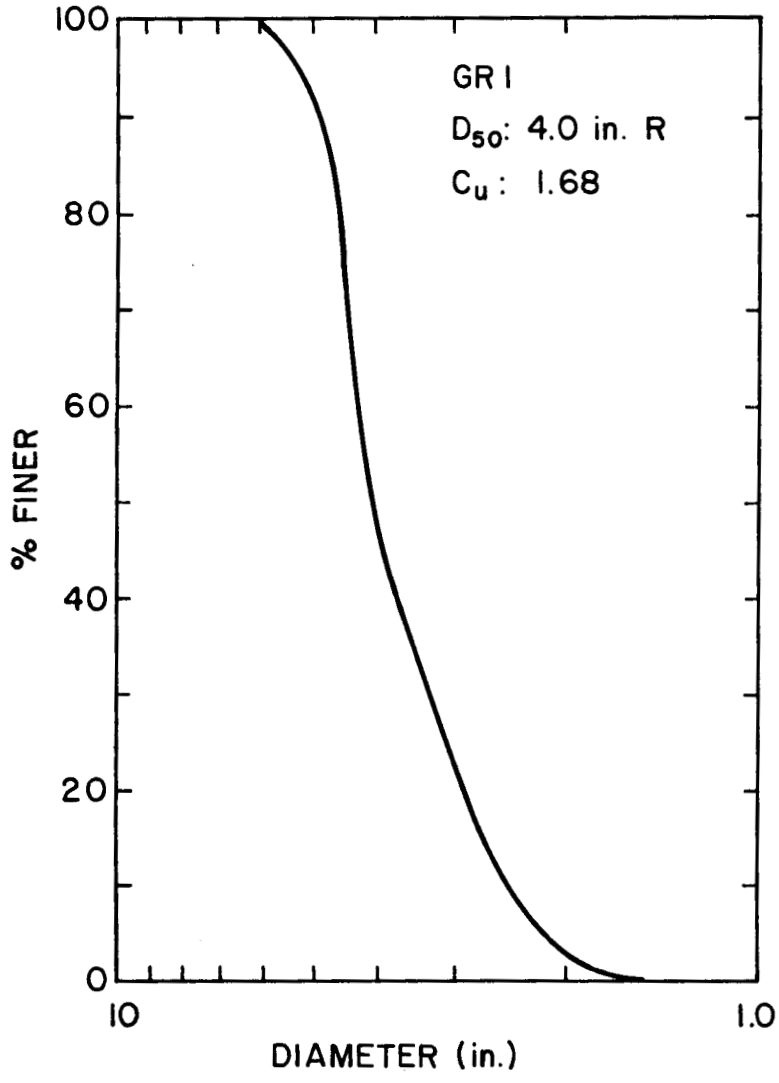

Figure A.1. Grain size distribution of grade 1 (GR1) riprap. D_{50} = median stone size, R = rounded shape, C_u = coefficient of uniformity.

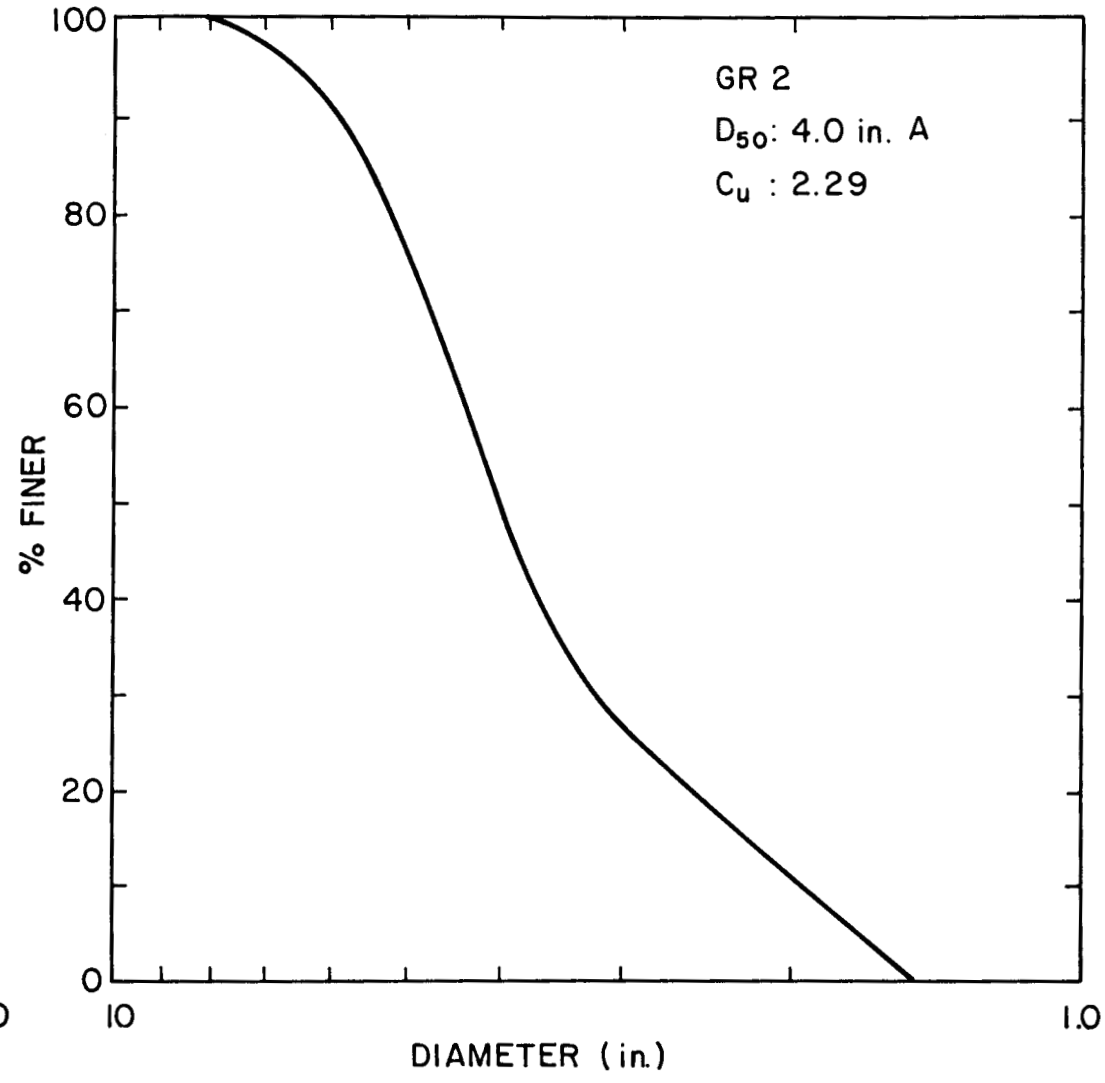

Figure A.2. Grain size distribution of grade 2 (GR2) riprap. D_{50} = median stone size, A = angular shape, C_u = coefficient of uniformity.

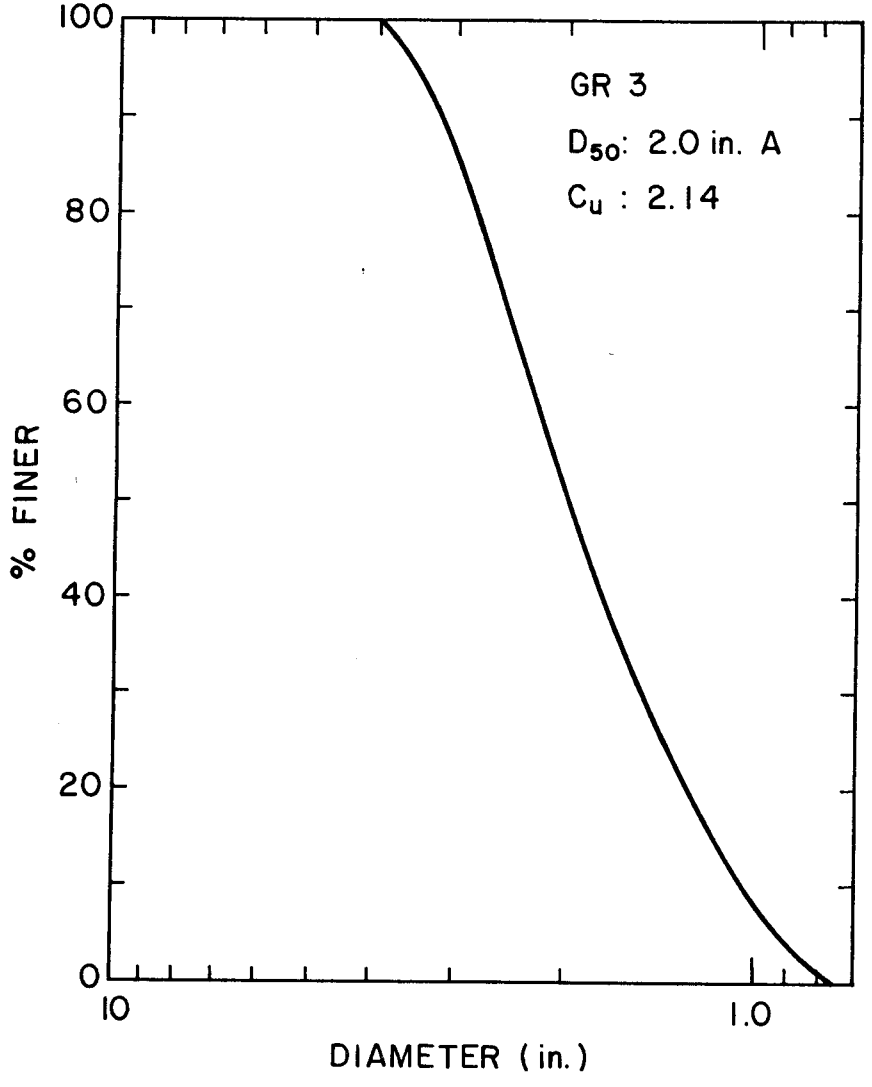

Figure A.3. Grain size distribution of grade 3 (GR3) riprap. D_{50} = median stone size, A = angular shape, C_u = coefficient of uniformity.

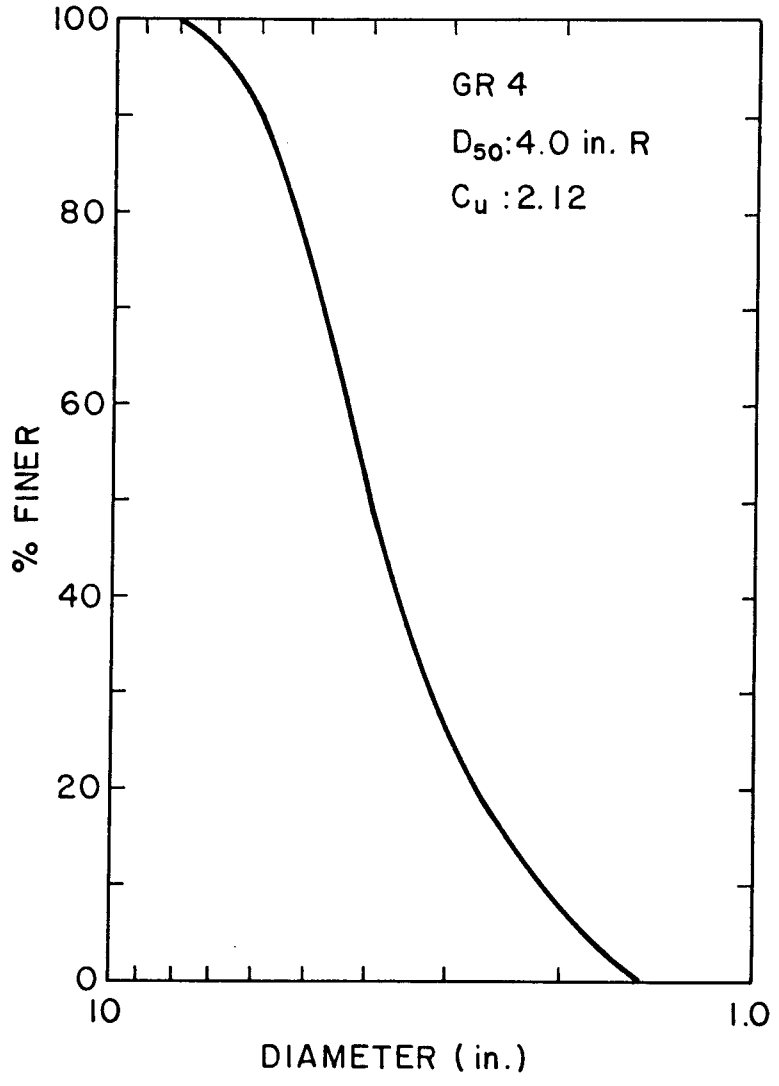

Figure A.4. Grain size distribution of grade 4 (GR4) riprap. D_{50} = median stone size, R = rounded shape, C_u = coefficient of uniformity.

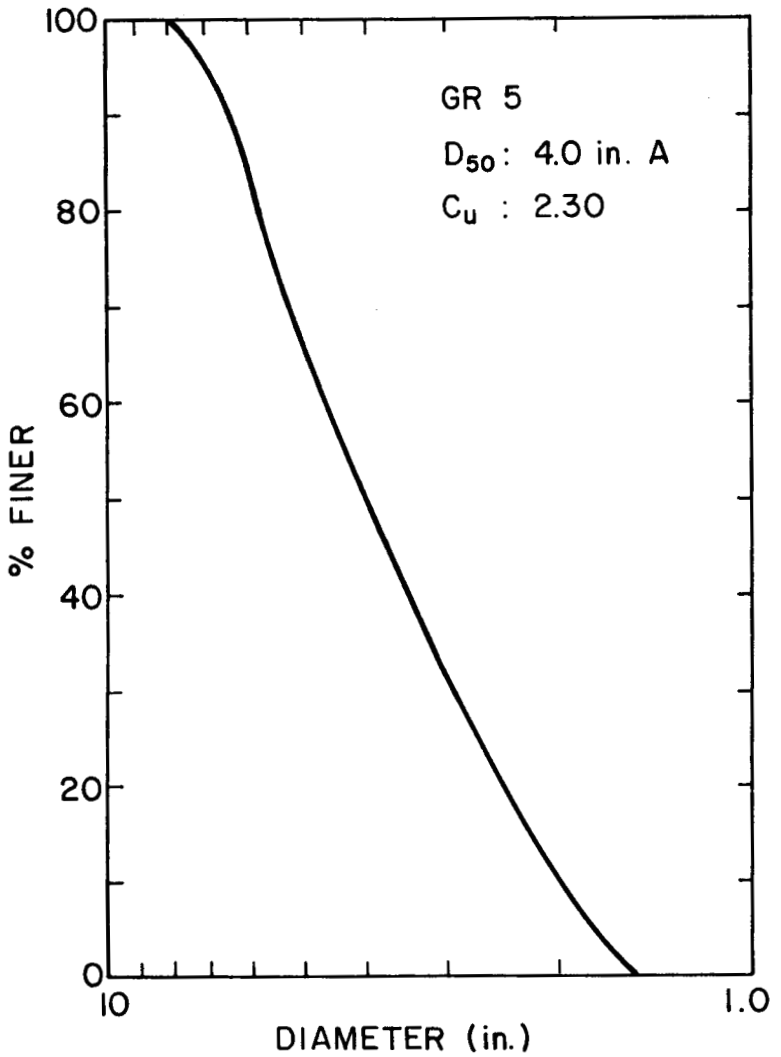

Figure A.5. Grain size distribution of grade 5 (GR5) riprap. D_{50} = median stone size, A = angular shape, C_u = coefficient of uniformity.

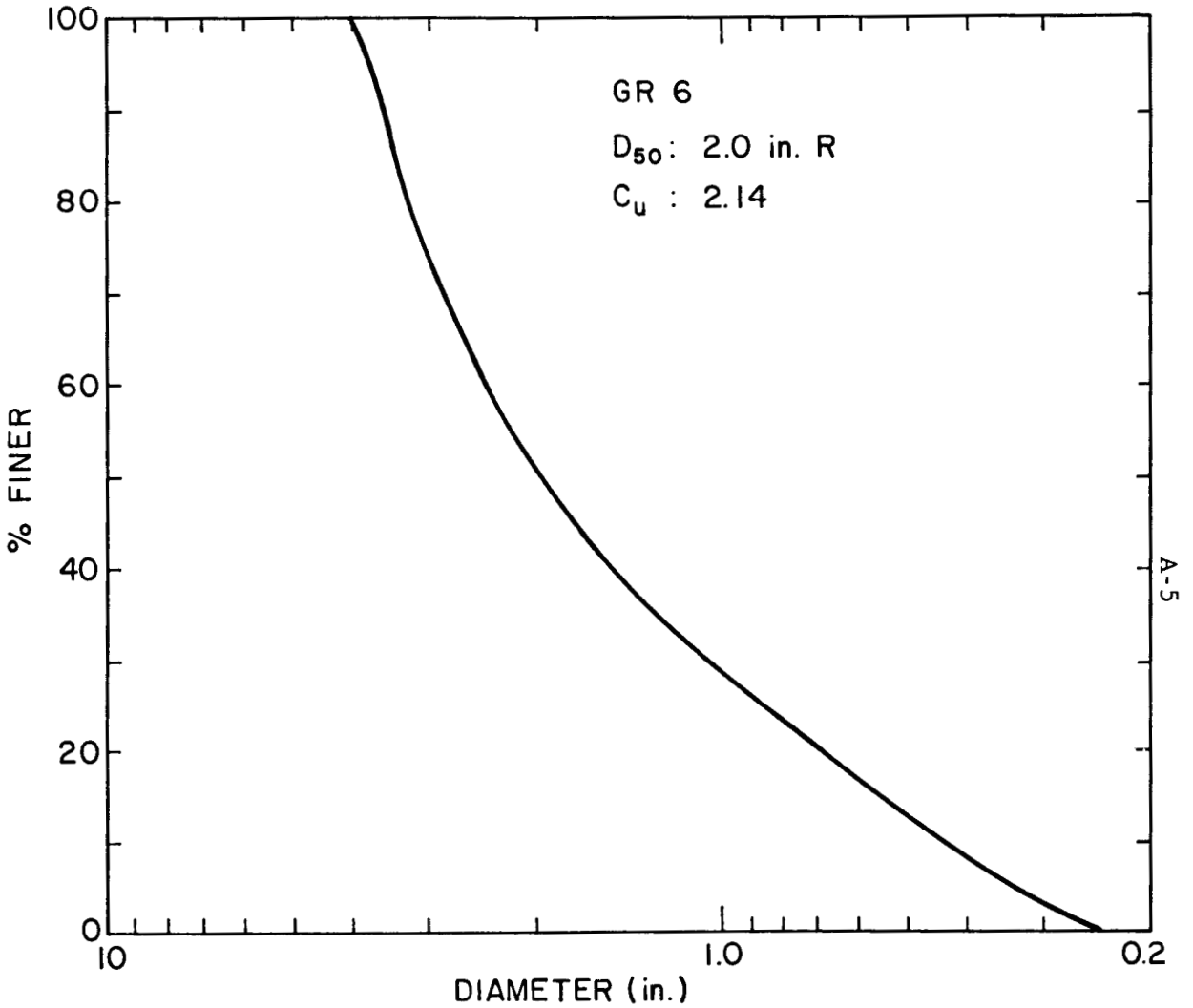

Figure A.6. Grain size distribution of grade 6 (GR6) riprap. D_{50} = median stone size, R = rounded shape, C_u = coefficient of uniformity.

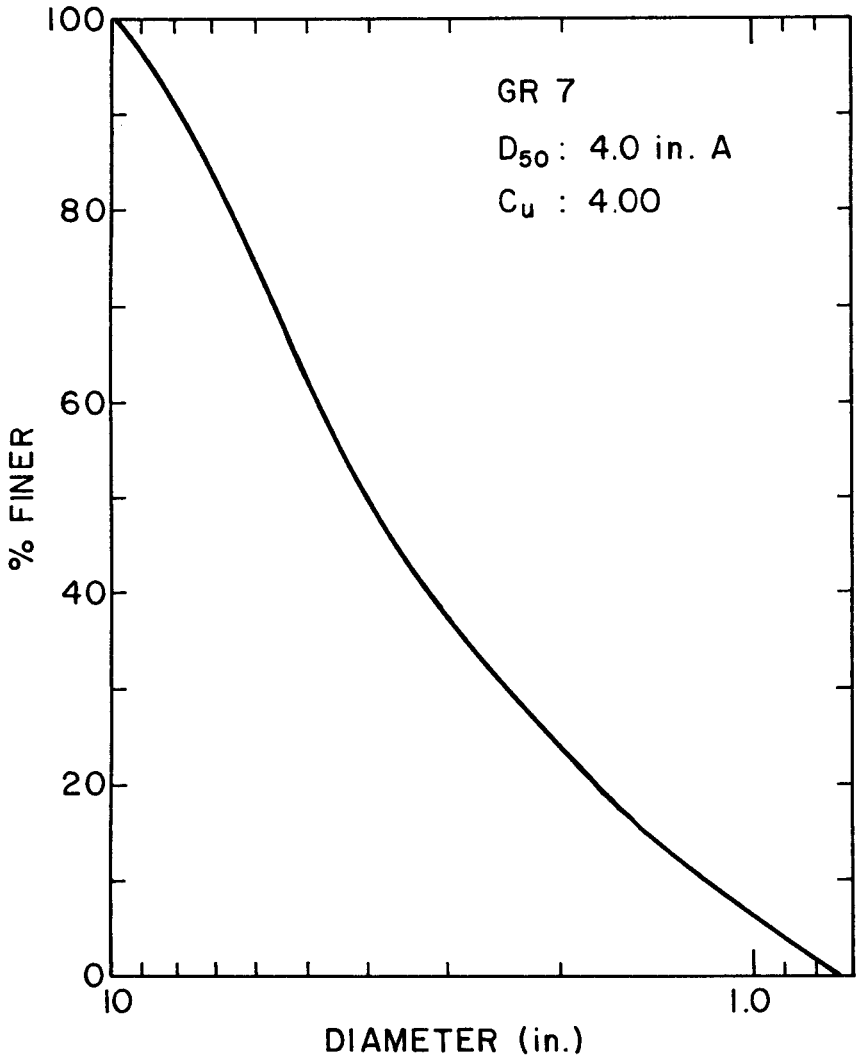

Figure A.7. Grain size distribution of grade 7 (GR7) riprap. D_{50} = median stone size, A = angular shape, C_u = coefficient of uniformity.

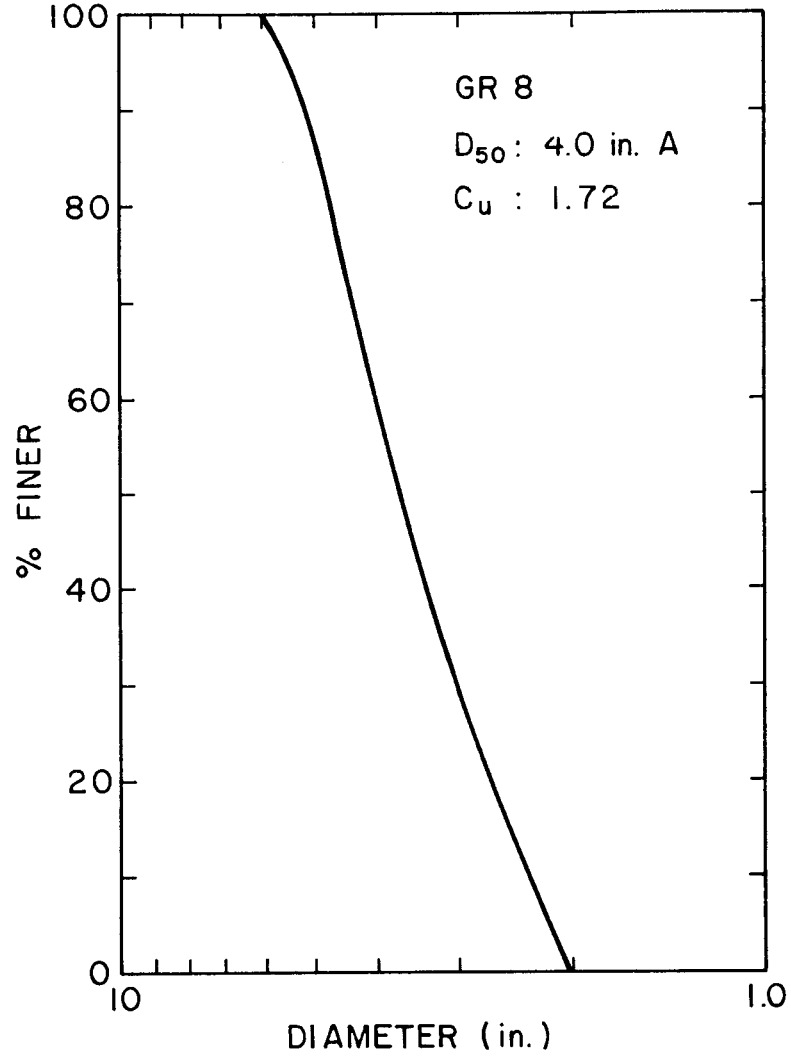

Figure A.8. Grain size distribution of grade 8 (GR8) riprap. D_{50} = median stone size, A = angular shape, C_u = coefficient of uniformity.

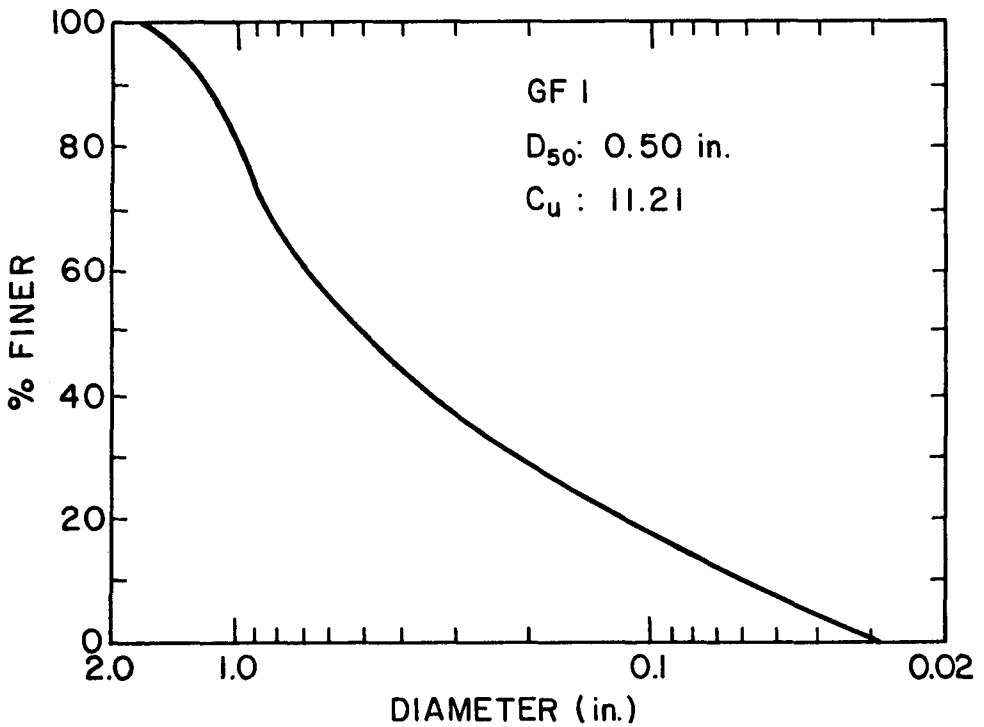

Figure A.9. Grain size distribution of filter filter gradation 1 (GF1) material. D_{50} = median stone size, C_u = coefficient of uniformity.

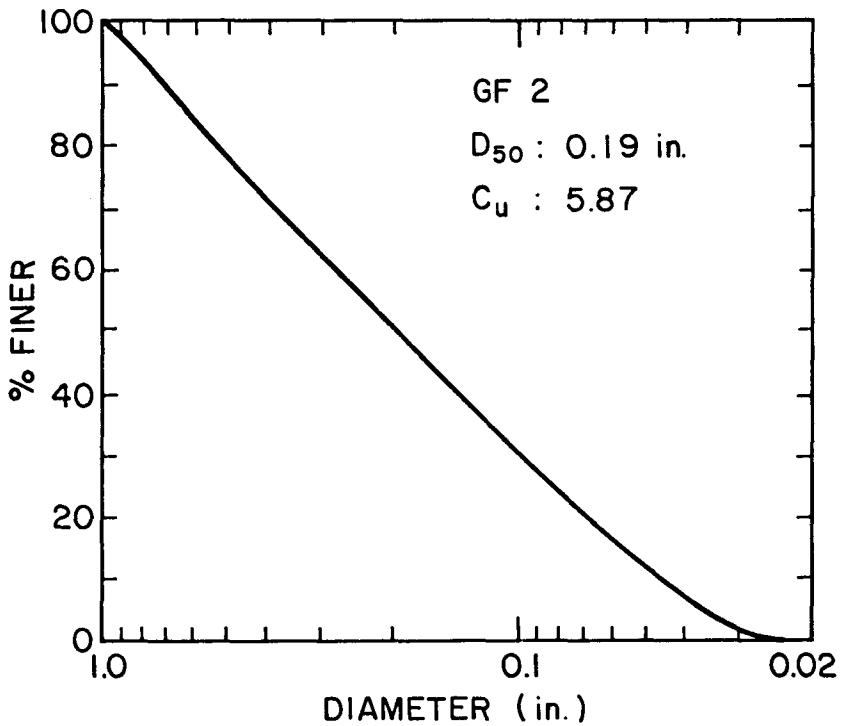

Figure A.10. Grain size distribution of filter gradation 2 material. D_{50} = median stone size, C_u = coefficient of uniformity.

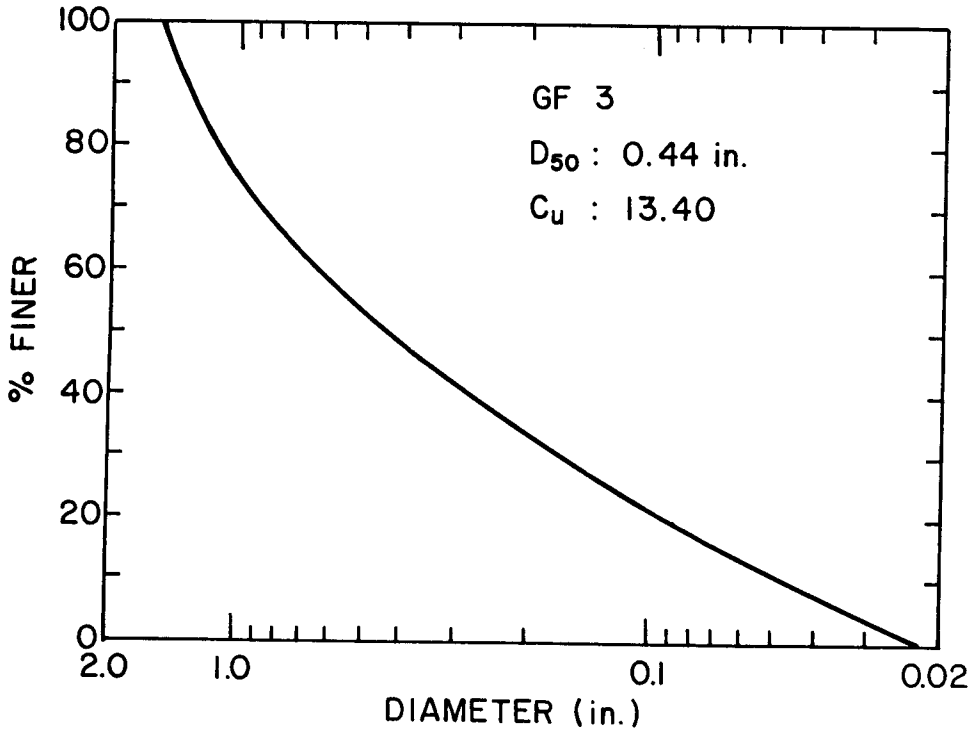

Figure A.11. Grain size distribution of filter gradation 3 (GF3) material. D_{50} = median stone size, C_u = coefficient of uniformity.

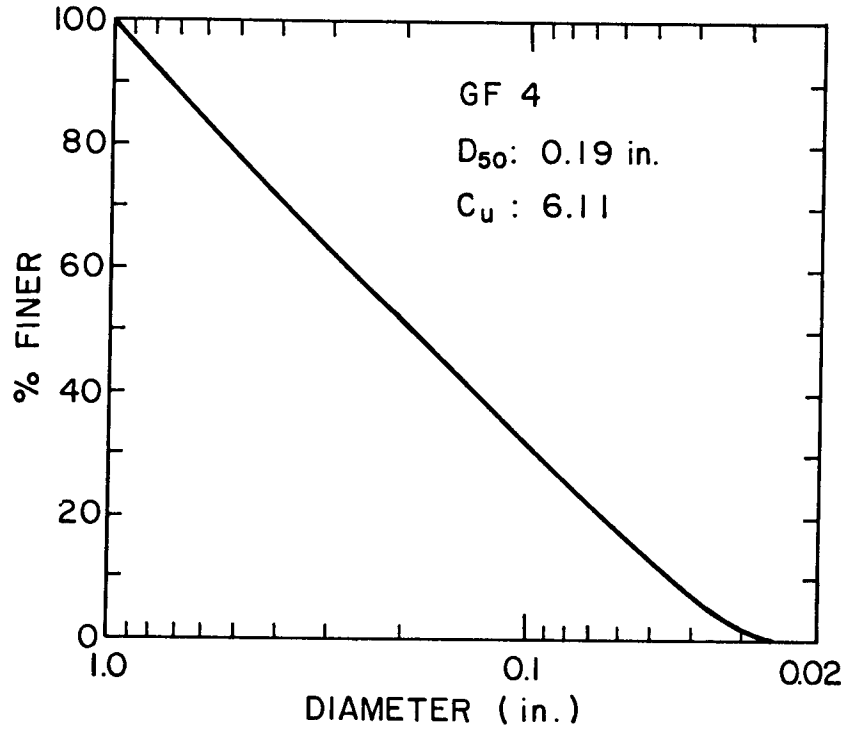

Figure A.12. Grain size distribution of filter gradation 4 (GF4) material. D_{50} = median stone size, C_u = coefficient of uniformity.

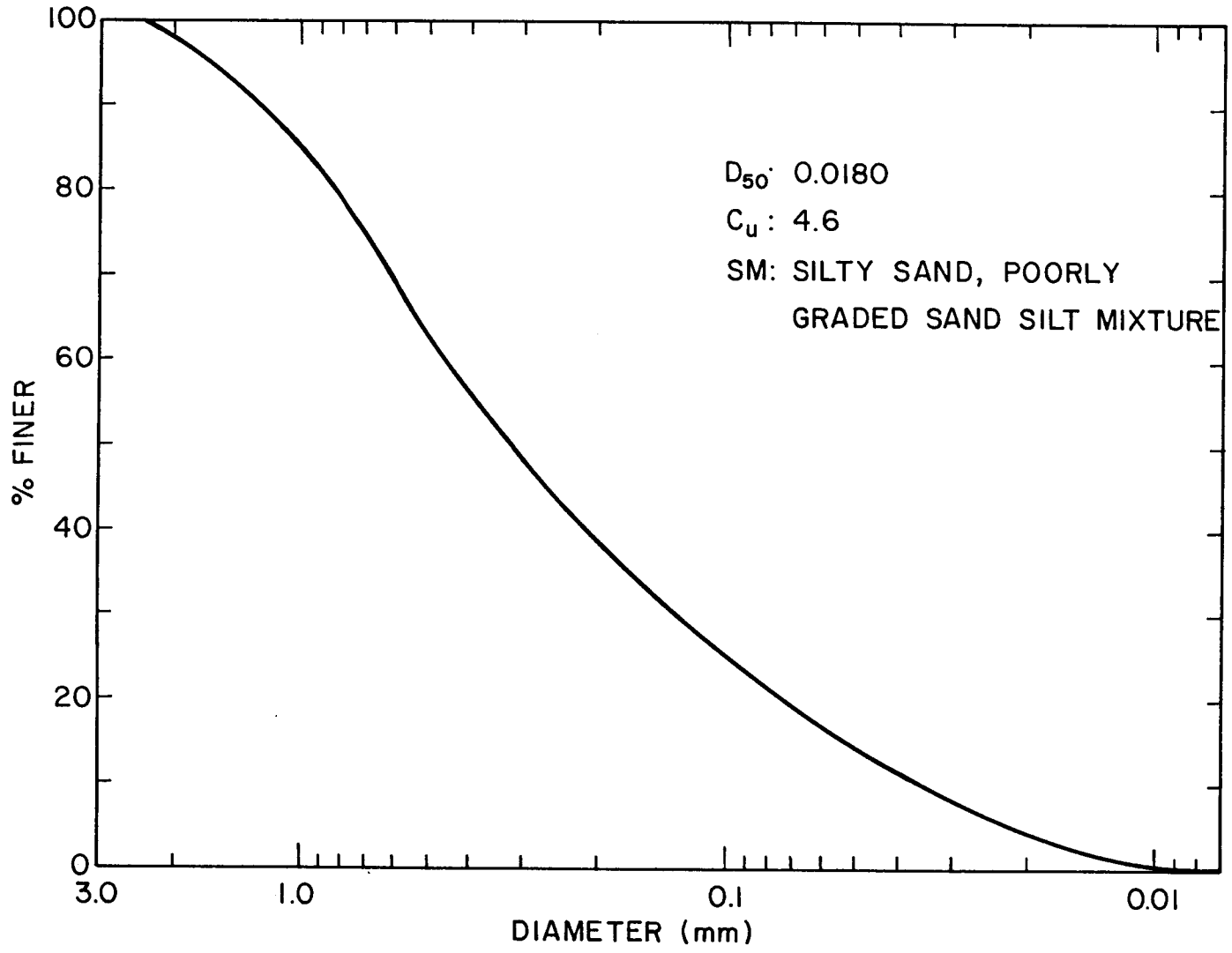

Figure A.13. Grain size distribution of sandy-silt soil mixture. D_{50} = median stone size, C_u = coefficient of uniformity.

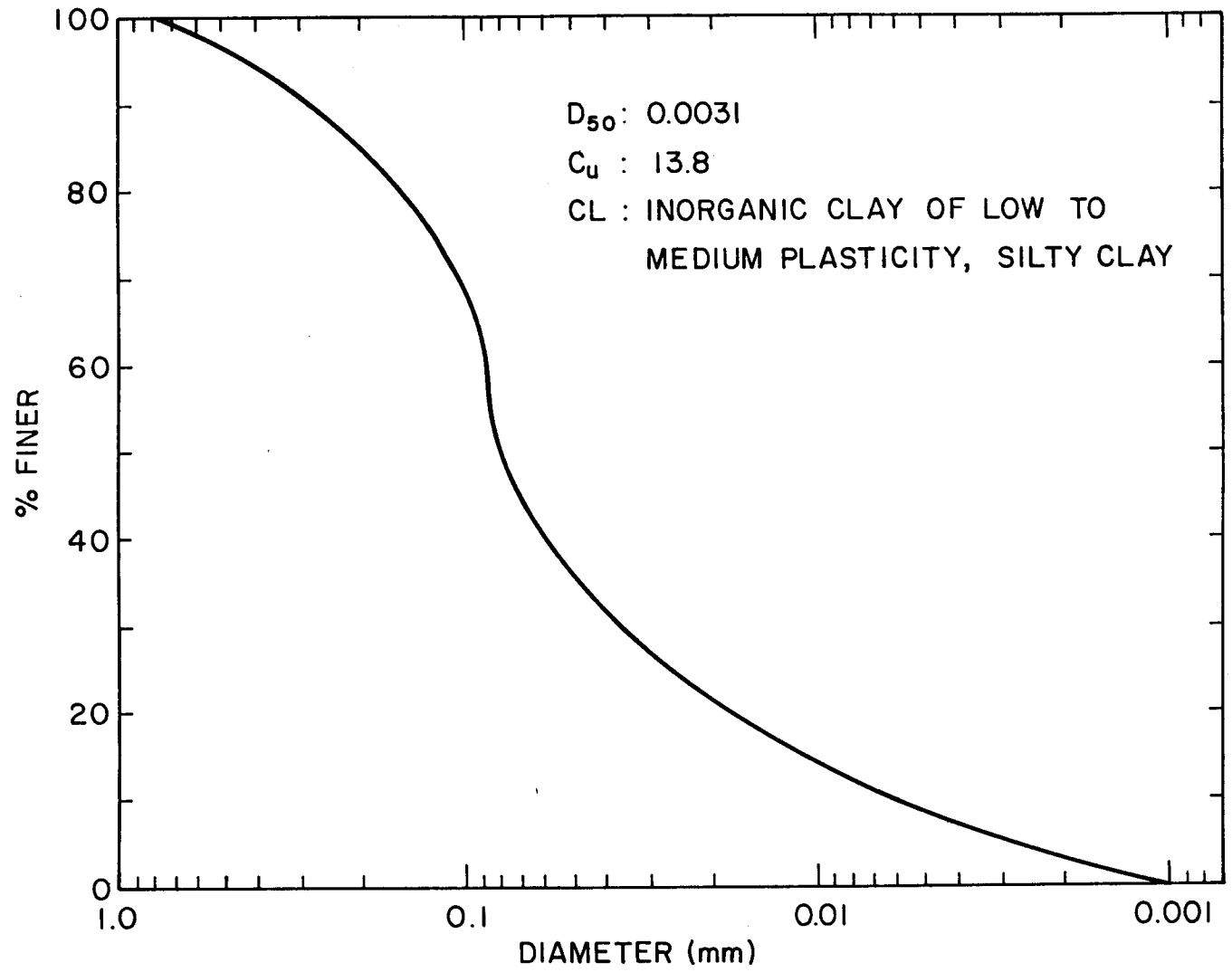

Figure A.14. Grain size distribution of silty-clay soil mixture. D_{50} = median stone size, C_u = coefficient of uniformity.

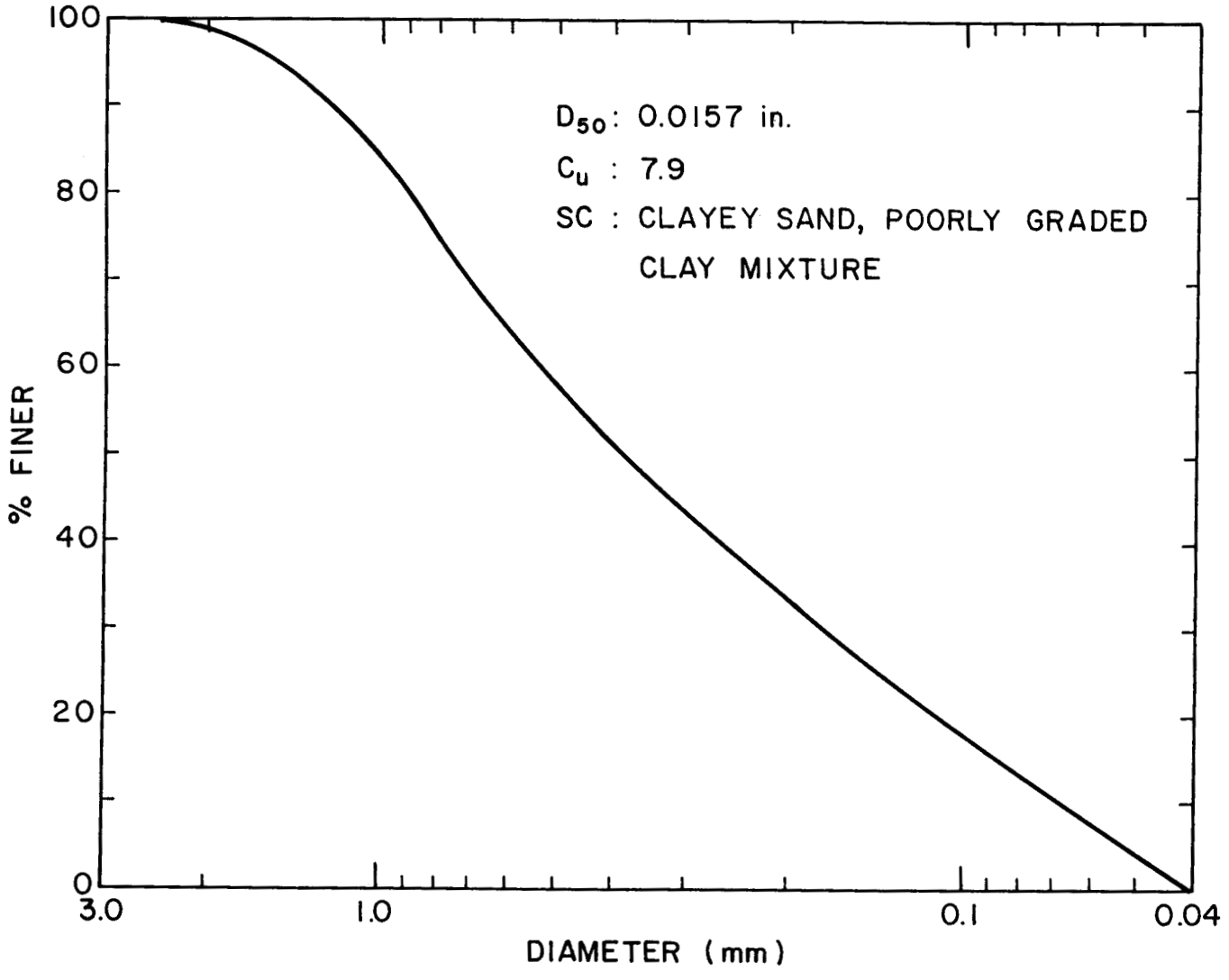

Figure A.15. Grain size distribution of the clayey-sand soil mixture. D_{50} = median stone size, C_u = coefficient of uniformity.

APPENDIX B

SUMMARY OF INTERSTITIAL VELOCITY PROFILES

APPENDIX B DEFINITIONS

d	depth of flow
D_{50}	median stone size
D_{10}	diameter at which 10% of the sample weight is finer
C_u	coefficient of uniformity
n_p	porosity
Q	channel discharge
q	discharge per foot of width
A	cross-sectional area
g	acceleration of gravity
S	gradient
V	velocity of flow

SUMMARY OF PHASE I AND PHASE II INTERSTITAL TESTS[a]

D-Test Number	D_{50}[b] (in.)	D_{10} (in.)	Slope (%)	Riprap Depth (in.)	C_u	n_p	Q (cfs)	Flow Depth (in.)	V_{tmax}	$\frac{Q}{A}$	$\frac{Q}{A\ n_p}$	$\sqrt{g\ D_{10} S}$	$0.232\ \sqrt{g\ D_{10} S}$	q* (cfs/ft)	$\frac{12\ q^*}{(g\ D_{50})^{0.5}\ (D_{50}\ ft)}$	$\frac{V}{(g\ D_{50})^{0.5}\ (D_{50}\ ft)}$
Phase II																
26	2.0	1.03	.10	3.0	2.14	0.45	1.10	0.198	0.45	0.2764	0.6142	1.8212	0.4225	0.0306	0.1606	0.1942
28	2.0	1.03	.10	4.0	2.14	0.45	1.16	0.013	0.47	0.2891	0.6424	1.8212	0.4225	0.0242	0.1243	0.2029
30	2.0	1.03	.10	6.0	2.14	0.45	1.84	0.156	0.63	0.2989	0.6642	1.8212	0.4225	0.0256	0.1295	0.2719
33	2.0	1.03	.10	8.0	2.14	0.45	2.05	1.150	0.50	0.2240	0.4979	1.8212	0.4225	0.0214	0.1088	0.2158
35	4.0 R	2.05	.10	6.0	2.12	0.36	0.97	-1.556	0.40	0.2183	0.6064	2.5692	0.5961	0.0135	0.0494	0.1221
37	4.0 R	2.05	.10	12.0	2.12	0.36	3.05	1.502	0.58	0.2259	0.6275	2.5692	0.5961	0.0212	0.0777	0.1770
39	4.0	2.00	.10	6.0	2.30	0.45	2.40	-0.624	0.49	0.4464	0.9920	2.5377	0.5887	0.0333	0.1209	0.1496
41	4.0	2.00	.10	8.0	2.30	0.45	2.52	0.017	0.62	0.3143	0.6984	2.5377	0.5887	0.0263	0.0952	0.2198
43	4.0	2.00	.10	12.0	2.30	0.45	3.33	1.430	0.75	0.2480	0.5511	2.5377	0.5887	0.0231	0.0842	0.2289
45	2.0 R	0.44	.10	6.0	2.14	0.36	1.64	1.042	0.39	0.2329	0.6469	1.1903	0.2761	0.0228	0.1181	0.1190
47	4.0	1.20	.10	12.0	4.00	0.39	2.46	0.000	0.36	0.2050	0.5256	1.9657	0.4560	0.0171	0.0623	0.1099
49	0.44	0.047	.10	6.0	13.40	0.33	0.23	0.477	0.08	0.0355	0.0911	0.3890	0.0902	0.0032	0.0331	0.0736
50	4.0	2.38	.10	12.0	1.72	0.46	5.58	3.907	0.66	0.3508	0.7626	2.7683	0.6422	0.0322	0.1172	0.2778
Phase I																
6	1.02	0.60	.01	3.0	1.75	0.44	0.11	0.000	0.10	0.0367	0.0833	0.4395	0.1020	0.0047	0.0341	0.0604
7	1.02	0.60	.02	3.0	1.75	0.44	0.11	0.000	0.13	0.0367	0.0833	0.6216	0.1442	0.0047	0.0341	0.0786
9	1.02	0.60	.10	3.0	1.75	0.44	0.21	0.000	0.24	0.0700	0.1591	1.3900	0.3225	0.0087	0.0631	0.1451
3	2.20	1.10	.02	6.0	2.09	0.45	0.33	0.000	0.23	0.0550	0.1222	0.8417	0.1953	0.0067	0.0331	0.0947
4	2.20	1.10	.01	6.0	2.09	0.45	0.23	0.000	0.15	0.0383	0.0852	0.5951	0.1381	0.0050	0.0247	0.0617
10	2.20	1.10	.10	6.0	2.09	0.45	0.56	0.000	0.36	0.0933	0.2074	1.8820	0.4366	0.0120	0.0593	0.1482
11	2.20	1.10	.10	6.0	2.09	0.45	0.56	0.000	0.37	0.0933	0.2074	1.8820	0.4366	0.0120	0.0593	0.1523
3	4.10	2.00	.20	12.0	2.15	0.44	4.34	0.000	0.72	0.3616	0.8212	3.5889	0.8326	0.030	0.1085	0.2171
4	4.10	2.00	.20	12.0	2.15	0.44	4.25	0.000	0.97	0.3542	0.8049	3.5889	0.8326	0.0290	0.1049	0.2924
8	5.10	3.45	.20	12.0	1.62	0.46	5.70	0.000	1.04	0.4750	1.0326	4.7136	1.0936	0.0396	0.1284	0.2811
8	5.10	3.45	.20	12.0	1.62	0.46	5.96	0.000	0.86	0.4967	1.0797	4.7136	1.0936	0.0414	0.1343	0.2325
14	6.20	3.80	.20	12.0	1.69	0.46	6.22	0.000	1.51	0.5138	1.1268	4.9469	1.1477	0.0432	0.1271	0.3702

[a]See preceding page for definitions.

[b]Angular-shaped rock except where noted "R" (rounded).

APPENDIX C

SUMMARY OF HYDRAULIC DATA

Table C.1. Summary of Phase II hydraulic data[a]

Run No.	Piezo No.	Median Stone Size D_{50} (in.)	Surface Discharge Q_s (cfs)	Total Discharge Q_T (cfs)	Slope S	Depth D=R (ft)	Velocity V (fps)	Area of Flow A (ft^2)	Froude Number F	Manning's n	Shields' Coefficient C_c	Reynold's Number R_e	Darcy-Weisbach Friction Factor f
21	8	4.00	7.30	9.00	0.20	0.09	6.70	1.09	3.92	0.020	0.033	18081	0.104
21	12	4.00	7.30	9.00	0.20	0.10	6.13	1.19	3.43	0.023	0.036	18892	0.136
22	9	4.00	4.96	6.66	0.20	0.07	5.57	0.89	3.61	0.021	0.027	16338	0.123
22	12	4.00	4.96	6.66	0.20	0.09	4.72	1.05	2.81	0.028	0.032	17746	0.202
22	9	4.00	6.98	8.68	0.20	0.12	5.02	1.39	2.60	0.031	0.042	20418	0.237
22	12	4.00	6.98	8.68	0.20	0.13	4.36	1.60	2.11	0.040	0.048	21906	0.361
22	9	4.00	8.00	9.70	0.20	0.13	5.03	1.59	2.44	0.034	0.048	21838	0.270
22	12	4.00	8.00	9.70	0.20	0.15	4.44	1.80	2.02	0.042	0.055	23235	0.391
22	7	4.00	8.52	10.22	0.20	0.11	6.71	1.27	3.63	0.022	0.038	19517	0.121
22	9	4.00	8.52	10.22	0.20	0.14	4.90	1.74	2.27	0.037	0.053	22845	0.312
22	12	4.00	8.52	10.22	0.20	0.16	4.48	1.90	1.99	0.043	0.058	82372	0.406
22	7	4.00	9.25	10.95	0.20	0.12	6.29	1.47	3.17	0.026	0.045	20998	0.159
22	9	4.00	9.25	10.95	0.20	0.15	5.17	1.79	2.36	0.036	0.054	23171	0.288
27	9	2.00	0.82	1.94	0.10	0.04	1.71	0.48	1.51	0.032	0.015	4242	0.353
27	9	2.00	1.86	2.98	0.10	0.07	2.24	0.83	1.50	0.035	0.025	5578	0.355
27	12	2.00	1.86	2.98	0.10	0.07	2.24	0.83	1.50	0.035	0.025	5578	0.355
27	9	2.00	4.27	5.39	0.10	0.12	2.99	1.43	1.52	0.038	0.043	7322	0.344
27	12	2.00	4.27	5.39	0.10	0.12	2.89	1.48	1.45	0.040	0.045	7449	0.382
27	9	2.00	6.44	7.56	0.10	0.16	3.34	1.93	1.47	0.042	0.058	8506	0.372
27	12	2.00	6.44	7.56	0.10	0.16	3.25	1.98	1.41	0.043	0.060	8616	0.402
27	8	2.00	8.09	9.21	0.10	0.13	5.06	1.60	2.44	0.024	0.048	7745	0.134
27	9	2.00	8.09	9.21	0.10	0.19	3.63	2.23	1.48	0.042	0.068	9144	0.364
27	12	2.00	8.09	9.21	0.10	0.19	3.55	2.28	1.43	0.044	0.069	9246	0.389
29	7	2.00	2.40	3.56	0.10	0.08	2.40	1.00	1.47	0.037	0.030	6123	0.373
29	7	2.00	3.57	4.73	0.10	0.11	2.64	1.35	1.39	0.041	0.041	7114	0.414
29	7	2.00	5.61	6.77	0.10	0.16	2.95	1.90	1.31	0.047	0.058	8440	0.468
29	8	2.00	5.61	6.77	0.10	0.21	2.22	2.53	0.85	0.075	0.077	9739	1.105
29	7	2.00	7.54	8.70	0.10	0.19	3.28	2.30	1.32	0.048	0.070	9286	0.459
29	8	2.00	7.54	8.70	0.10	0.24	2.62	2.88	0.94	0.069	0.087	10391	0.902
29	9	2.00	7.54	8.70	0.10	0.25	2.50	3.01	0.88	0.075	0.091	10623	1.030
29	10	2.00	7.54	8.70	0.10	0.26	2.38	3.17	0.82	0.081	0.096	10902	1.203
29	11	2.00	7.54	8.70	0.10	0.24	2.61	2.89	0.94	0.070	0.088	10409	0.911
29	7	2.00	9.05	10.21	0.10	0.21	3.55	2.55	1.36	0.047	0.077	9778	0.435
29	8	2.00	9.05	10.21	0.10	0.26	2.89	3.13	1.00	0.066	0.095	10833	0.804
29	11	2.00	9.05	10.21	0.10	0.27	2.75	3.29	0.93	0.072	0.100	11106	0.933
31	7	2.00	2.45	4.29	0.10	0.06	3.55	0.69	2.61	0.020	0.021	5086	0.117
31	10	2.00	2.45	4.29	0.10	0.06	3.22	0.76	2.26	0.023	0.023	5338	0.157
31	7	2.00	5.56	7.40	0.10	0.11	4.31	1.29	2.32	0.025	0.039	6954	0.149
31	10	2.00	5.56	7.40	0.10	0.13	3.68	1.51	1.83	0.032	0.046	7524	0.239

Table C.1. (continued)

Run No.	Piezo No.	Median Stone Size D_{50} (in.)	Surface Discharge Q_s (cfs)	Total Discharge Q_T (cfs)	Slope S	Depth D-R (ft)	Velocity V (fps)	Area of Flow A (ft^2)	Froude Number F	Manning's n	Shields' Coefficient C_c	Reynold's Number R_e	Darcy-Weisbach Friction Factor f
31	11	2.00	5.56	7.40	0.10	0.11	4.31	1.29	2.32	0.025	0.039	6954	0.149
31	7	2.00	7.20	9.04	0.10	0.14	4.26	1.69	2.00	0.030	0.051	7960	0.200
31	10	2.00	7.20	9.04	0.10	0.15	3.98	1.81	1.81	0.033	0.055	8238	0.246
31	11	2.00	7.20	9.04	0.10	0.15	4.14	1.74	1.92	0.031	0.053	8077	0.218
31	12	2.00	7.20	9.04	0.10	0.11	5.26	1.37	2.74	0.021	0.042	7167	0.106
31	7	2.00	7.99	9.83	0.10	0.14	4.59	1.74	2.13	0.028	0.053	8077	0.177
31	9	2.00	7.99	9.83	0.10	0.12	5.59	1.43	2.85	0.020	0.043	7322	0.098
31	10	2.00	7.99	9.83	0.10	0.16	4.08	1.96	1.78	0.034	0.059	8572	0.253
31	11	2.00	7.99	9.83	0.10	0.16	4.23	1.89	1.88	0.032	0.057	8418	0.227
31	12	2.00	7.99	9.83	0.10	0.12	5.44	1.47	2.74	0.021	0.045	7424	0.107
31	7	2.00	10.15	11.99	0.10	0.17	4.86	2.09	2.05	0.030	0.063	8852	0.190
31	10	2.00	10.15	11.99	0.10	0.18	4.59	2.21	1.89	0.033	0.067	9103	0.225
31	11	2.00	10.15	11.99	0.10	0.20	4.25	2.39	1.68	0.038	0.072	9466	0.284
31	12	2.00	10.15	11.99	0.10	0.23	3.73	2.72	1.38	0.047	0.082	10098	0.419
32	11	2.00	5.50	7.34	0.10	0.16	2.79	1.97	1.21	0.050	0.060	8594	0.543
32	12	2.00	5.50	7.34	0.10	0.14	3.33	1.65	1.58	0.038	0.050	7865	0.319
32	11	2.00	7.01	8.85	0.10	0.19	3.02	2.32	1.21	0.052	0.070	9326	0.545
32	12	2.00	7.01	8.85	0.10	0.15	3.79	1.85	1.70	0.036	0.056	8328	0.277
32	11	2.00	8.28	10.12	0.10	0.21	3.35	2.47	1.30	0.049	0.075	9623	0.472
32	12	2.00	8.28	10.12	0.10	0.18	3.94	2.10	1.66	0.037	0.064	8873	0.290
32	11	2.00	9.57	11.41	0.10	0.22	3.65	2.62	1.38	0.047	0.079	9911	0.422
32	12	2.00	9.57	11.41	0.10	0.19	4.16	2.30	1.67	0.038	0.070	9286	0.285
32	11	2.00	10.69	12.53	0.10	0.23	3.93	2.72	1.45	0.044	0.082	10098	0.378
32	12	2.00	10.69	12.53	0.10	0.20	4.55	2.35	1.81	0.035	0.071	9386	0.244
32	7	2.00	11.48	13.32	0.10	0.30	3.18	3.61	1.02	0.066	0.109	11634	0.766
32	11	2.00	11.48	13.32	0.10	0.23	4.24	2.71	1.57	0.041	0.082	10080	0.324
32	12	2.00	11.48	13.32	0.10	0.21	4.59	2.50	1.77	0.036	0.076	9681	0.255
34	7	2.00	5.94	7.94	0.10	0.21	2.36	2.52	0.91	0.070	0.076	9720	0.974
34	8	2.00	5.94	7.94	0.10	0.20	2.49	2.39	0.98	0.064	0.072	9466	0.831
34	9	2.00	5.94	7.94	0.10	0.21	2.38	2.50	0.92	0.070	0.076	9681	0.951
34	10	2.00	5.94	7.94	0.10	0.11	4.60	1.29	2.47	0.023	0.039	6954	0.131
34	11	2.00	5.94	7.94	0.10	0.16	3.05	1.95	1.33	0.046	0.059	8550	0.451
34	12	2.00	5.94	7.94	0.10	0.14	3.49	1.70	1.64	0.037	0.052	7983	0.299
34	7	2.00	8.06	10.06	0.10	0.24	2.81	2.87	1.01	0.064	0.087	10373	0.781
34	8	2.00	8.06	10.06	0.10	0.23	2.89	2.79	1.06	0.062	0.085	10227	0.718
34	9	2.00	8.06	10.06	0.10	0.24	2.78	2.90	1.00	0.066	0.088	10427	0.806
34	10	2.00	8.06	10.06	0.10	0.13	5.07	1.59	2.45	0.024	0.048	7721	0.133
34	11	2.00	8.06	10.06	0.10	0.20	3.29	2.45	1.28	0.050	0.074	9584	0.486
34	12	2.00	8.06	10.06	0.10	0.15	4.36	1.85	1.96	0.031	0.056	8328	0.209
34	7	2.00	9.62	11.62	0.10	0.25	3.24	2.97	1.15	0.057	0.090	10552	0.608
34	8	2.00	9.62	11.62	0.10	0.24	3.33	2.89	1.20	0.055	0.088	10409	0.560
34	9	2.00	9.62	11.62	0.10	0.26	3.05	3.15	1.05	0.063	0.095	10867	0.725
34	10	2.00	9.62	11.62	0.10	0.17	4.83	1.99	2.09	0.029	0.060	8638	0.183
34	11	2.00	9.62	11.62	0.10	0.24	3.38	2.85	1.22	0.053	0.086	10337	0.537
34	12	2.00	9.62	11.62	0.10	0.18	4.47	2.15	1.86	0.033	0.065	8978	0.231
34	7	2.00	11.15	13.15	0.10	0.27	3.41	3.27	1.15	0.058	0.099	11072	0.604

Table C.1. (continued)

Run No.	Piezo No.	Median Stone Size D_{50} (in.)	Surface Discharge Q_s (cfs)	Total Discharge Q_T (cfs)	Slope S	Depth D-R (ft)	Velocity V (fps)	Area of Flow A (ft^2)	Froude Number F	Manning's n	Shields' Coefficient C_c	Reynold's Number R_e	Darcy-Weisbach Friction Factor f
34	8	2.00	11.15	13.15	0.10	0.27	3.50	3.19	1.19	0.056	0.097	10936	0.561
34	9	2.00	11.15	13.15	0.10	0.28	3.28	3.40	1.09	0.062	0.103	11290	0.679
34	10	2.00	11.15	13.15	0.10	0.19	4.87	2.29	1.96	0.032	0.069	9266	0.207
34	11	2.00	11.15	13.15	0.10	0.25	3.72	3.00	1.31	0.050	0.091	10605	0.466
34	12	2.00	11.15	13.15	0.10	0.18	5.19	2.15	2.16	0.029	0.065	8978	0.172
34	7	2.00	12.17	14.17	0.10	0.28	3.67	3.32	1.23	0.054	0.101	11157	0.530
34	8	2.00	12.17	14.17	0.10	0.27	3.70	3.29	1.24	0.054	0.100	11106	0.516
34	9	2.00	12.17	14.17	0.10	0.29	3.48	3.50	1.13	0.059	0.106	11455	0.621
34	10	2.00	12.17	14.17	0.10	0.21	4.79	2.54	1.84	0.035	0.077	9759	0.238
34	11	2.00	12.17	14.17	0.10	0.26	3.86	3.15	1.33	0.050	0.095	10867	0.453
34	12	2.00	12.17	14.17	0.10	0.19	5.29	2.30	2.13	0.030	0.070	9286	0.176
34	7	2.00	12.80	14.80	0.10	0.28	3.80	3.37	1.26	0.053	0.102	11240	0.501
34	8	2.00	12.80	14.80	0.10	0.28	3.78	3.39	1.25	0.054	0.103	11274	0.510
34	9	2.00	12.80	14.80	0.10	0.30	3.51	3.65	1.12	0.061	0.111	11698	0.637
34	11	2.00	12.80	14.80	0.10	0.25	4.20	3.05	1.47	0.045	0.092	10693	0.372
34	12	2.00	12.80	14.80	0.10	0.18	6.10	2.10	2.57	0.024	0.064	8873	0.121
36	7	4.00	4.10	5.10	0.10	0.15	2.26	1.81	1.02	0.059	0.030	16492	0.762
36	10	4.00	4.10	5.10	0.10	0.12	2.90	1.41	1.49	0.039	0.024	14560	0.361
36	7	4.00	6.91	7.91	0.10	0.20	2.86	2.41	1.12	0.056	0.040	19025	0.632
36	8	4.00	6.91	7.91	0.10	0.11	5.26	1.31	2.80	0.020	0.022	14036	0.102
36	9	4.00	6.91	7.91	0.10	0.13	4.39	1.57	2.14	0.028	0.026	15362	0.175
36	10	4.00	6.91	7.91	0.10	0.17	3.43	2.01	1.48	0.042	0.034	17377	0.367
36	7	4.00	9.57	10.57	0.10	0.25	3.18	3.01	1.12	0.059	0.050	21259	0.642
36	8	4.00	9.57	10.57	0.10	0.16	5.14	1.86	2.30	0.026	0.031	16718	0.152
36	9	4.00	9.57	10.57	0.10	0.18	4.51	2.12	1.89	0.033	0.035	17846	0.224
36	10	4.00	9.57	10.57	0.10	0.23	3.53	2.71	1.31	0.049	0.045	20173	0.468
36	12	4.00	9.57	10.57	0.10	0.14	5.86	1.63	2.80	0.021	0.027	15652	0.102
36	7	4.00	10.89	11.89	0.10	0.25	3.61	3.01	1.27	0.052	0.050	21259	0.495
36	8	4.00	10.89	11.89	0.10	0.18	5.03	2.16	2.09	0.030	0.036	18013	0.183
36	9	4.00	10.89	11.89	0.10	0.20	4.49	2.42	1.76	0.036	0.040	19065	0.258
36	10	4.00	10.89	11.89	0.10	0.25	3.61	3.01	1.27	0.052	0.050	21259	0.495
36	12	4.00	10.89	11.89	0.10	0.17	5.49	1.98	2.38	0.026	0.033	17247	0.141
36	7	4.00	13.04	14.04	0.10	0.30	3.66	3.56	1.18	0.057	0.059	23118	0.571
36	8	4.00	13.04	14.04	0.10	0.21	5.09	2.56	1.94	0.033	0.043	19607	0.213
36	9	4.00	13.04	14.04	0.10	0.23	4.79	2.72	1.77	0.037	0.045	20210	0.255
36	10	4.00	13.04	14.04	0.10	0.29	3.76	3.46	1.23	0.055	0.058	22791	0.525
36	12	4.00	13.04	14.04	0.10	0.20	5.47	2.38	2.16	0.029	0.040	18907	0.171
36	7	4.00	14.09	15.09	0.10	0.30	3.95	3.56	1.28	0.053	0.059	23118	0.489
36	8	4.00	14.09	15.09	0.10	0.21	5.50	2.56	2.10	0.031	0.043	19607	0.182
36	9	4.00	14.09	15.09	0.10	0.24	4.99	2.82	1.81	0.036	0.047	20578	0.243
36	10	4.00	14.09	15.09	0.10	0.29	4.01	3.51	1.31	0.052	0.059	22955	0.469
36	12	4.00	14.09	15.09	0.10	0.21	5.56	2.53	2.13	0.030	0.042	19492	0.176
36	7	4.00	16.62	17.62	0.10	0.32	4.36	3.81	1.36	0.050	0.064	23915	0.431
36	9	4.00	16.62	17.62	0.10	0.27	5.16	3.22	1.75	0.038	0.054	21987	0.260
36	10	4.00	16.62	17.62	0.10	0.32	4.36	3.81	1.36	0.050	0.064	23915	0.431
36	12	4.00	16.62	17.62	0.10	0.24	5.76	2.88	2.07	0.032	0.048	20795	0.186
36	7	4.00	16.65	17.65	0.10	0.33	4.25	3.91	1.31	0.052	0.065	24226	0.464

Table C.1. (continued)

Run No.	Piezo No.	Median Stone Size D_{50} (in.)	Surface Discharge Q_s (cfs)	Total Discharge Q_T (cfs)	Slope S	Depth D=R (ft)	Velocity V (fps)	Area of Flow A (ft^2)	Froude Number F	Manning's n	Shields' Coefficient C_c	Reynold's Number R_e	Darcy-Weisbach Friction Factor f
36	8	4.00	16.65	17.65	0.10	0.23	5.96	2.79	2.18	0.030	0.047	20468	0.169
36	9	4.00	16.65	17.65	0.10	0.28	5.01	3.32	1.68	0.040	0.055	22326	0.284
36	10	4.00	16.65	17.65	0.10	0.32	4.37	3.81	1.36	0.050	0.064	23915	0.429
36	12	4.00	16.65	17.65	0.10	0.24	5.77	2.88	2.08	0.031	0.048	20795	0.186
36	7	4.00	17.11	18.11	0.10	0.33	4.28	3.99	1.31	0.053	0.067	24473	0.467
36	8	4.00	17.11	18.11	0.10	0.26	5.50	3.11	1.90	0.035	0.052	21609	0.221
36	9	4.00	17.11	18.11	0.10	0.28	5.15	3.32	1.72	0.039	0.055	22326	0.269
36	10	4.00	17.11	18.11	0.10	0.32	4.49	3.81	1.40	0.049	0.064	23915	0.407
36	12	4.00	17.11	18.11	0.10	0.25	5.64	3.03	1.98	0.033	0.051	21329	0.205
36	7	4.00	18.26	19.26	0.10	0.36	4.28	4.26	1.27	0.055	0.071	25286	0.499
36	8	4.00	18.26	19.26	0.10	0.28	5.35	3.41	1.77	0.038	0.057	22626	0.256
36	9	4.00	18.26	19.26	0.10	0.30	5.11	3.57	1.65	0.041	0.060	23150	0.294
36	10	4.00	18.26	19.26	0.10	0.30	5.05	3.61	1.62	0.042	0.060	23279	0.304
36	12	4.00	18.26	19.26	0.10	0.29	5.24	3.48	1.71	0.039	0.058	22857	0.272
36	7	4.00	19.03	20.03	0.10	0.36	4.41	4.31	1.30	0.054	0.072	25434	0.476
36	8	4.00	19.03	20.03	0.10	0.29	5.53	3.44	1.82	0.037	0.057	22725	0.242
36	9	4.00	19.03	20.03	0.10	0.31	5.11	3.72	1.62	0.042	0.062	23631	0.306
36	10	4.00	19.03	20.03	0.10	0.31	5.12	3.71	1.62	0.042	0.062	23599	0.304
36	12	4.00	19.03	20.03	0.10	0.33	4.78	3.98	1.46	0.047	0.066	24442	0.375
36	7	4.00	22.84	23.84	0.10	0.39	4.85	4.71	1.36	0.052	0.079	26587	0.431
36	8	4.00	22.84	23.84	0.10	0.32	5.91	3.86	1.84	0.037	0.064	24071	0.237
36	9	4.00	22.84	23.84	0.10	0.34	5.54	4.12	1.67	0.042	0.069	24868	0.289
36	10	4.00	22.84	23.84	0.10	0.30	6.32	3.61	2.03	0.033	0.060	23279	0.194
36	12	4.00	22.84	23.84	0.10	0.30	6.37	3.58	2.06	0.033	0.060	23182	0.189
38	7	4.00	3.22	6.47	0.10	0.12	2.24	1.44	1.14	0.051	0.022	14695	0.618
38	9	4.00	3.22	6.47	0.10	0.14	1.87	1.72	0.87	0.069	0.026	16061	1.054
38	7	4.00	7.51	10.76	0.10	0.21	2.96	2.54	1.13	0.056	0.038	19517	0.624
38	8	4.00	7.51	10.76	0.10	0.13	4.97	1.51	2.47	0.024	0.023	15048	0.131
38	9	4.00	7.51	10.76	0.10	0.23	2.76	2.72	1.02	0.063	0.041	20197	0.766
38	11	4.00	7.51	10.76	0.10	0.15	4.13	1.82	1.87	0.032	0.028	16521	0.229
38	7	4.00	11.24	14.49	0.10	0.25	3.70	3.04	1.29	0.051	0.046	21352	0.477
38	8	4.00	11.24	14.49	0.10	0.17	5.46	2.06	2.32	0.026	0.031	17576	0.149
38	9	4.00	11.24	14.49	0.10	0.28	3.34	3.37	1.11	0.060	0.051	22481	0.650
38	10	4.00	11.24	14.49	0.10	0.30	3.13	3.59	1.01	0.067	0.054	23203	0.786
38	11	4.00	11.24	14.49	0.10	0.20	4.64	2.42	1.82	0.035	0.037	19050	0.241
38	7	4.00	13.44	16.69	0.10	0.28	4.02	3.34	1.34	0.050	0.051	22381	0.443
38	8	4.00	13.44	16.69	0.10	0.20	5.69	2.36	2.26	0.028	0.036	18813	0.156
38	9	4.00	13.44	16.69	0.10	0.31	3.66	3.67	1.17	0.058	0.056	23460	0.587
38	10	4.00	13.44	16.69	0.10	0.37	3.03	4.44	0.88	0.080	0.067	25804	1.040
38	11	4.00	13.44	16.69	0.10	0.24	4.77	2.82	1.73	0.038	0.043	20565	0.267
38	7	4.00	17.77	21.02	0.10	0.35	4.24	4.19	1.26	0.055	0.063	25067	0.500
38	8	4.00	17.77	21.02	0.10	0.26	5.73	3.10	1.99	0.033	0.047	21561	0.203
38	9	4.00	17.77	21.02	0.10	0.38	3.93	4.52	1.13	0.062	0.068	26036	0.628
38	11	4.00	17.77	21.02	0.10	0.30	4.91	3.62	1.58	0.043	0.055	23300	0.322
40	8	4.00	17.93	20.13	0.10	0.33	4.48	4.00	1.37	0.050	0.061	24492	0.427
40	11	4.00	17.93	20.13	0.10	0.36	4.13	4.34	1.21	0.058	0.066	25512	0.546

Table C.1. (continued)

Run No.	Piezo No.	Median Stone Size D_{50} (in.)	Surface Discharge Q_s (cfs)	Total Discharge Q_T (cfs)	Slope S	Depth D-R (ft)	Velocity V (fps)	Area of Flow A (ft^2)	Froude Number F	Manning's n	Shields' Coefficient C_c	Reynold's Number R_e	Darcy-Weisbach Friction Factor f
40	8	4.00	19.14	21.34	0.10	0.34	4.73	4.05	1.43	0.048	0.061	24645	0.389
40	11	4.00	19.14	21.34	0.10	0.39	4.08	4.69	1.15	0.062	0.071	26521	0.605
40	7	4.00	26.33	28.53	0.10	0.54	4.08	6.45	0.98	0.076	0.098	31101	0.831
40	8	4.00	26.33	28.53	0.10	0.42	5.21	5.05	1.42	0.051	0.077	27520	0.399
40	7	4.00	30.35	32.55	0.10	0.58	4.34	6.99	1.00	0.075	0.106	32377	0.796
40	8	4.00	30.35	32.55	0.10	0.47	5.37	5.65	1.38	0.053	0.086	29109	0.420
40	11	4.00	30.35	32.55	0.10	0.55	4.61	6.59	1.10	0.068	0.100	31437	0.667
40	12	4.00	30.35	32.55	0.10	0.55	4.58	6.63	1.09	0.069	0.100	31532	0.679
40	7	4.00	35.78	37.98	0.10	0.60	4.94	7.25	1.12	0.068	0.110	32974	0.639
40	8	4.00	35.78	37.98	0.10	0.58	5.15	6.95	1.19	0.063	0.105	32284	0.563
40	9	4.00	35.78	37.98	0.10	0.64	4.65	7.69	1.02	0.075	0.117	33959	0.763
40	11	4.00	35.78	37.98	0.10	0.60	4.98	7.19	1.13	0.067	0.109	32837	0.623
40	12	4.00	35.78	37.98	0.10	0.59	5.02	7.13	1.15	0.066	0.108	32700	0.608
40	7	4.00	38.60	40.80	0.10	0.64	5.05	7.65	1.11	0.069	0.116	33871	0.645
40	8	4.00	38.60	40.80	0.10	0.55	5.80	6.65	1.37	0.055	0.101	31580	0.424
40	9	4.00	38.60	40.80	0.10	0.67	4.83	7.99	1.04	0.074	0.121	34615	0.735
40	11	4.00	38.60	40.80	0.10	0.38	8.41	4.59	2.40	0.029	0.070	26236	0.139
40	12	4.00	38.60	40.80	0.10	0.53	6.10	6.33	1.48	0.050	0.096	30811	0.365
42	7	4.00	14.40	16.70	0.10	0.31	3.87	3.72	1.23	0.056	0.056	23619	0.533
42	8	4.00	14.40	16.70	0.10	0.33	3.68	3.91	1.14	0.060	0.059	24215	0.619
42	9	4.00	14.40	16.70	0.10	0.33	3.62	3.98	1.11	0.062	0.060	24431	0.653
42	10	4.00	14.40	16.70	0.10	0.19	6.34	2.27	2.57	0.024	0.034	18451	0.121
42	11	4.00	14.40	16.70	0.10	0.21	5.62	2.56	2.15	0.030	0.039	19594	0.174
42	12	4.00	14.40	16.70	0.10	0.27	4.18	3.29	1.47	0.045	0.050	22212	0.369
42	7	4.00	19.56	21.86	0.10	0.38	4.23	4.62	1.20	0.059	0.070	26322	0.553
42	8	4.00	19.56	21.86	0.10	0.38	4.24	4.61	1.21	0.059	0.070	26293	0.550
42	9	4.00	19.56	21.86	0.10	0.39	4.28	4.68	1.18	0.060	0.071	26492	0.575
42	10	4.00	19.56	21.86	0.10	0.25	6.59	2.97	2.33	0.028	0.045	21105	0.147
42	11	4.00	19.56	21.86	0.10	0.27	6.00	3.26	2.03	0.033	0.049	22111	0.194
42	12	4.00	19.56	21.86	0.10	0.32	5.16	3.79	1.62	0.042	0.057	23841	0.305
42	7	4.00	24.76	27.06	0.10	0.43	4.84	5.12	1.30	0.055	0.078	27710	0.470
42	8	4.00	24.76	27.06	0.10	0.44	4.66	5.31	1.24	0.059	0.080	28219	0.524
42	9	4.00	24.76	27.06	0.10	0.43	4.78	5.18	1.28	0.056	0.078	27872	0.487
42	10	4.00	24.76	27.06	0.10	0.29	7.14	3.47	2.34	0.029	0.053	22812	0.146
42	11	4.00	24.76	27.06	0.10	0.33	6.25	3.96	1.92	0.036	0.060	24369	0.217
42	12	4.00	24.76	27.06	0.10	0.36	5.71	4.34	1.67	0.042	0.066	25512	0.286
42	7	4.00	30.32	32.62	0.10	0.51	4.95	6.12	1.22	0.061	0.093	30295	0.535
42	8	4.00	30.32	32.62	0.10	0.50	5.04	6.01	1.26	0.059	0.091	30022	0.507
42	9	4.00	30.32	32.62	0.10	0.46	5.53	5.48	1.44	0.050	0.083	28667	0.384
42	10	4.00	30.32	32.62	0.10	0.30	8.49	3.57	2.74	0.025	0.054	23138	0.106
42	11	4.00	30.32	32.62	0.10	0.36	6.95	4.36	2.03	0.034	0.066	25571	0.194
42	12	4.00	30.32	32.62	0.10	0.41	6.14	4.94	1.69	0.042	0.075	27218	0.282
42	7	4.00	36.10	38.40	0.10	0.55	5.45	6.62	1.29	0.058	0.100	31508	0.478
42	8	4.00	36.10	38.40	0.10	0.54	5.55	6.51	1.33	0.056	0.099	31245	0.454
42	9	4.00	36.10	38.40	0.10	0.49	6.14	5.88	1.55	0.048	0.089	29695	0.335
42	10	4.00	36.10	38.40	0.10	0.33	9.09	3.97	2.79	0.025	0.060	24400	0.103
42	11	4.00	36.10	38.40	0.10	0.37	8.09	4.46	2.34	0.030	0.068	25862	0.146

Table C.1. (continued)

Run No.	Piezo No.	Median Stone Size D_{50} (in.)	Surface Discharge Q_s (cfs)	Total Discharge Q_T (cfs)	Slope S	Depth D-R (ft)	Velocity V (fps)	Area of Flow A (ft^2)	Froude Number F	Manning's n	Shields' Coefficient C_c	Reynold's Number R_e	Darcy-Weisbach Friction Factor f
42	12	4.00	36.10	38.40	0.10	0.44	6.82	5.29	1.81	0.040	0.080	28166	0.244
42	7	4.00	39.83	42.13	0.10	0.59	5.59	7.12	1.28	0.059	0.108	32677	0.488
42	8	4.00	39.83	42.13	0.10	0.58	5.68	7.01	1.31	0.058	0.106	32423	0.466
42	9	4.00	39.83	42.13	0.10	0.52	6.34	6.28	1.55	0.048	0.095	30689	0.335
44	7	4.00	20.99	24.39	0.10	0.30	5.90	3.56	1.91	0.035	0.054	23106	0.220
44	8	4.00	20.99	24.39	0.10	0.25	7.12	2.95	2.53	0.026	0.045	21033	0.125
44	9	4.00	20.99	24.39	0.10	0.32	5.44	3.86	1.69	0.041	0.058	24060	0.280
44	11	4.00	20.99	24.39	0.10	0.47	3.71	5.66	0.95	0.077	0.086	29134	0.883
44	7	4.00	26.80	30.20	0.10	0.38	5.94	4.51	1.71	0.041	0.068	26007	0.274
44	8	4.00	26.80	30.20	0.10	0.33	6.70	4.00	2.05	0.034	0.061	24492	0.191
44	9	4.00	26.80	30.20	0.10	0.38	5.94	4.51	1.71	0.041	0.068	26007	0.274
44	10	4.00	26.80	30.20	0.10	0.55	4.10	6.54	0.98	0.077	0.099	31317	0.836
44	11	4.00	26.80	30.20	0.10	0.53	4.21	6.36	1.02	0.073	0.096	30883	0.769
44	7	4.00	31.98	35.38	0.10	0.43	6.26	5.11	1.69	0.042	0.077	27683	0.280
44	8	4.00	31.98	35.38	0.10	0.38	6.95	4.60	1.98	0.036	0.070	26265	0.204
44	9	4.00	31.98	35.38	0.10	0.42	6.32	5.06	1.72	0.042	0.077	27547	0.272
44	10	4.00	31.98	35.38	0.10	0.59	4.51	7.09	1.03	0.073	0.107	32608	0.748
44	11	4.00	31.98	35.38	0.10	0.56	4.80	6.66	1.14	0.066	0.101	31603	0.620
44	12	4.00	31.98	35.38	0.10	0.60	4.44	7.21	1.01	0.075	0.109	32882	0.787
44	P7	4.00	35.51	38.91	0.10	0.45	6.50	5.46	1.70	0.043	0.083	28615	0.277
44	8	4.00	35.51	38.91	0.10	0.38	7.72	4.60	2.20	0.032	0.070	26265	0.166
44	9	4.00	35.51	38.91	0.10	0.44	6.75	5.26	1.80	0.040	0.080	28086	0.248
44	10	4.00	35.51	38.91	0.10	0.59	5.04	7.04	1.16	0.065	0.107	32493	0.594
44	11	4.00	35.51	38.91	0.10	0.55	5.37	6.61	1.28	0.059	0.100	31485	0.492
44	12	4.00	35.51	38.91	0.10	0.57	5.23	6.78	1.23	0.061	0.103	31896	0.532
44	9	4.00	37.17	40.57	0.10	0.46	6.81	5.46	1.78	0.041	0.083	28615	0.253
44	10	4.00	37.17	40.57	0.10	0.53	5.84	6.37	1.41	0.053	0.097	30908	0.402
44	11	4.00	37.17	40.57	0.10	0.51	6.13	6.06	1.52	0.049	0.092	30146	0.346
44	12	4.00	37.17	40.57	0.10	0.57	5.46	6.81	1.28	0.059	0.103	31957	0.491
44	7	4.00	42.05	45.45	0.10	0.49	7.18	5.86	1.81	0.041	0.089	29645	0.244
44	9	4.00	42.05	45.45	0.10	0.45	7.87	5.34	2.08	0.035	0.081	28299	0.185
44	10	4.00	42.05	45.45	0.10	0.54	6.48	6.49	1.55	0.048	0.098	31197	0.332
44	11	4.00	42.05	45.45	0.10	0.48	7.24	5.81	1.83	0.040	0.088	29518	0.238
44	12	4.00	42.05	45.45	0.10	0.61	5.71	7.36	1.29	0.059	0.112	33223	0.484
46	8	2.00	1.86	3.50	0.10	0.11	1.40	1.33	0.74	0.078	0.040	7061	1.460
46	12	2.00	1.86	3.50	0.10	0.08	1.84	1.01	1.12	0.049	0.031	6154	0.639
46	7	2.00	3.85	5.49	0.10	0.14	2.23	1.73	1.03	0.058	0.052	8054	0.750
46	8	2.00	3.85	5.49	0.10	0.16	2.01	1.92	0.88	0.069	0.058	8484	1.025
46	12	2.00	3.85	5.49	0.10	0.09	3.47	1.11	2.01	0.028	0.034	6451	0.198
46	7	2.00	5.25	6.89	0.10	0.17	2.64	1.99	1.14	0.054	0.060	8638	0.614
46	8	2.00	5.25	6.89	0.10	0.19	2.35	2.23	0.96	0.065	0.068	9144	0.864
46	12	2.00	5.25	6.89	0.10	0.11	3.86	1.36	2.02	0.029	0.041	7141	0.196
46	7	2.00	6.63	8.27	0.10	0.19	2.96	2.24	1.21	0.052	0.068	9164	0.549
46	8	2.00	6.63	8.27	0.10	0.21	2.62	2.53	1.01	0.064	0.077	9739	0.791
46	10	2.00	6.63	8.27	0.10	0.11	4.95	1.34	2.61	0.022	0.041	7088	0.118
46	11	2.00	6.63	8.27	0.10	0.11	5.22	1.27	2.83	0.020	0.038	6900	0.100

Table C.1. (continued)

Run No.	Piezo No.	Median Stone Size D_{50} (in.)	Surface Discharge Q_s (cfs)	Total Discharge Q_T (cfs)	Slope S	Depth D-R (ft)	Velocity V (fps)	Area of Flow A (ft^2)	Froude Number F	Manning's n	Shields' Coefficient C_c	Reynold's Number R_e	Darcy-Weisbach Friction Factor f
46	12	2.00	6.63	8.27	0.10	0.16	3.38	1.96	1.48	0.042	0.059	8572	0.368
48	8	4.00	7.76	9.94	0.10	0.20	3.30	2.35	1.31	0.048	0.036	18773	0.463
48	10	4.00	7.76	9.94	0.10	0.18	3.64	2.13	1.52	0.041	0.032	17873	0.344
48	8	4.00	10.93	13.11	0.10	0.28	3.26	3.35	1.09	0.062	0.051	22414	0.676
48	10	4.00	10.93	13.11	0.10	0.23	4.00	2.73	1.48	0.044	0.041	20234	0.366
48	11	4.00	10.93	13.11	0.10	0.32	2.81	3.89	0.87	0.079	0.059	24153	1.058
48	8	4.00	16.35	18.53	0.10	0.36	3.80	4.30	1.12	0.062	0.065	25394	0.638
48	9	4.00	16.35	18.53	0.10	0.41	3.36	4.86	0.93	0.076	0.074	26997	0.922
48	10	4.00	16.35	18.53	0.10	0.29	4.74	3.45	1.56	0.043	0.052	22746	0.330
48	11	4.00	16.35	18.53	0.10	0.38	3.56	4.59	1.01	0.070	0.070	26236	0.777
48	7	4.00	20.36	22.54	0.10	0.47	3.58	5.69	0.92	0.080	0.086	29211	0.954
48	8	4.00	20.36	22.54	0.10	0.34	5.03	4.05	1.52	0.045	0.061	24645	0.344
48	9	4.00	20.36	22.54	0.10	0.45	3.76	5.41	0.99	0.073	0.082	28484	0.820
48	10	4.00	20.36	22.54	0.10	0.34	5.00	4.07	1.51	0.046	0.062	24706	0.349
48	11	4.00	20.36	22.54	0.10	0.45	3.78	5.39	0.99	0.073	0.082	28431	0.811
48	7	4.00	23.91	26.09	0.10	0.51	3.88	6.16	0.95	0.078	0.093	30394	0.878
48	8	4.00	23.91	26.09	0.10	0.38	5.22	4.58	1.49	0.047	0.069	26208	0.361
48	9	4.00	23.91	26.09	0.10	0.48	4.12	5.81	1.04	0.070	0.088	29518	0.736
48	10	4.00	23.91	26.09	0.10	0.34	5.90	4.05	1.79	0.039	0.061	24645	0.249
48	11	4.00	23.91	26.09	0.10	0.38	5.27	4.54	1.51	0.047	0.069	26093	0.351
48	12	4.00	23.91	26.09	0.10	0.44	4.53	5.28	1.20	0.060	0.080	28139	0.553
48	7	4.00	26.75	28.93	0.10	0.52	4.27	6.27	1.04	0.071	0.095	30664	0.739
48	8	4.00	26.75	28.93	0.10	0.43	5.21	5.13	1.41	0.051	0.078	27737	0.405
48	9	4.00	26.75	28.93	0.10	0.48	4.60	5.81	1.17	0.063	0.088	29518	0.588
48	10	4.00	26.75	28.93	0.10	0.33	6.77	3.95	2.08	0.033	0.060	24339	0.185
48	11	4.00	26.75	28.93	0.10	0.40	5.52	4.85	1.53	0.047	0.073	26969	0.342
48	12	4.00	26.75	28.93	0.10	0.47	4.79	5.58	1.24	0.059	0.085	28928	0.521
51	7	4.00	25.61	29.76	0.10	0.47	4.57	5.61	1.18	0.062	0.085	29005	0.578
51	8	4.00	25.61	29.76	0.10	0.36	6.01	4.26	1.78	0.039	0.065	25276	0.253
51	9	4.00	25.61	29.76	0.10	0.45	4.71	5.44	1.23	0.059	0.082	28563	0.527
51	10	4.00	25.61	29.76	0.10	0.29	7.34	3.49	2.40	0.028	0.053	22878	0.139
51	11	4.00	25.61	29.76	0.10	0.33	6.45	3.97	1.98	0.035	0.060	24400	0.205
51	12	4.00	25.61	29.76	0.10	0.35	6.08	4.21	1.81	0.038	0.064	25127	0.244
51	7	4.00	33.05	37.20	0.10	0.53	5.24	6.31	1.27	0.058	0.096	30762	0.494
51	8	4.00	33.05	37.20	0.10	0.47	5.84	5.66	1.50	0.049	0.086	29134	0.356
51	9	4.00	33.05	37.20	0.10	0.52	5.25	6.29	1.28	0.058	0.095	30713	0.489
51	10	4.00	33.05	37.20	0.10	0.38	7.20	4.59	2.05	0.034	0.070	26236	0.190
51	11	4.00	33.05	37.20	0.10	0.43	6.39	5.17	1.72	0.042	0.078	27845	0.272
51	12	4.00	33.05	37.20	0.10	0.42	6.60	5.01	1.80	0.040	0.076	27410	0.247
51	7	4.00	39.95	44.10	0.10	0.58	5.78	6.91	1.34	0.056	0.105	32191	0.444
51	8	4.00	39.95	44.10	0.10	0.53	6.28	6.36	1.52	0.049	0.096	30883	0.346
51	9	4.00	39.95	44.10	0.10	0.57	5.88	6.79	1.38	0.055	0.103	31910	0.421
51	10	4.00	39.95	44.10	0.10	0.42	8.01	4.99	2.19	0.033	0.076	27356	0.167
51	11	4.00	39.95	44.10	0.10	0.48	6.92	5.77	1.76	0.042	0.087	29416	0.258
51	12	4.00	39.95	44.10	0.10	0.46	7.25	5.51	1.89	0.039	0.083	28746	0.225
51	7	4.00	45.26	49.41	0.10	0.63	5.95	7.61	1.32	0.058	0.115	33782	0.462

Table C.1. (continued)

Run No.	Piezo No.	Median Stone Size D_{50} (in.)	Surface Discharge Q_s (cfs)	Total Discharge Q_T (cfs)	Slope S	Depth D-R (ft)	Velocity V (fps)	Area of Flow A (ft^2)	Froude Number F	Manning's n	Shields' Coefficient C_c	Reynold's Number R_e	Darcy-Weisbach Friction Factor f
51	8	4.00	45.26	49.41	0.10	0.56	6.70	6.76	1.57	0.048	0.102	31840	0.324
51	9	4.00	45.26	49.41	0.20	0.63	5.96	7.59	1.32	0.058	0.115	33738	0.458
51	10	4.00	45.26	49.41	0.10	0.42	8.89	5.09	2.41	0.030	0.077	27628	0.138
51	11	4.00	45.26	49.41	0.10	0.46	8.13	5.57	2.10	0.035	0.084	28902	0.181
51	12	4.00	45.26	49.41	0.10	0.46	8.21	5.51	2.14	0.034	0.083	28746	0.175

[a]Data computed by IBM PC; therefore, rounding effects may be neglected.

$$F = \frac{Q_s/12}{\sqrt{gD^3}}$$

$$C_c = \frac{DS}{(G_s-1)\,D_{50}}$$

$$n = \frac{1.486}{Q_s} D^{2/3} S^{1/2} A$$

$$R_e = \frac{\sqrt{gDS}\,D_{50}}{\nu}$$

$$V = \frac{Q_s}{A} \text{ ft/s}$$

$$\nu = 1.41 \times 10^{-5} \text{ ft}^2/\text{s at } 50°\text{F}$$

$$A = 12 \times D \text{ ft}^2$$

$$f = \frac{8gDS}{V^2}$$

INTERNAL DISTRIBUTION

1. J. B. Cannon
2. W. Fulkerson
3. S. G. Hildebrand
4. N. E. Hinkle
5. R. H. Ketelle
6. D. W. Lee
7-14. R. B. Mclean
15. R. M. Reed
16. D. E. Reichle
17. R. B. Shelton
18. W. P. Staub
19. A. J. Witten
20. ORNL Patent Office
21. Central Research Library
22. Document Reference Section
23-24. Laboratory Records
25. Laboratory Records (RC)

EXTERNAL DISTRIBUTION

26-34. S. R. Abt, Colorado State University, Fort Collins, CO 80523.

35. J. J. Cuttica, Vice President of Research and Development, Gas Research Institute, 8600 W. Bryn Mawr Avenue, Chicago, IL 60631.

36. J. P. Kalt, Professor of Economics, Kennedy School of Government, Harvard University, 79 John F. Kennedy Street, Cambridge, MA 02138.

37. M. S. Khattak, Colorado State University, Fort Collins, CO 80523.

38. D. L. LaGrone, Colorado State University, Fort Collins, CO 80523.

39. D. E. Morrison, Professor of Sociology, Michigan State University, 201 Berkey Hall, East Lansing, MI 48824-1111.

40. J. D. Nelson, Colorado State University, Fort Collins, CO 80523.

41. R. L. Perrine, Professor, Engineering and Applied Sciences, Civil Engineering Department, Engineering I, Room 2066, University of California, Los Angeles, CA 90024.

42. J. F. Ruff, Colorado State University, Fort Collins, CO 80523.

43. R. J. Wittler, Colorado State University, Fort Collins, CO 80523.

44-45. OSTI, U.S. Department of Energy, P.O. Box 62, Oak Ridge, TN 37831.

46. Assistant Manager, Energy Research and Development, DOE/ORO.

NRC FORM 335 (2 84) NRCM 1102, 3201, 3202

U.S. NUCLEAR REGULATORY COMMISSION

BIBLIOGRAPHIC DATA SHEET

SEE INSTRUCTIONS ON THE REVERSE

1. REPORT NUMBER (Assigned by TIDC, add Vol. No., if any)
NUREG/CR-4651
ORNL/TM-10100/V2
Vol.2

2. TITLE AND SUBTITLE
Development of Riprap Design Criteria by Riprap Testing in Flumes: Phase II

3. LEAVE BLANK

4. DATE REPORT COMPLETED
MONTH: August | YEAR: 1988

5. AUTHOR(S)
S. R. Abt, R. J. Wittler, J. F. Ruff, D. L. LaGrone, M. S. Khattak, J. D. Nelson, N. E. Hinkle, and D. W. Lee

6. DATE REPORT ISSUED
MONTH: September | YEAR: 1988

7. PERFORMING ORGANIZATION NAME AND MAILING ADDRESS (Include Zip Code)
Oak Ridge National Laboratory
P.O.Box 2008
Oak Ridge, Tennessee 37831

8. PROJECT/TASK/WORK UNIT NUMBER

9. FIN OR GRANT NUMBER
B-0279

10. SPONSORING ORGANIZATION NAME AND MAILING ADDRESS (Include Zip Code)
Division of Low Level Waste Management & Decommissioning
Office of Nuclear Material Safety and Safeguards
U.S. Nuclear Regulatory Commission
Washington, D.C. 20555

11a. TYPE OF REPORT
Technical

b. PERIOD COVERED (Inclusive dates)

12. SUPPLEMENTARY NOTES

13. ABSTRACT (200 words or less)

Flume studies were conducted in which riprap embankments were subjected to overtopping flows. Embankment slopes of 1, 2, 8, 10, and 20% were protected with riprap containing median stone sizes of 1, 2, 4, 5, and/or 6 in. Riprap layer thickness ranged from 1.5 D_{50} to 4 D_{50}. Riprap design criteria for overtopping flows were developed in terms of unit discharge at failure, interstitital velocities and discharges through the riprap layer, resistance to flow over the riprap surface, effects of riprap layer thickness and gradation on riprap stability, and potential impacts of integrating soil into the riprap layer for riprap stabilization. A riprap design procedure is presented for overtopping flow conditions.

14. DOCUMENT ANALYSIS - a. KEYWORDS/DESCRIPTORS
Riprap Design Criteria, Riprap Stability
Riprap Testing
Riprap
Riprap Embankments

b. IDENTIFIERS/OPEN-ENDED TERMS

15. AVAILABILITY STATEMENT
Unlimited

16. SECURITY CLASSIFICATION
(This page)
Unclassified
(This report)
Unclassified

17. NUMBER OF PAGES

18. PRICE